On the Industrial Crystallization of Proteins

Habilitationsschrift

zur Erlangung des akademischen Grades
Dr.-Ing. habil.

vorgelegt dem
Zentrum für Ingenieurwissenschaften
der Martin-Luther-Universität Halle-Wittenberg
als organisatorische Grundeinheit für Forschung und Lehre im Range einer Fakultät
(§ 75 Abs. 1 HSG LSA, § 19 Abs. 1 Grundordnung)

von
Herrn Matthew Jonathan Jones, PhD
geb. am: 06. August 1967 in: Rinteln

Gutachter
1. Professor Dr.-Ing. habil. Dr. h.c. Joachim Ulrich (ZIW, MLU)
2. Professor Dr. rer. nat. habil. Dr. h.c. Reinhard Neubert (Pharmazie, MLU)
3. Professor Dr. Gérard Coquerel (Université de Rouen, Frankreich)

Halle (Saale), 9. Dezember 2014

Acknowledgements

I wish to express my gratitude to all who have enabled, encouraged and supported the work presented here.

First and foremost my thanks go to Professor Joachim Ulrich for having sufficient faith in the value of my idea to study the large scale crystallization of proteins to provide me with the opportunity to carry out this research. The many fruitful discussions in the time we worked together helped me develop and grow as a scientist. His continuous support and encouragement was an essential and much appreciated contribution to the success of this work.

A large part of the work presented here would not have been possible without the efforts of the numerous PhD-, Diplom-, Masters-, and undergraduate project students I supervised during my time in Halle. In particular I would like to thank Dr Maxim Weber and Dr Naser Aldabaibeh for their sterling work, as well as for the many stimulating and at times very lively discussions and debates. I also thank Dr Bo-Hyun Ryu for her contribution to the solvent freeze-out technology.

My gratitude also goes to Professor Markus Pietzsch and Dr Thomas Hertel for their hospitality in the early stages of this work, allowing me and my students to work in their laboratories, for patiently teaching us the techniques necessary for the characterisation of our samples and for their continuing interest in our progress and the many valuable discussions we had along the way.

I also wish to thank all my friends for their support and encouragement, in particular Anke and Christian Marx, Aniko Szepes and Sabrina Pfennig, as well as my former colleagues from the Thermische Verfahrenstechnik research group who contributed by sharing the pleasure (and the pain) of research and university life and made my time in Halle a positively memorable experience.

Finally, my heartfelt gratitude to my parents Regine and Keith Jones and to my sister, Dr Nicola G. Jones, who supported me all the way, through thick and thin, without ever doubting.

Table of Contents

1. Introduction

Crystallization is a well-established unit operation for separation, purification and form-giving of solid products from a liquid phase and is employed as a matter of routine in those industry sectors producing such products. The general principles governing the crystallization process are sufficiently well understood to consider the technology mature (see, for example, (Myerson 1993, Mullin 2001, Beckmann 2013)). Nonetheless, there are still aspects of crystallization, concerning both existing gaps in the understanding of the fundamental physics of the formation of crystalline solids as well as emerging technological application of this unit operation, that merit continuing research.

One area where crystallization technology is decidedly in its infancy is the application of crystallization as a unit operation for purification, isolation and form-giving for crystalline proteins. The main reason for this situation is the absence of a comprehensive body of knowledge regarding those physical properties of proteins required to design such technology.

Protein crystallization itself has been practiced since the first half of the 19th century, ever since haemoglobin was first crystallized from both porcine and human blood (Hünefeld 1840). Crystallization has since been used as a method for separating proteins from their natural sources (although chromatographic techniques are currently the methods of choice for high-performance purification, see, for example, (Walsh 2002)) and presently its predominant application is firmly rooted in structural science, where the primary task is to generate single crystals of sufficient quality for diffraction studies towards structure solution. To this date, the paucity of solubility data for proteins, the absence of techniques capable of generating these data routinely, in an acceptably short period of time and with a minimum amount of material has led to a situation where screening a large range of potential crystallization conditions, more or less at random, is still the preferred approach for generating protein single crystals.

Industrial crystallization of proteins, that is the large scale crystallization of proteins for the sake of purification and form-giving, is certainly of interest to the relevant industry sectors, though very little information is made public. For example, glucose isomerase produced by Genencor International is purified by crystallization and a paper by Visuri (Visuri 2000) clearly demonstrates the advantage of this unit operation over preparative chromatography both in terms of the quality of the product obtained and the investment and running costs of equipment required for the respective operations. Insulin, a therapeutic protein, on the other hand is purified by chromatography (Barfoed 1987, Kroeff 1989, Hazra 2010), but crystallization is employed as a finishing operation.

There are only few examples of protein crystallization in industrial use to be found in the scientific literature. To the best knowledge of this author, prior to the year 2000 the publication of Visuri cited above, together with an investigation of ovalbumin purification by Judge *et al.* (Judge 1995) were the only recent academic publications in this field since those concerning ‘large scale’ crystallization of proteins for the purpose of isolating and

characterising these components in selected natural resources published in the late 19th and first half of the 20th century (see for example (Hofmeister 1890, Sumner 1919, Abel 1927, Young 1937)). However, in the years since there has been a noticeable increase in interest in large scale protein crystallization in the academic community.

As the market for protein products grows (Braun 2006), it is not unlikely that the demand for cost effective unit operations will increase in the long term. Although it is not always the case that preparative chromatography is more cost intensive than crystallization and given the likelihood that crystallization will not always be able to satisfy purity requirements for products such as therapeutic proteins, it is nonetheless imperative to build a better understanding of this unit operation as applied to protein products. First and foremost this means establishing a better body of knowledge of the physical properties of proteins governing the crystallization process, as well as gaining an understanding of the type of crystallization equipment that is most suitable for achieving a given product quality for defined quality criteria. Even if crystallization is employed merely for form-giving, a solid body of knowledge is essential to guarantee good process control and to avoid unexpected results with respect to crystal modification or size distribution obtained.

The major obstacle towards obtaining this improved knowledge is the availability and cost of the materials to be investigated. The availability is currently limited either by the source of a given protein, or the cost of manufacturing a protein using suitable biotechnological approaches. In the case of proteins obtained from natural resources, the protein itself might be present in minute quantities representing merely a fraction of a percent of the total biomass available. This is certainly the case for urease, one of the model proteins used in the studies presented herein, which accounts for less than 0.1 % of the mass of the jack bean meal it is extracted from. For other proteins frequently used as model systems for the investigation of crystallization behaviour, the natural abundance in their respective sources is generally greater. Ovalbumin for example, a storage protein found in egg white, has a much greater abundance (> 60 % of total protein content (Longsworth 1940, Forsythe 1950, Warner 1954)). Lysozyme, a bacteriolytic enzyme found in egg white (amongst other sources) is the classic and best understood protein in terms of crystallization; its abundance is an order of magnitude lower than that of ovalbumin (Longsworth 1940, Forsythe 1950, Warner 1954), which is still high compared to urease. Manufactured proteins are expensive since the prerequisite research essential to establish and modify microorganisms suitable for production is involved and time consuming and the manufacturing technology required is inherently inefficient in terms of yield. Moreover, the quantities required are small compared to commodity and speciality chemicals, and price prohibits any more than the essential research required to develop a workable manufacturing process.

In addition to these limitations, the amounts of material necessary to obtain the fundamental data required for the rational design of manufacturing processes is comparatively large when considering methodologies routinely employed in the small-molecule manufacturing industries. The complexity of the phase behaviour of proteins, discussed in detail in chapter 2 below, together with the size of the molecules, means that more experiments are required to

fully map phase space and evaluate kinetics of nucleation and crystal growth as a function of the relevant physical parameters, and that the individual experiments require a greater amount of time.

In this work a number of these issues are addressed. A novel method for measuring solubility data is presented, which significantly reduces the time required to establish the phase diagram of a protein. As a result of this improvement, it was possible for the first time to establish the regions of stability of different crystal modification of the model protein lysozyme. In addition, crystallization technologies have been investigated and two case studies are presented and discussed. The first is concerned with the crystallization of urease, an enzyme found in jack beans, with the focus upon understanding the interplay between crystallization and conditions product quality criteria such as purity, crystal size and enzymatic activity. The second case study demonstrates the utility of freezing out the solvent as a means of generating supersaturation as opposed to the more established salting-out. Here, product quality criteria are evaluated as a function of the processing conditions and are considered together with the potential environmental advantages afforded by reduced use of crystallizing agents.

2. Thermodynamics of Protein Solutions - Solubility

For the purpose of designing a large-scale crystallization process for a protein, the primary thermodynamic property of interest is the solubility of this protein. In general, the solubility defines the operating range for any crystallization process. In order to crystallize a solid from a liquid the system has to be driven to a state of disequilibrium where the route to regaining a state of equilibrium is via a decomposition of the liquid into two components, one of which is the desired solid material. The latter qualification is important, as a second pathway breaking disequilibrium via a liquid-liquid phase separation exists, commonly called oiling-out. These spontaneous liquid-liquid phase separations are undesirable in the context of industrial process development, as the composition of the two new phases often remains unknown and control over processes is therefore lost.

The solubility of a crystalline solid is the maximum amount of that solid that can be dissolved in a liquid of given composition, strictly the chemical potential (μ) of the individual components, conveniently their respective concentrations (c), at a given temperature (T) and pressure (p). The main difficulty in representing the solubility of a given protein lies in the fact that proteins solutions suitable for crystallization are complex in their composition and cannot be presented in simple binary or ternary phase diagrams (Jones 2010). In the very simplest case a protein solution for crystallization will contain water as solvent, the dissolved protein itself, a precipitating agent and a buffer to control and maintain the pH at a constant value during the crystallization process. Depending upon the buffer required, this leads to a minimum of four, more frequently five compositional variables that need to be accounted for.

2.1 Measurement of Solubility

Solubility can be measured using any analytical method capable of quantifying the amount of dissolved solid in systems where the solid and liquid phases are in thermodynamic equilibrium. A frequently employed method of analysis for determining protein concentration in a solution is the measurement of UV absorbance (Edelhoch 1967, Pace 1995, Grimsley 2003, Noble 2009), commonly at a wavelength of 280 nm. The chromophores responsible for the absorption of proteins the UV range are the amino acids tyrosine, tryptophan and phenylalanine, histidine and cysteine, the latter in the form of its oxidised dimer cystine. Tryptophan has an absorption maximum λ_{max} at exactly 280 nm (Table 1) and also has the highest extinction coefficient (ε) and together with tyrosine, $\lambda_{max} = 275.5$ nm, is responsible for the absorption maximum of most proteins around $\lambda = 280$ nm. While phenylalanine, histidine and cysteine/cystine absorb UV-light, their absorption maxima lie at considerably lower wavelengths. As a consequence their contribution to the absorption at $\lambda = 280$ nm is negligible and when calculating protein or peptide extinction coefficients at this wavelength, based upon a known amino acid sequence, it is common to consider only the number of tryptophan, tyrosine and cystine units present (Gill 1989, Pace 1995). The concentration range

accessible for a given protein depends upon its absorption coefficient at the selected wavelength and is therefore a function of the number of the above amino acids in the protein.
Two major limitations exist for optical concentration measurements. One is the availability of a suitably pure protein sample for calibration and determination of the extinction coefficient, if the latter is not already known to sufficient accuracy, the other is that relatively 'large' sample volumes of the order of a few μL are required, limiting this analytical technique to proteins available in sufficient abundance. Manipulation of the optical path length (using short path cuvettes) can increase the concentration range accessible, in very dilute solutions other means of characterisation are required. Various chromophore-based assays (Lowry 1951, Winterbourne 1986) are available to increase the sensitivity of optical concentration measurements, alternatively suitable chromatographic methods may be employed.

Table 1: Wavelength of maximum absorbance and molar extinction coefficients for the three aromatic amino acids (Mihalyi 1968) and cystine (Ison 2006).

Amino acid	λ_{max}**/nm**	ε **/ M^{-1}cm^{-1}**
Cystine	250	356
Phenylalanine	258	195
Tryptophan	280	5,559
Tyrosine	275	1,405

The method of obtaining thermodynamic equilibrium between the protein crystal and the solution is at least as important as the method of concentration analysis is, if not more so. Solubility data have been obtained from hanging drop/sitting drop experiments (Chayen 1988, Mikol 1989a, Cacioppo 1992, Ninomiya 2001, Tamagawa 2002). Here, a small drop, typically a few μL, of a protein/precipitant solution under defined conditions is brought into indirect contact with a significantly more concentrated salt reservoir. Equilibrium is obtained by exchange of solvent between the protein-rich liquid phase with the salt reservoir via the vapour phase and simultaneous growth of a protein crystal. The process ends when the chemical potential of the solvent in the salt reservoir is the same as in the protein reservoir and therefore the same as the chemical potential of the solvent in the vapour phase. This approach suffers from several drawbacks. The major disadvantage is the time required to achieve equilibrium, which typically lies in the range of several weeks to months (Chayen 1988, Ninomiya 2001). The timescale of equilibration gives plenty of opportunity for sample decomposition and therefore failure of the experiment. The second disadvantage is the sample size. Hanging drop/sitting drop experiments necessarily require repeated sampling from a small volume, introducing significant scope for experimental error.
Isothermal micro-batch crystallization is a method more commonly employed (Ataka 1986, Boistelle 1992, Budayova-Spano 2000, Benas 2002, Sleutel 2009). Here, a slurry of protein crystals is allowed to equilibrate with a solution at defined pH, buffer and precipitant concentration. Larger sample volumes are possible using this approach, but these also

necessitate larger protein amounts, which can be a disadvantage for expensive proteins or those with low abundance and availability. Batch samples can be agitated, which decreases equilibration times. The method of agitation used should ensure that the protein crystals are not subjected to mechanical degradation leading to the formation of amorphous components changing the nature and number of components of the system. Magnetic stirring bars should therefore be avoided and overhead stirring kept to a minimum so that the slurry is just suspended. Nutating shaking tables may present the best alternative providing sufficient agitation while avoiding excessive mechanical stresses on the protein crystals. Despite the advantages of agitated slurries, most of the literature reports using this method cite equilibration times of days to weeks (Ataka 1988, Howard 1988, Vuolanto 2003), making data acquisition for the purpose of phase diagram determination almost as arduous as static microbatch or hanging drop/sitting drop methods.

Pusey and Gernert (Pusey 1988) presented a method facilitating mass transfer between the solid and solution phases (or vice versa) and thus improving equilibration times by allowing a solution to pass through a static bed of protein crystals. The set-up described is simple: a slurry of protein crystals is loaded into a small column which is connected to a reservoir containing a protein solution with defined pH, buffer and precipitant concentration. The solution is allowed to flow through the protein bed, which is kept at constant temperature in a thermal bath, under the action of gravity. The eluent is collected and recycled into the reservoir and samples can be drawn at any time.

The time gain in this approach is significant: for validation samples the measured solution protein concentrations were within 5 % of known equilibrium values within 6 - 8 hours and approached 1 % accuracy within 24 hours. As pointed out by the authors, the 'formidable task' of generating accurate phase diagrams, including the regions of stability and solubility of metastable phases, becomes feasible with this improvement. The major drawback is once again the relatively large amount of crystalline solid required for generating the static bed of crystals (a few mg), which is somewhat mitigated by reusability of one and the same bed for several measurements. Based upon this methodology, several papers (Pusey 1988, Cacioppo 1991a, Cacioppo 1991b, Forsythe 1996, Forsythe 1999a) were published elucidating the solubility of tetragonal lysozyme chloride over a range of temperatures and sodium chloride concentrations at pH values between 4.0 and 5.4. These are discussed in some detail in chapter 2.4 below.

Building upon this method, Weber *et al.* (Weber 2005) reported a fully automated approach to measuring protein solubility resulting in a further and significant reduction of the equilibration times. The major innovation compared to the method of Pusey and Gernert (Pusey 1988) is the introduction of a continuous flow of solution through the protein bed. At the same time, the concentration is measured continuously via UV absorption using a standard laboratory UV spectrophotometer and recorded with digital data-acquisition and storage. Equilibration times can be reduced to as little as 20 minutes and the fact that equilibration has been achieved is immediately apparent when viewing the data acquired – in real time and without sampling.

The set-up is illustrated in Figure 1. A standard chromatography column is used to contain the particle suspension which is confined within the column by means of two sintered glass frits. The position of the frits can be adjusted in order to accommodate a variable slurry volume. A length of small diameter tubing is connected to either end of the column and the circuit is closed by inserting a flow-through cuvette between the opposing ends of that tubing. A peristaltic pump is used to transport the solution through the protein reservoir and the flow through-cuvette, which is inserted into a standard laboratory UV photo-spectrometer. An auxiliary circuit containing a second column is coupled to the main system using three-way valves. This circuit is employed both to fill the system with protein solution and to remove any air bubbles introduced during filling, as these may facilitate undesired denaturing of the protein in solution at the air-liquid interface. The auxiliary circuit is de-coupled from the main system during solubility measurements.

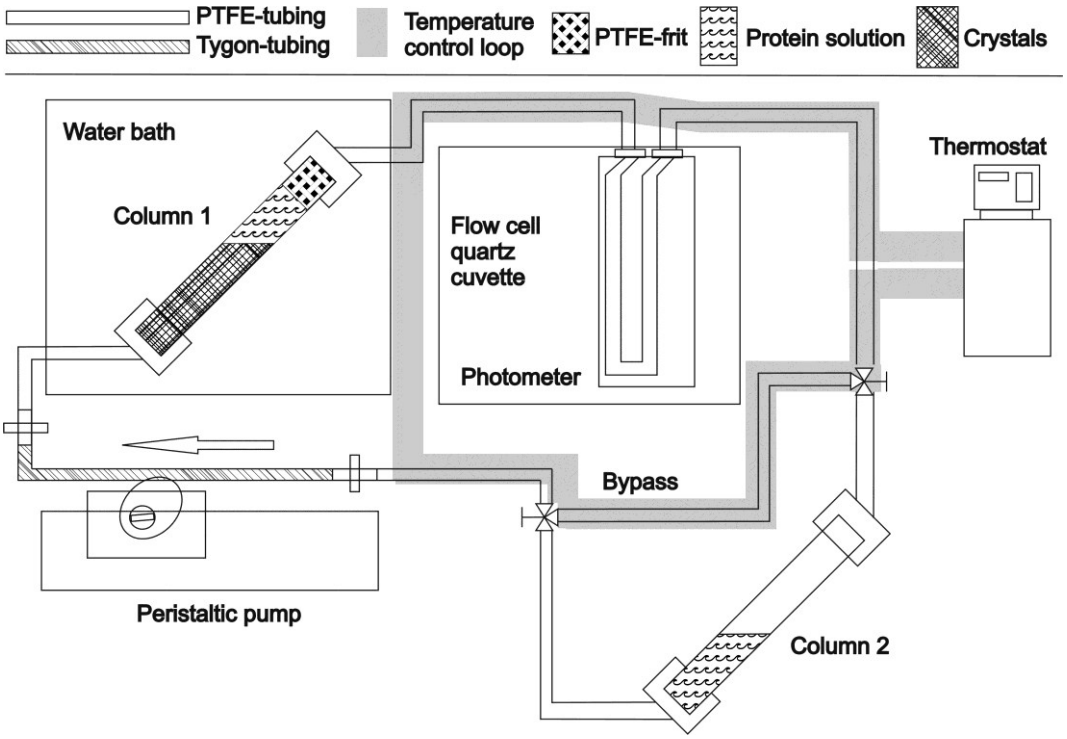

Figure 1: Apparatus for continuous, real-time concentration measurements in protein solutions (Weber 2005). The water bath controls the temperature of the crystal bed in contact with the solution, which is pumped into the measuring chamber of the UV-Vis photometer by the peristaltic pump. The concentration range accessible in the measurement can be adjusted using cuvettes of different optical path lengths.

The column containing the protein slurry reservoir is placed into a thermal bath where the temperature is controlled. Those sections of tubing not contained within the thermal bath are conveniently insulated to prevent any crystal nucleation due to large temperature differences between the bath and the environment. At the same time, their length is kept to a minimum and is limited only by the distance required to connect the column to the cuvette. The total volume in the system is of the order of 2 – 5 mL and is largely determined by the volume of the column.

This set-up allows rapid equilibration when approaching the solubility from an undersaturated solution, whereas equilibration times were considerably longer when approaching from a supersaturated solution. Clearly the kinetics of dissolution and crystal growth are different for the protein investigated (various lysozyme modifications, see discussion in chapter 2.4). Validation experiments showed that equilibration times were of the order of 20 – 90 minutes (from undersaturated solution) and depended somewhat on the nature of the crystal slurry employed, though exact factors contributing to this variation were never identified. Nucleation of crystalline protein outside of the reservoir column was only rarely observed, a much greater problem was the formation of insoluble proteinaceous plaques in the tubing, possibly due to mechanical stress provided by the pump and leading to denaturing of the protein or denaturing of the protein at a liquid-gas interface. However, plaque formation was usually only observed after several days of operation using one and the same crystal bed and is easily overcome by careful cleaning of the column and replacement of the crystal bed and the connecting tubing.

Once equilibrium has been reached, as evidenced by a constant UV-absorbance, the temperature in the thermal bath can be increased or decreased in order to obtain further solubility data points at otherwise identical solution composition. In order to obtain solubility data for additional solution compositions (change of pH, buffer-type, buffer concentration and precipitant concentration) the solution has to be exchanged, conveniently changing the crystal reservoir to one generated under similar composition conditions at the same time. This avoids the need for extensive washing of the crystal bed with the new solution and any risk that the composition with respect to the non-protein components differs from the nominal composition due to incomplete elution of the solution previously under investigation.

Using this approach, the solubility of several crystal modifications of lysozyme was determined over a range of conditions (Aldabaibeh 2009) as discussed in chapter 2.4 below.

2.2 Solubility of Selected Proteins - Compilation of Literature Data

Table 2 provides an overview of proteins for which solubility data have been published. The table provides information the protein studied and the literature source and where available, the source organism for the protein and the method of equilibration. The method of concentration measurement is omitted as this would make the table unwieldy. The majority of authors employ UV photometry for the determination of concentration, either directly or via a colorimetric assay, though other techniques such as interferometry, scintillation measurements and even direct observation of cessation of growth or dissolution can be encountered. Older literature frequently employs the determination of total nitrogen content via the Kjeldal method as a means of quantifying protein concentration. The method of equilibration differentiates between vapour diffusion from hanging drops/sitting drops, batch methods, the column method developed by Pusey and Gernert (Pusey 1988) discussed above, the continuous flow through method developed by Weber *et al.* (Weber 2005) and other approaches requiring dedicated equipment. The batch methods incorporate a range of

different approaches at different experimental scales and include turbidity-based detection methods that do not strictly measure an equilibrium concentration (see chapter 2.7). While it can certainly be argued that the column method is also a type of batch equilibration, it is sufficiently distinct from the other batch methods to merit a separate classification.

Table 2: Overview of published solubility data. The methods used for solubility determination refers only to the equilibration method, analytical methods applied can be found in the cited papers. 1: vapour diffusion (hanging drop/sitting drop); 2: (micro-)batch; 3: static bed column; 4: flow-through crystal bed; 5: dedicated sample cells (high pressure studies, interferometry). This compilation lays no claim to completeness.

Protein	**Source organism**	**Method**	**Literature reference**
Lysozyme	*gallus gallus* (hen egg white)	1	(Riès-Kautt 1989, Guilloteau 1992, Skouri 1995, Vaney 2001)
		2	(Cole 1969, Ataka 1988, Howard 1988, Guilloteau 1992, Shih 1992, Rosenberger 1993, Chin 1994, Broutin 1995, Coen 1995, Coen 1997, Gripon 1997, Retailleau 1997, Moretti 2000, Haire 2001, Benas 2002, Legrand 2002, Retailleau 2002, Lu 2003, Annunziata 2008, Lu 2011, Wang 2011, Maosoongnern 2012)
		3	(Pusey 1988, Cacioppo 1991a, Cacioppo 1991b, Ewing 1994, Forsythe 1996, Forsythe 1999a, Forsythe 1999b)
		4	(Weber 2005, Aldabaibeh 2009)
		5	(Suzuki 2000, Gray 2001, Nakazato 2004, Van Driessche 2009, Suzuki 2011)
Ovalbumin	*Gallus gallus* (hen egg white)	2	(Judge 1996, Dumetz 2008, Dumetz 2009)
Haemoglobin	*Equus ferus caballus* (horse)	2	(Landsteiner 1923, Green 1931a, Green 1931b, Green 1932, Green 1935)
	Homo sapiens sapiens (human)	5	(Feeling-Taylor 1999)
	Canis lupus familiaris (dog)	2	(Landsteiner 1923)
Human γ-Globulin	*homo sapiens sapiens* (human)	-	(Galeotti 1906)
Ribonuclease A	*Bos primigenius* (cattle)	2	(Dumetz 2008, Dumetz 2009)
β-lactoglobulin	*Bos primigenius* (cattle)	2	(Dumetz 2008)
Insulin	*Bos primigenius* (cattle)	2	(Lens 1946)

Protein	Source organism	Method	Literature reference
Insulin	*Not specified*	2	(Widmark 1923, Schwert 1950)
	sus scrofa (pig)	-	(Bergeron 2003)
Chymotrypsin Chymotrypsinogen	*Bos primigenius* (cattle) (Kunitz: not specified)	2	(Kunitz 1938, Kubacki 1949, Deshpande 1989, Przybycien 1989, Lu 2003)
Casein	*Bos primigenius* (cattle)	-	(Cohn 1922, Cohn 1923)
Bovine pancreatic trypsin inhibitor	*Bos primigenius* (cattle)	2	(Lafont 1994, Lafont 1997, Budayova-Spano 2000, Veesler 2004)
Edestin	*Cannabis sativa* (hemp)	2	(Osborne 1905, Kodama 1922)
Collagenase	*Hypoderma lineatum* (gad fly)	1	(Carbonnaux 1995)
Pea protein hydrolysates	*Pisum sativum* (garden pea)	-	(Soral-Smietana 1998)
Xylose isomerase	Sleutel, Vuolanto: *Streptomyces rubiginosus* Chayen: *Arthrobacter strain B3728*	1, 2	(Chayen 1988, Vuolanto 2003, Sleutel 2009)
Concanavalin A	*canavalia ensiformis* (jack bean)	1, 2, 3	(Mikol 1989a, Cacioppo 1992, Moré 1995, Kashimoto 1998)
Canavalin	*canavalia ensiformis* (jack bean)	1	(DeMattei 1991)
α-Amylase	*Sus scrofa* (pig)	2	(Boistelle 1992)
β-Amylase	*Hordeum vulgare* (barley)	2	(Visuri 1972)
Taka-amylase	*Aspergillus oryzae*	1	(Ninomiya 2001)
Zein	*Zea mays* (maize)	-	(Cohn 1924)
Thaumatin	*Thaumatococcus daniellii* (katemfe)	5	(Malkin 1996, Juarez-Martinez 2001)
Endoglucanase A	*Clostridium Cellulolyticum*	2	(Budayova 1999)
Subtilisin	*Bacillus lentus*	2	(Pan 2002)
Asparaginase II	Recombinant *Escherichia coli*	2	(Liu 2014)

2.3 Crystal Modifications of Lysozyme

The following discussion focuses upon the solubility of various lysozyme modifications in order to highlight the progress made in determining protein solid-liquid phase-diagrams in recent years.

At least eight crystal modifications of hen egg white lysozyme are known for which crystal structures have been reported (see Table 3, some of the structures are illustrated in Figure 2). These are the tetragonal, high temperature orthorhombic (HTO), low temperature orthorhombic (LTO), two monoclinic, two triclinic and a hexagonal modification. The first three are related as they are all modifications of lysozyme chloride, *i.e.*, can be crystallized with chloride counter ions using sodium chloride as precipitating agent (Jolles 1972, Artymiuk 1982, Oki 1999, Sukumar 1999, Biswal 2000). In addition, the work of Jolles and Berthou (Jolles 1972) demonstrated that a pathway for transition exists between tetragonal and high temperature orthorhombic lysozyme and that this transition can be effected simply by heating a slurry of tetragonal lysozyme chloride above 25 °C. In a second paper Jolles and Berthou also identified the low temperature orthorhombic modification (Berthou 1974).

Of these three modifications, tetragonal lysozyme chloride is by far the best studied, perhaps due to the relative ease with which it can be crystallized (McPherson 1999). The modifications belonging to the remaining three crystal classes represent more than just three modifications and are not related to the first group since they generally require different anions to crystallize and are therefore chemically distinct. Steinrauf (Steinrauf 1959) was the first to investigate monoclinic and triclinic crystal modifications of lysozyme. He reported the unit cells of monoclinic lysozyme nitrate, iodide and sulfate. Despite the striking similarity of the unit cells, these three solids must be regarded as distinct but isostructural modifications of the respective lysozyme salts (for a more detailed discussion see, for example, Jones and Ulrich (Jones 2010)) due to the differences in chemical composition. The triclinic modification described in Steinrauf's paper is also obtained as a nitrate salt. Although Steinrauf was not able to solve the structures, later work (Madhusudan 1993, Walsh 1998) confirmed the presence of nitrate ions in both monoclinic and triclinic lysozyme nitrate, sulfate ions in monoclinic lysozyme sulfate (Majeed 2003), which, in addition to the chemical difference, crystallizes in a different space group when compared to the nitrate salt, and iodide ions in the structure of lysozyme iodide (Steinrauf 1998). The structure of hexagonal lysozyme nitrate was solved by Brinkmann *et al.* (Brinkmann 2006) and additional salts of lysozyme and their crystal structures have been reported (Lim 1998, Vaney 2001). To complicate matters further, both monoclinic and triclinic lysozyme nitrate have two known and distinct crystal modifications (Madhusudan 1993, Nagendra 1995, Nagendra 1996, Harata 2004). In both cases the two modifications differ in their water content and the high-humidity structure can be converted into the low-humidity variant by dehydration (Madhusudan 1993, Harata 2004, Harata 2006). Finally, a monoclinic lysozyme chloride has been reported (Harata 1994), suggesting that the two groups defined above are not wholly unrelated. It must be noted, though, that this modification was only obtained in the presence of 1-propanol.

Table 3: Overview of crystal modifications of hen egg white lysozyme with known crystal structures. Data were obtained from the RCSB Protein Data Bank (Berman 2000), the PDB reference is that used in the data bank.

Crystal Class	**Space Group**	**Counter Ion**	**Lattice Parameters**	**PDB reference**	**Resolution**	**Authors**
Hexagonal	$P\,6_122$	Nitrate	$a = b = 85.64$ Å, $c = 67.93$ Å, $\alpha = \beta = 90$ °, $\gamma = 120$ °	1FBB	1.46 Å	(Brinkmann 2006)
Tetragonal	$P4_32_12$	Chloride	$a = b = 78.54$, $c = 37.77$ Å, $\alpha = \beta = \gamma = 90$ °	197L	1.33 Å	(Vaney 1996)
Orthorhombic I (LTO)	$P2_12_12_1$	Chloride	$a = 30.50$ Å, $b = 55.39$ Å, $c = 68.85$ Å, $\alpha = \beta = \gamma = 90$ °	1HSW	1.9 Å	(Sukumar 1999)
Orthorhombic I (LTO)	$P2_12_12_1$	Chloride	$a = 59.06$ Å, $b = 68.45$ Å, $c = 30.52$ Å, $\alpha = \beta = \gamma = 90$ °	1AKI	1.5 Å	(Artymiuk 1982)
Orthorhombic II (HTO)	$P2_12_12_1$	Chloride	$a = 56.44$ Å, $b = 73.73$ Å, $c = 30.43$ Å, $\alpha = \beta = \gamma = 90$ °	1BGI	1.7 Å	(Oki 1999)
Monoclinic (high humidity)	$P2_1$	Nitrate	$a = 27.94$ Å, $b = 62.73$ Å, $c = 60.25$ Å, $\alpha = \gamma = 90$ °, $\beta = 90.76$ °	1HF4	1.45 Å	(Vaney 2001)
Monoclinic (low humidity)	$P2_1$	Nitrate	$a = 26.90$ Å, $b = 68.95$ Å, $c = 31.33$ Å, $\alpha = \gamma = 90$ °, $\beta = 111.93$ °	1LMA	1.75 Å	(Madhusudan 1993)
Monoclinic	$P2_1$	Chloride	$a = 27.23$ Å, $b = 63.66$ Å, $c = 59.12$ Å, $\alpha = \gamma = 90$ °, $\beta = 92.90$ °	1LYS	1.72 Å	(Harata 1994)
Triclinic (high humidity)	P 1	Nitrate	$a = 25.93$ Å, $b = 39.97$ Å, $c = 42.39$ Å, $\alpha = 88.00$ °, $\beta = 95.44$ °, $\gamma = 90.58$ °	1V7T	1.13 Å	(Harata 2004)
Triclinic (low humidity)	P 1	Nitrate	$a = 27.23$ Å, $b = 31.97$ Å, $c = 34.27$ Å, $\alpha = 88.44$ °, $\beta = 108.62$ °, $\gamma = 111.71$ °	1V7S	1.14 Å	(Harata 2004)

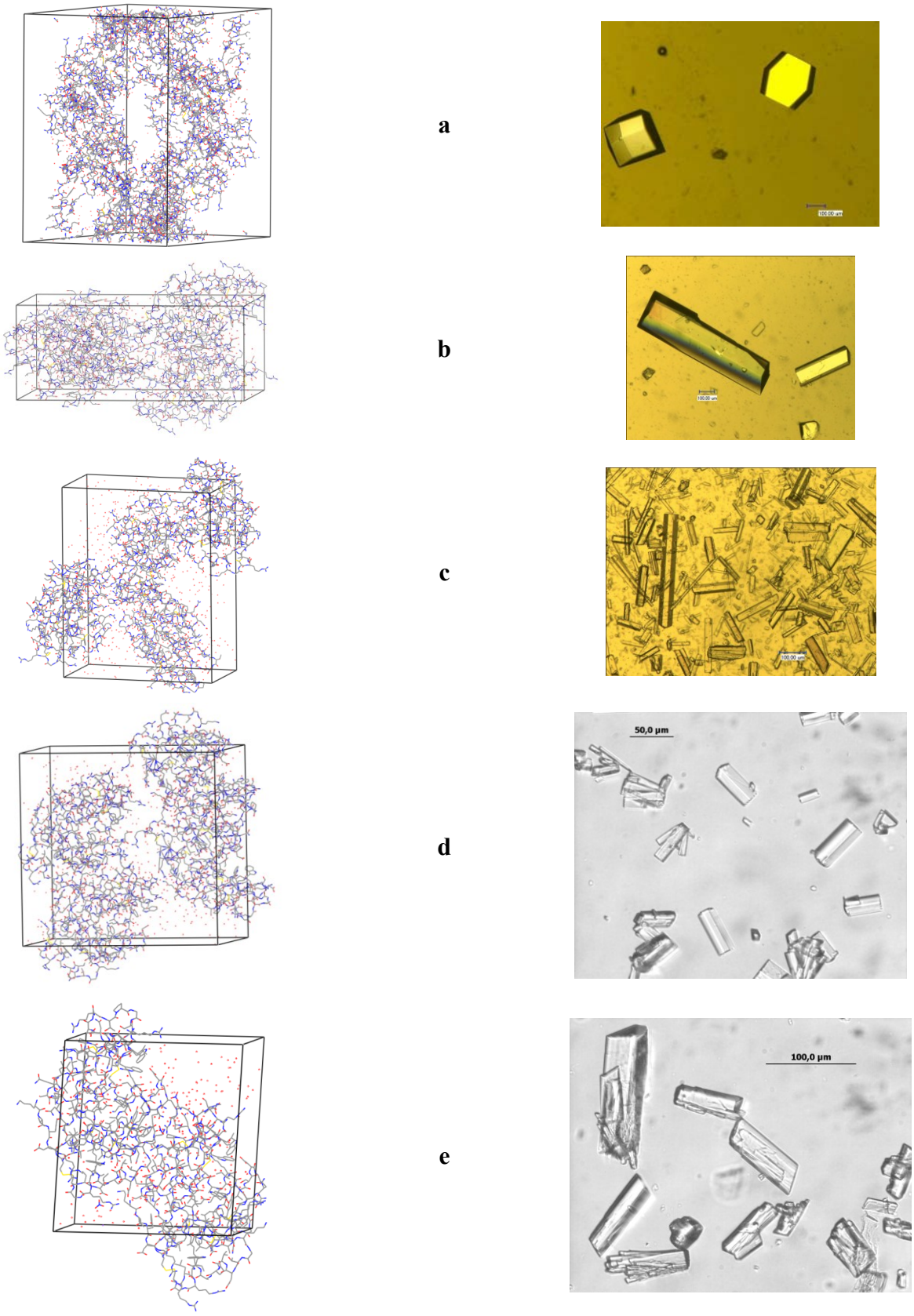

Figure 2: Crystal structure and optical microscope images for selected lysozyme crystal modifications. a: tetragonal, b: high temperature orthorhombic, c: low temperature orthorhombic, d: monoclinic, e: triclinic. Hydrogen atoms are omitted from the crystal structures for reasons of clarity. The isolated red dots in the crystal structures represent oxygen atoms from water.

While Harata's analysis and discussion of his diffraction data does not reveal the presence of the alcohol in the crystal structure, his inability to crystallize a monoclinic lysozyme in the absence of 1-propanol can be taken as a strong indication that the organic solvent is essential to stabilise the structure. Furthermore, Berthou and Jolles (Berthou 1978) discussed a transition of monoclinic lysozyme nitrate to an orthorhombic modification that strongly resembles the high temperature chloride. This observation suggests that the anion has a subtle but important role in steering the solid modification. Clearly, hen egg white lysozyme has a rich phase space where the chemical composition of the system is essential in defining the solid modifications that may be obtained under given conditions of crystallization. Despite this, solubility has been investigated for only a very limited part of this phase space.

2.4 Solubility of Lysozyme Chloride

The solubility of tetragonal lysozyme chloride has been studied extensively as evidenced by the significant number of literature references in Table 2. The first major investigation was conducted by Howard *et al.* (Howard 1988), who studied the temperature dependence of lysozyme solubility over a range of pH values covering $4 \leq \mathrm{pH} \leq 7.5$. In the range $4 \leq \mathrm{pH} \leq 5.5$ a sodium acetate buffer was used, a sodium phosphate buffer was employed in the higher pH range. Both buffer concentrations were 0.05 M. Salt concentrations were between 1.5 %(w/v) and 10 %(w/v), equivalent to $0.257 \text{ mol } L^{-1} \leq c_{salt} \leq 1.711 \text{ mol } L^{-1}$. The equilibration method used was a microbatch method starting from a clear solution and allowing the system to nucleate and thereafter reach equilibrium. No agitation was applied and the samples were sampled after 4 weeks with further sampling after 6 weeks and, in some cases, again after 11 weeks.

The first sampling point was selected based upon preliminary experiments and no changes to solution concentrations were observed at the later sampling points. The crystal modification of the solid phase was checked using X-ray diffraction and the protein concentration in the supernatant was determined by UV-photometry.

The solubility data reported in this paper is given in mg protein mL^{-1} solution and is of low precision (one decimal). Plotting the data as solubility versus salt concentration at constant temperature (Figure 3) shows that the solubility is strongly dependent upon the salt concentration at low pH, decreasing rapidly with increasing sodium chloride concentration, and while this behaviour is still apparent at higher pH, the effect is markedly less pronounced. This qualitative behaviour is consistent with 'inverse Hofmeister series behaviour' (Riès-Kautt 1991, Zhang 2009) expected for a basic protein. In addition to decreasing sensitivity of the lysozyme solubility to salt concentration with increasing pH, the solubility also appears to become less temperature dependent as both the salt concentration and the pH increase.

Figure 4 shows the solubility of lysozyme chloride against the temperature for a range of salt concentrations at fixed pH. Again, the strong dependence on the salt concentration is apparent. Interestingly, the solubility increases at low temperature and appears to have a maximum at around 20 °C, decreasing thereafter. The authors only briefly discuss this

behaviour in terms of a transition to a different solid modification as previously reported by (Jolles 1972) and stress the thermodynamic significance of the change in slope of the solubility curve.

This maximum solubility is also clearly observable in the plot of solubility vs. temperature (Figure 5) for a salt concentration of 1.5 % NaCl and variable pH, though only at low pH. At higher pH the solubility appears to have a considerably less pronounced maximum.

A considerably more comprehensive study of tetragonal lysozyme chloride solubility was carried out over a period of more than a decade by the Pusey group (Pusey 1988, Cacioppo 1991a, Cacioppo 1991b, Forsythe 1996, Forsythe 1999a) using the column method published in 1988 (Pusey 1988) culminating in the publication of a densely sampled data set (Forsythe 1999a) covering the pH range from 4.0 to 5.4, the temperature range from 1 to 30 °C and sodium chloride concentrations from 1.5 %(w/v) to 7 %(w/v) using a 0.1 molar sodium acetate buffer. Figure 6 presents a small selection of data from that publication.

The temperature range covered in these investigations was between 0 °C and 30 °C and the pH range studied was $4.0 \leq pH \leq 5.4$. Salt concentrations varied from 1 % to 7 % and a 0.1 molar acetate buffer was employed in the majority of studies. The results show clearly, that protein solubility behaves in a similar manner when compared to the majority of small molecule organic compounds, in that the solubility increases with temperature. The behaviour of the solubility as a function of the precipitant concentration is also as expected and decreases with increasing salt concentration. With regard to pH, the interpretation of some of the data is not straight-forward as oscillations were observed within small pH intervals (see, for example, Figure 3 in (Cacioppo 1991b)), although overall the expected trend of a solubility decrease as the pH approaches the pI (the pH at which the protein exhibits overall charge neutrality) is seen. Interestingly, the solubility appears to have a minimum for an acetate buffer concentration of 1 M. In (Forsythe 1996), the dependence of the solubility is reported as a function of acetate buffer concentrations between 0.01 M and 0.5 M and as a function of salt concentration and temperature. Irrespective of the precipitant concentration investigated, the solubility initially decreases with increasing buffer concentration and reaches a minimum at 0.1 M, after which the solubility begins to increase before decreasing again at the higher buffer concentrations employed. The authors offer only speculative explanations for the underlying phenomena leading to this observation, citing competition between chloride and acetate ions interacting with basic sites on the protein molecule and, at the higher buffer concentrations, acetate itself acting as a suitable precipitant for the protein. Despite the fact that this issue has not been satisfactorily resolved, it is important to highlight the mere fact that the buffer salt also influences the solubility of a protein.

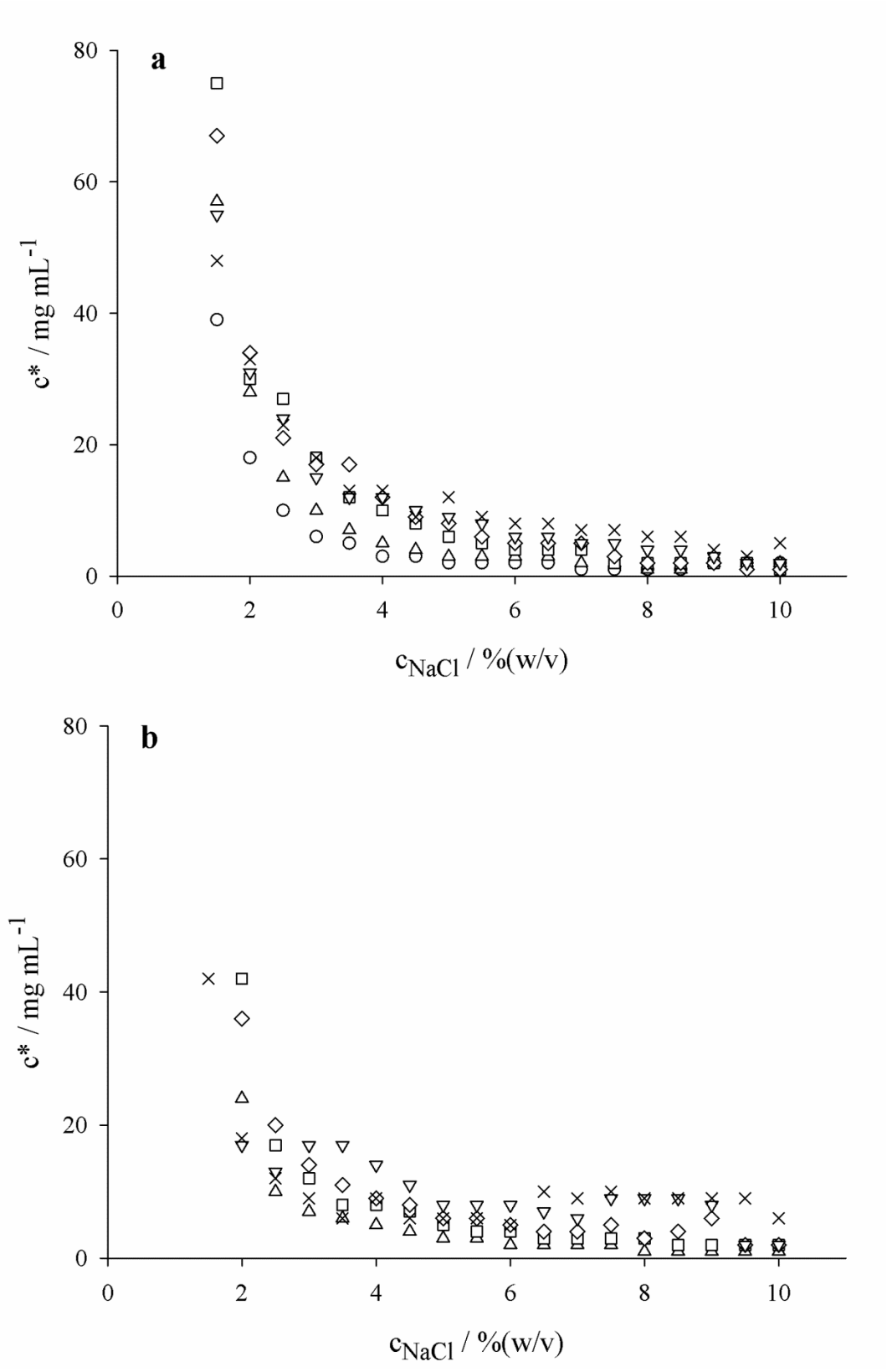
a
b
c* / mg mL-1
cNaCl / %(w/v)
0
20
40
60
80
0
2
4
6
8
10

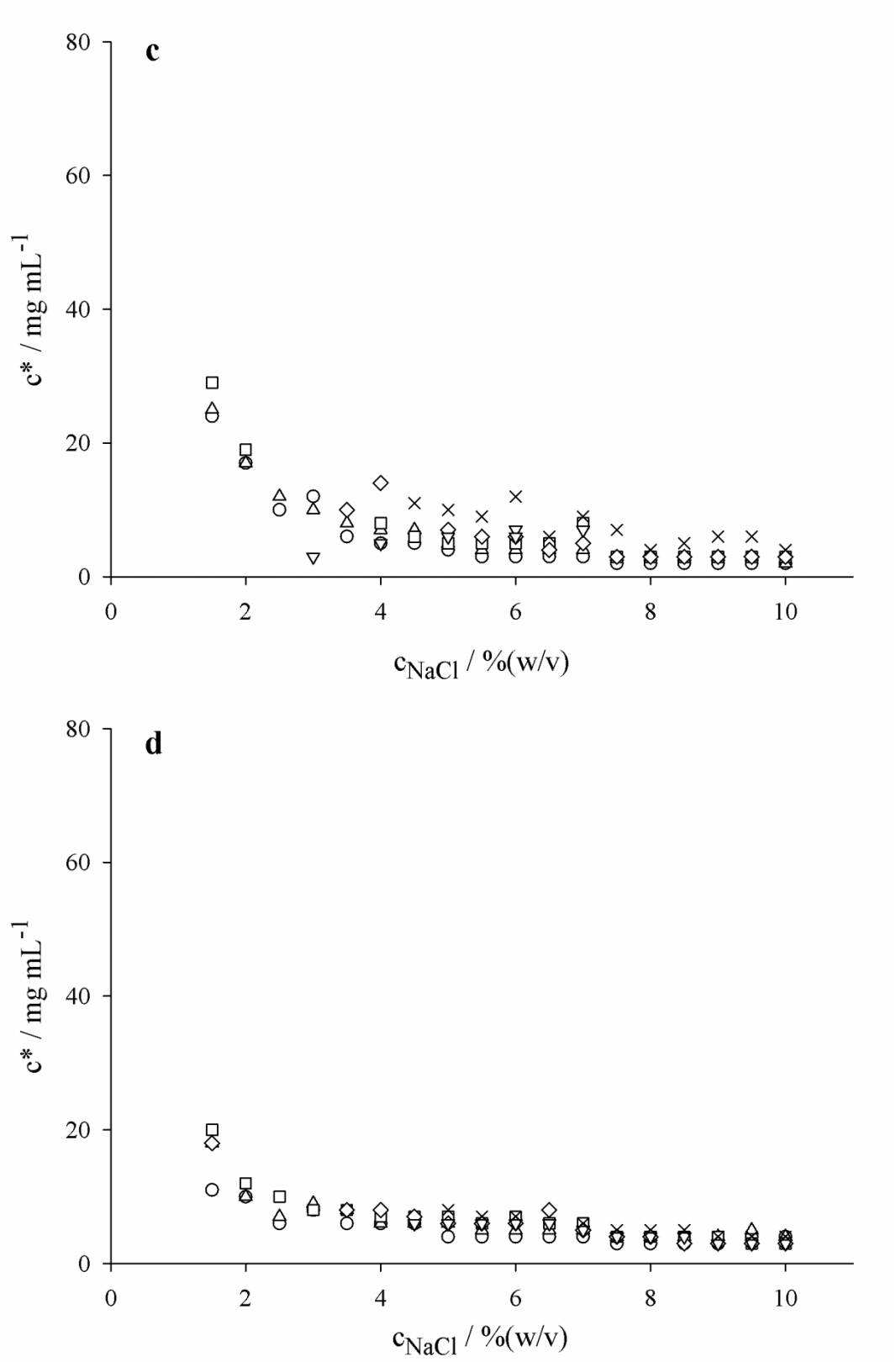

Figure 3: Solubility of lysozyme chloride as a function of NaCl concentration at constant pH and variable temperature according to Howard *et al.* (Howard 1988). a: pH = 4.0, b: pH = 5.0, c: pH = 6.0, d: pH = 7.0. The symbols represent ○ T = 10 °C, Δ T = 15 °C, □ T = 20 °C, ◊ T = 25 °C, ∇ T = 30 °C, × T = 40 °C. The solubility decreases significantly with increasing pH, while the temperature dependence becomes weaker. At high pH the solubility is less sensitive to the salt concentration of the solution than at low pH.

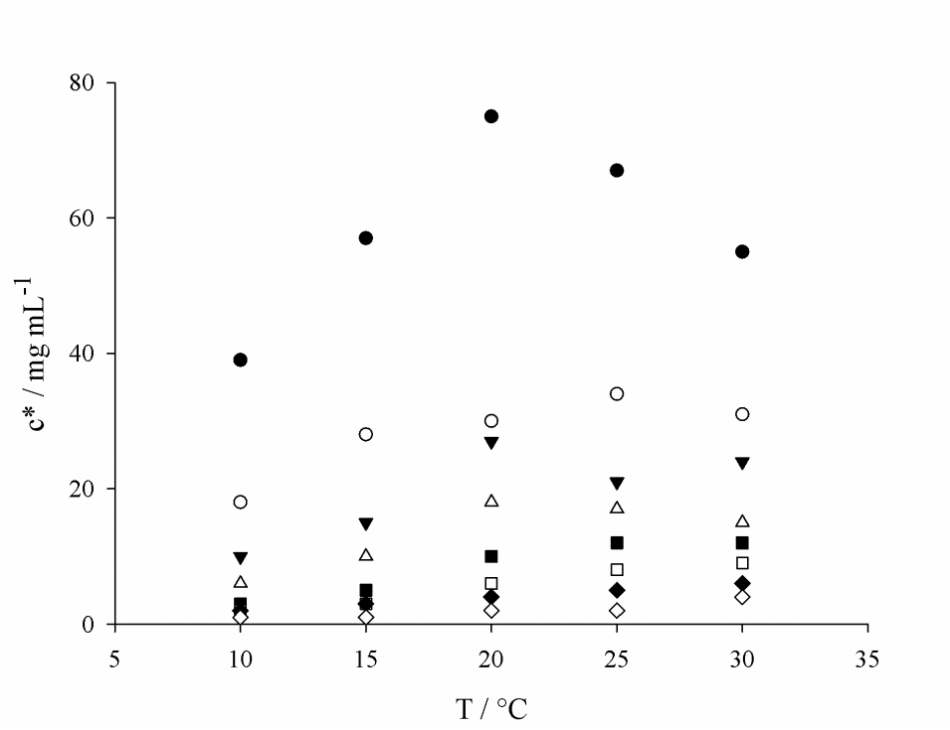

Figure 4: Solubility of lysozyme chloride as a function of temperature for different salt concentrations at constant pH = 4 (Howard 1988). The respective NaCl concentrations are: ● 1.5 %(w/v), ○ 2.0 %(w/v), ▼ 2.5 %(w/v), ∆ 3.0 %(w/v), ■ 4.0 %(w/v), □ 5.0 %(w/v), ♦ 6.0 %(w/v), and ◊ 8.0 %(w/v). The maximum in solubility and subsequent decrease observed around 20 °C for low salt concentrations was ascribed to a change in crystal modification crystallized.

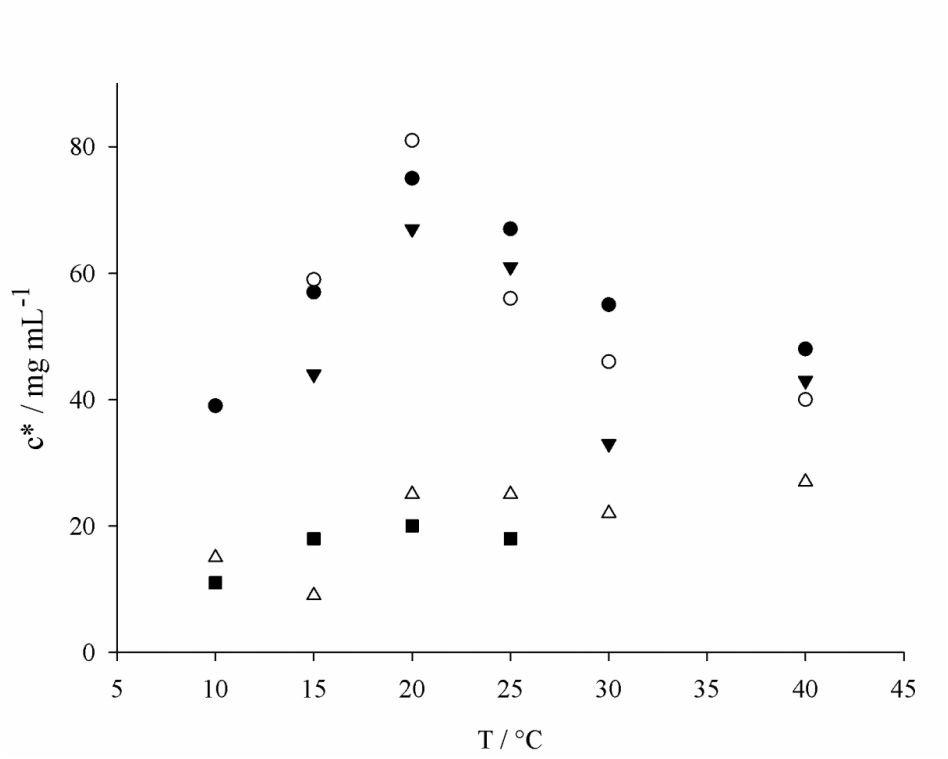

Figure 5: Solubility of lysozyme chloride as a function of temperature for different pH values at constant salt concentration (1.5 %(w/v) (Howard 1988). As for the representation in Figure 4 above, at low pH the solubility initially increases with temperature and decreases after a maximum around 20 °C. ● pH = 4.0, ○ pH = 4.5, ▼ pH = 5.5, Δ pH = 6.5, ■ pH = 7.0.

The clear difference between the earlier Howard data (Howard 1988) and data presented by Forsythe *et al.* (Forsythe 1999a) is the extension of the temperature range accessible for the crystal modification studied. Since the column method requires the presence of a crystal bed with defined crystal modification and the solubility is measured rapidly compared to the micro-batch method applied by Howard *et al.* (Howard 1988), which relied upon nucleation of the crystalline phase from a clear but supersaturated solution, there is no ambiguity over the nature of the crystalline phase present and in equilibrium with the solution. This is evidenced by the absence of a maximum in solubility with subsequent decrease towards higher temperature in the data derived from the column method (Figure 6 and Figure 7).

Moreover, the solubility shows a monotonic increase with temperature consistent with an exponential temperature dependence as clearly shown by Cacioppo *et al.* (Cacioppo 1991a).

In addition to the difference in behaviour with regard to temperature, Figure 7 also shows that the solubility of lysozyme chloride also depends upon the concentration of the buffer used – while the data shown were generated at otherwise identical solution conditions, Howard *et al.* used a 0.05 M acetate buffer while Forsythe *et al.* employed a buffer at twice the concentration. Forsythe and Pusey (Forsythe 1996) noted the difficulty in comparing solubility data acquired under different solution conditions and also investigated the effect of buffer concentration upon lysozyme solubility.

Surprisingly, the results show that a minimum in solubility exists at a buffer concentration of 0.1 mol L^{-1} and that the solubility increases towards lower buffer concentrations and initially also towards higher buffer concentrations, where a maximum is reached at ca. 0.2 mol L^{-1}, after which a further increase in buffer concentration leads to a decrease in lysozyme solubility. These observations were shown to be independent of the sodium chloride concentration present. Forsythe and Pusey (Forsythe 1996) discussed their observations qualitatively and with reference to the Hofmeister series (see above), but no satisfactory quantitative explanation was provided.

Although some data published by the Pusey group (Cacioppo 1991a) also related to an orthorhombic crystal modification of lysozyme chloride, the main focus of the work was clearly upon tetragonal lysozyme chloride.

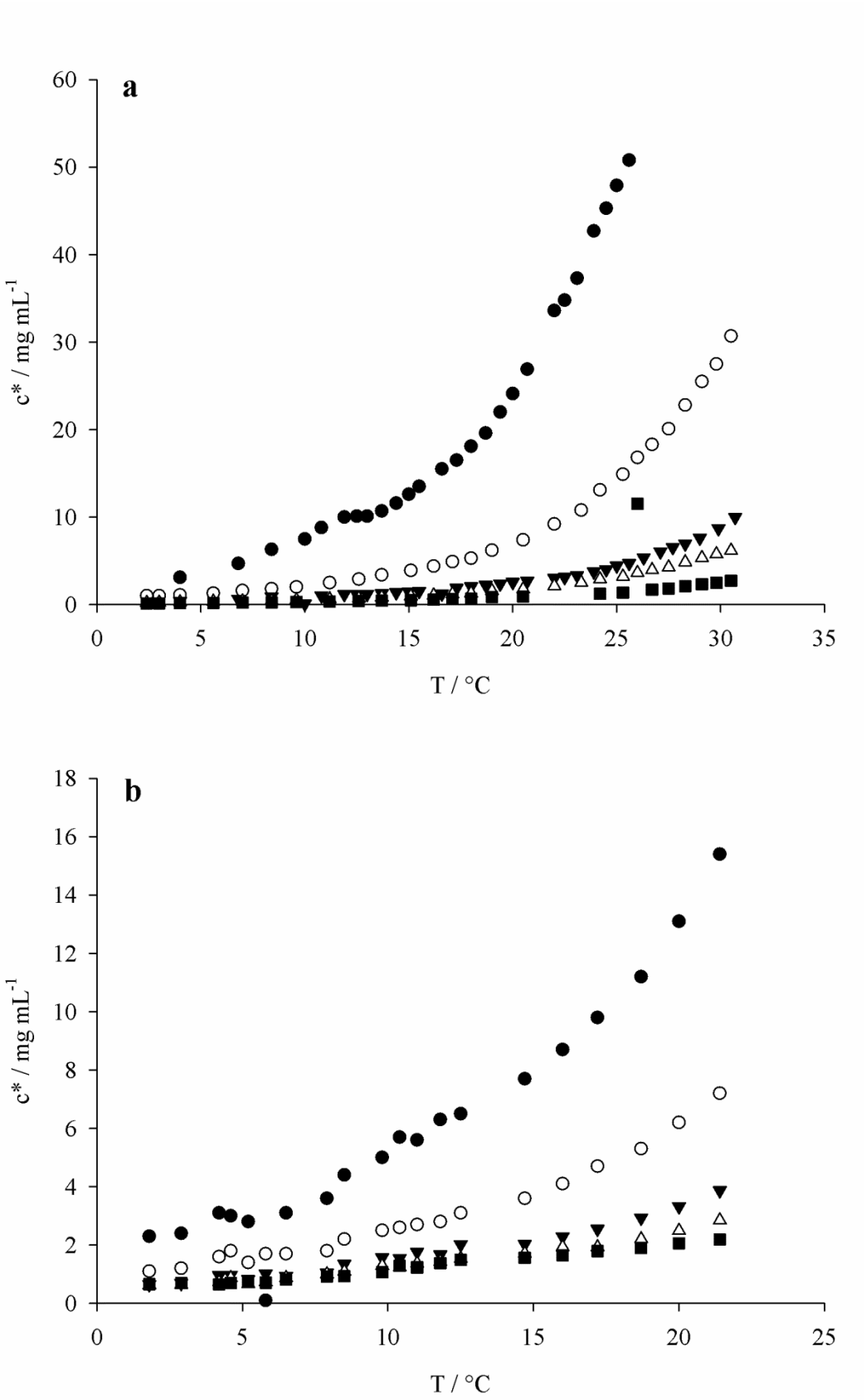

Figure 6: Solubility of lysozyme chloride as a function of temperature for different salt concentrations at constant pH. The data were measured by the static column method and are taken from Forsythe *et al.* (Forsythe 1999a). a) pH = 4.0, b) pH = 5.0. ● 2 %(w/v) NaCl, ○ 3 %(w/v) NaCl, ▼ 4 %(w/v) NaCl, Δ 5 %(w/v) NaCl, ■ 7 %(w/v) NaCl. The maximum in solubility previously reported by Howard *et al.* (Howard 1988) is absent.

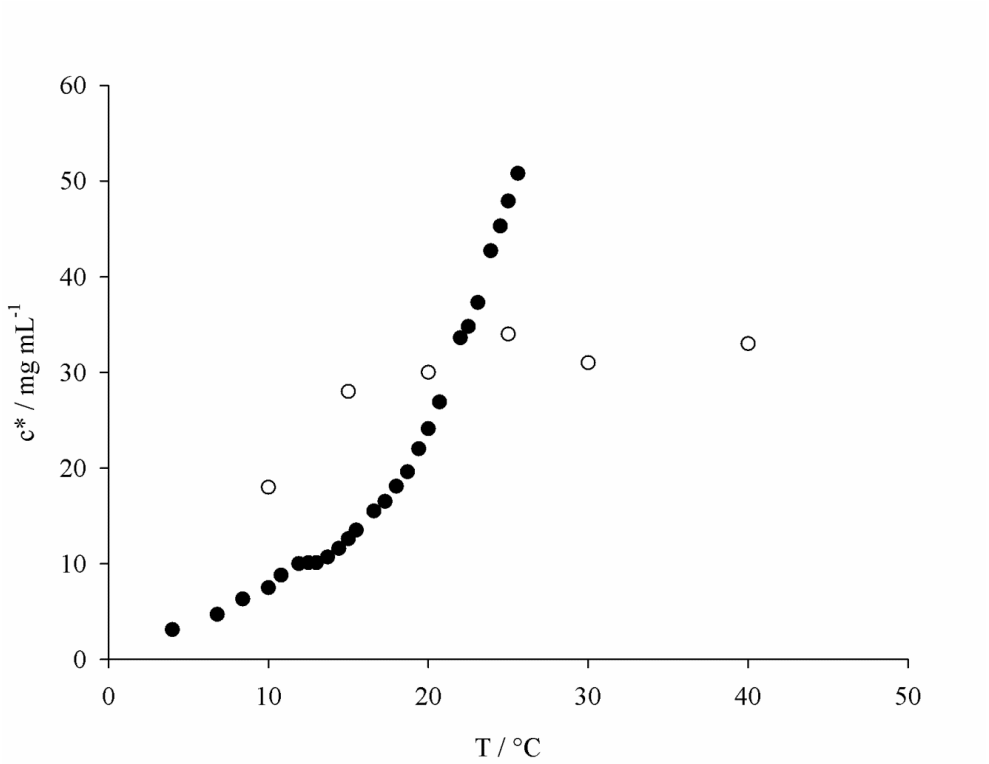

Figure 7: Comparison of lysozyme chloride solubility as a function of temperature measured under otherwise identical conditions (pH = 4.0, 2 %(w/v) NaCl) but differing in buffer concentration and equilibration method. ● 0.1 M sodium acetate buffer, static column method (Forsythe 1999a),○ 0.05 M sodium acetate buffer, microbatch equilibration (Howard 1988).

With the development of the rapid, automated equilibration and solubility measurement set-up by Weber *et al.* (Weber 2005), the new possibilities opened up by the speed of measurement were exploited to explore a wider range of phase space and to extend the phase diagram to other crystal modifications.

Extensive validation experiments reported by Weber *et al.* (Weber 2005) showed that equilibration times could be reduced to just under 20 minutes (*cf.* Figure 8) when approached from an undersaturated solution, whereas equilibration from a supersaturated solution required several hours. This behaviour has been reported previously (Pusey 1988), though the overall equilibration times were considerably longer with the static column method. A comparison of the validation data acquired using the flow through cell and literature data from (Forsythe 1999a) (Figure 9) shows the good agreement of both methods when applied for identical solution compositions.

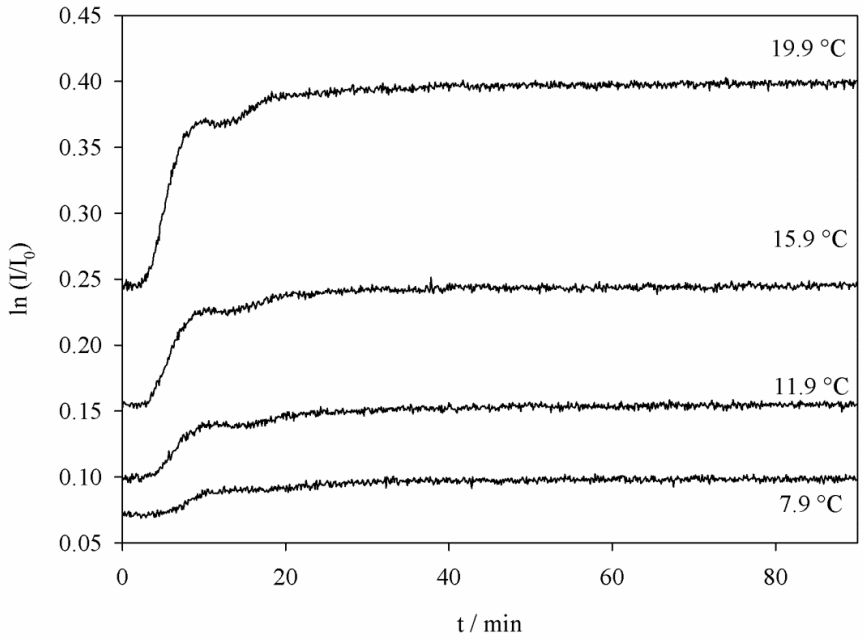

Figure 8: Typical UV-absorption traces as a function of equilibration time for lysozyme chloride solubility measurements using the flow-through cell in Figure 1 (Weber 2005). These traces represent a single, continuous measurement and the data have been separated for ease of comparison. The time t = 0 represents the time at which the respective temperatures were set. Equilibrium values are reached within 20 minutes for all temperatures.

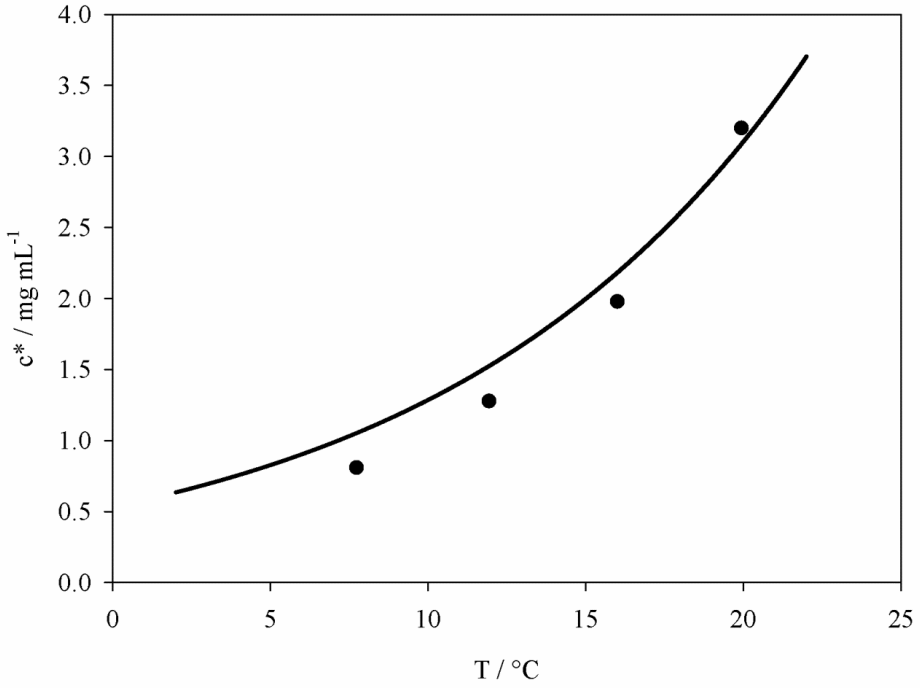

Figure 9: Comparison of lysozyme chloride solubility data obtained under otherwise identical conditions with ▬ the static column method (Forsythe 1999a) and ● the flow-through cell (Weber 2005) for a solution containing 4 %(w/v) sodium chloride at pH = 4.5.

The pH range studied for tetragonal lysozyme chloride could be extended to pH = 10 while the salt concentration was increased to 9 %(w/v) (Aldabaibeh 2010). Figure 10 shows data acquired at solution pH values of 5.7, 7.0 and 8.0 and salt concentrations from 2 %(w/v) to 9 %(w/v). While the general shape of the solubility curve resembles that observed previously by other researchers as described above, the data demonstrate that the solubility becomes increasingly insensitive to pH changes at high salt concentrations and almost overlap at the highest NaCl concentration employed. However, increasing the pH above a value of 8.0 (Figure 11) leads to behaviour of the solubility that is somewhat unexpected in view of the dictum that protein solubility is at its lowest close to the isoelectric point, namely an increase in solubility with increasing pH. While this observation is not entirely understood, it is important to point out that the tetragonal modification is not the stable crystal modification at high pH values, as will be discussed in the following.

The same range of solution salt concentrations and pH-values was employed in a study of the orthorhombic II, high temperature, modification of lysozyme chloride. At this point the focus will be on the pH range from $5.7 \leq pH \leq 8.0$ whereas the higher pH range will be discussed in the context of the comparison of the two orthorhombic solid phases below. Here, the temperature range accessible is limited by denaturing of the protein at higher temperature and the rate of phase transition to other crystal modifications (tetragonal or orthorhombic I, also called the low temperature orthorhombic phase) at lower temperature.

The upper useful limit in temperature was 40 °C for this modification, the lower limit was dependent upon the solution conditions, in particular the salt concentration in the solution. As Figure 12 shows, the solubility of the high temperature orthorhombic (HTO) modification of lysozyme chloride is clearly pH dependent for the three lower salt concentrations and decreases with increasing pH and salt concentration. As observed for the tetragonal modification at high salt concentration and $7.0 \leq pH \leq 8.0$, the pH dependence of the solubility is negligible at the highest salt concentration even for this modification.

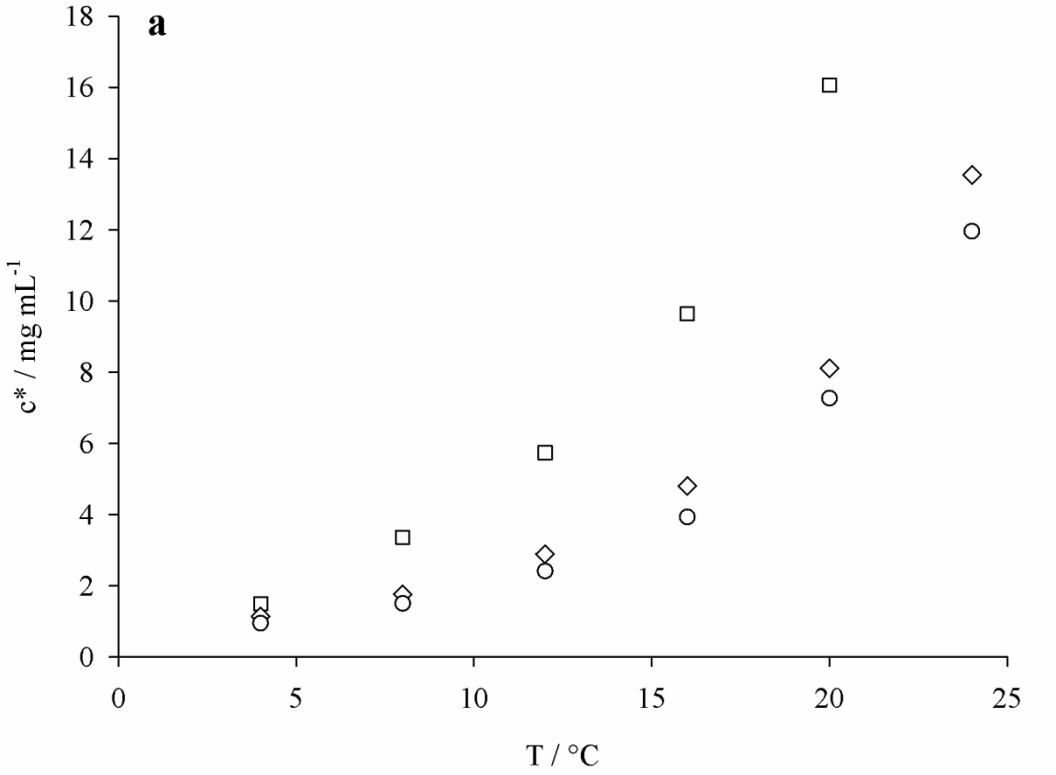
a
c* / mg mL-1
T / °C
0
2
4
6
8
10
12
14
16
18
0
5
10
15
20
25

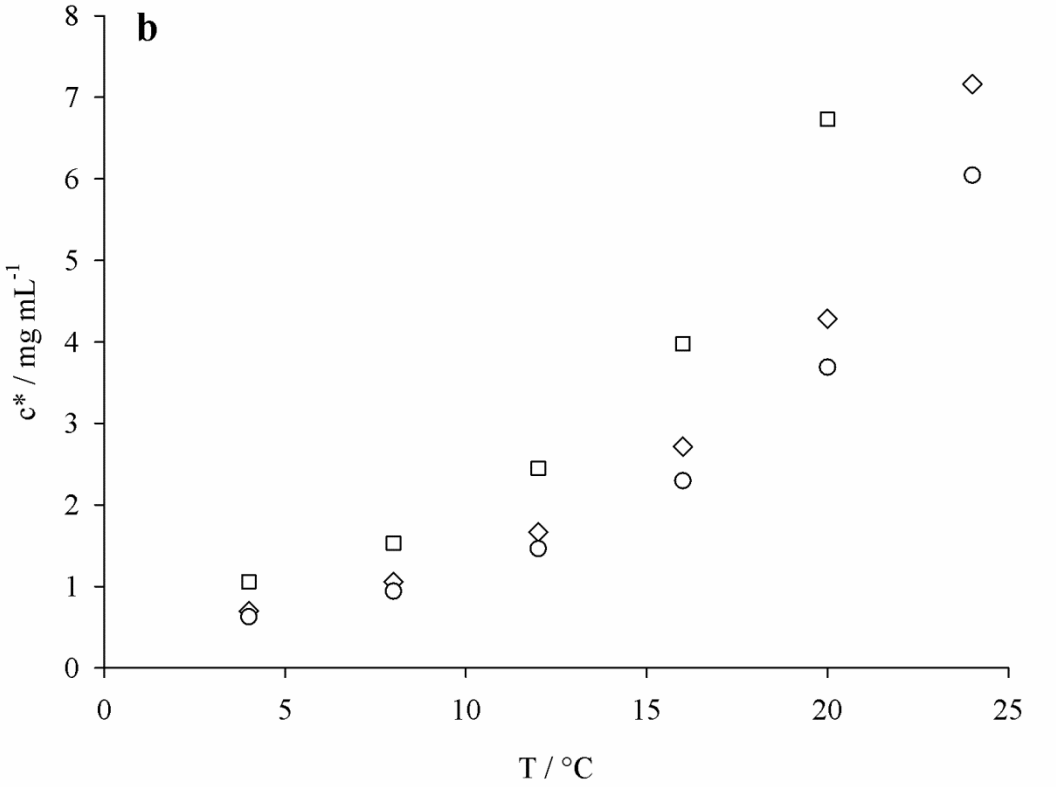
b
c* / mg mL-1
T / °C
0
1
2
3
4
5
6
7
8
0
5
10
15
20
25

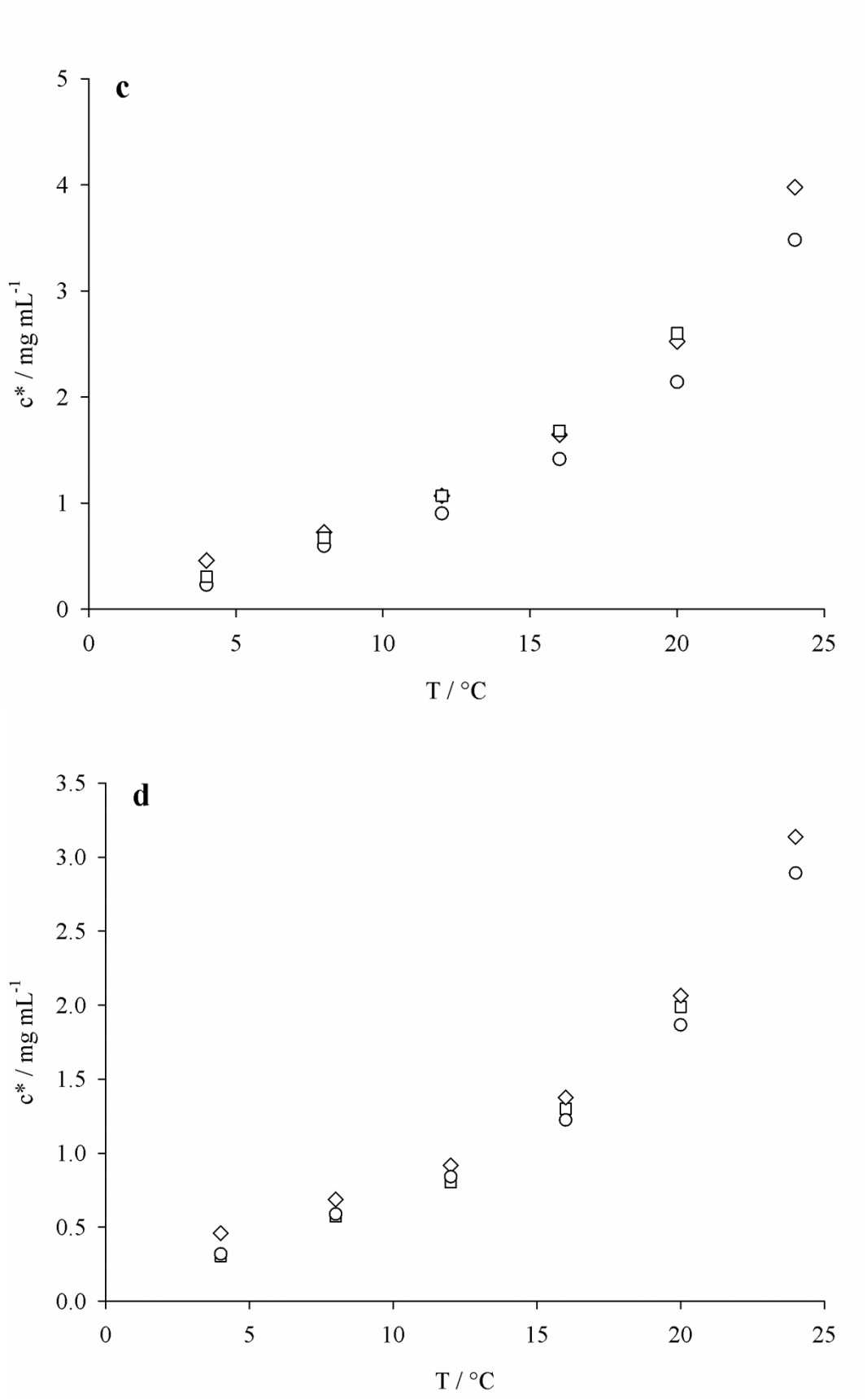

Figure 10: Solubility of tetragonal lysozyme chloride at 5.7 ≤ pH ≤ 8.0 for constant NaCl concentrations (Aldabaibeh 2009). a) 2 %(w/v) NaCl, b) 3 %(w/v) NaCl, c) 5 %(w/v) NaCl, d) 7 %(w/v) NaCl. ○ pH = 5.7, ◊ pH = 7.0, □ pH = 8.0. With increasing salt concentration the solubility becomes almost independent of pH.

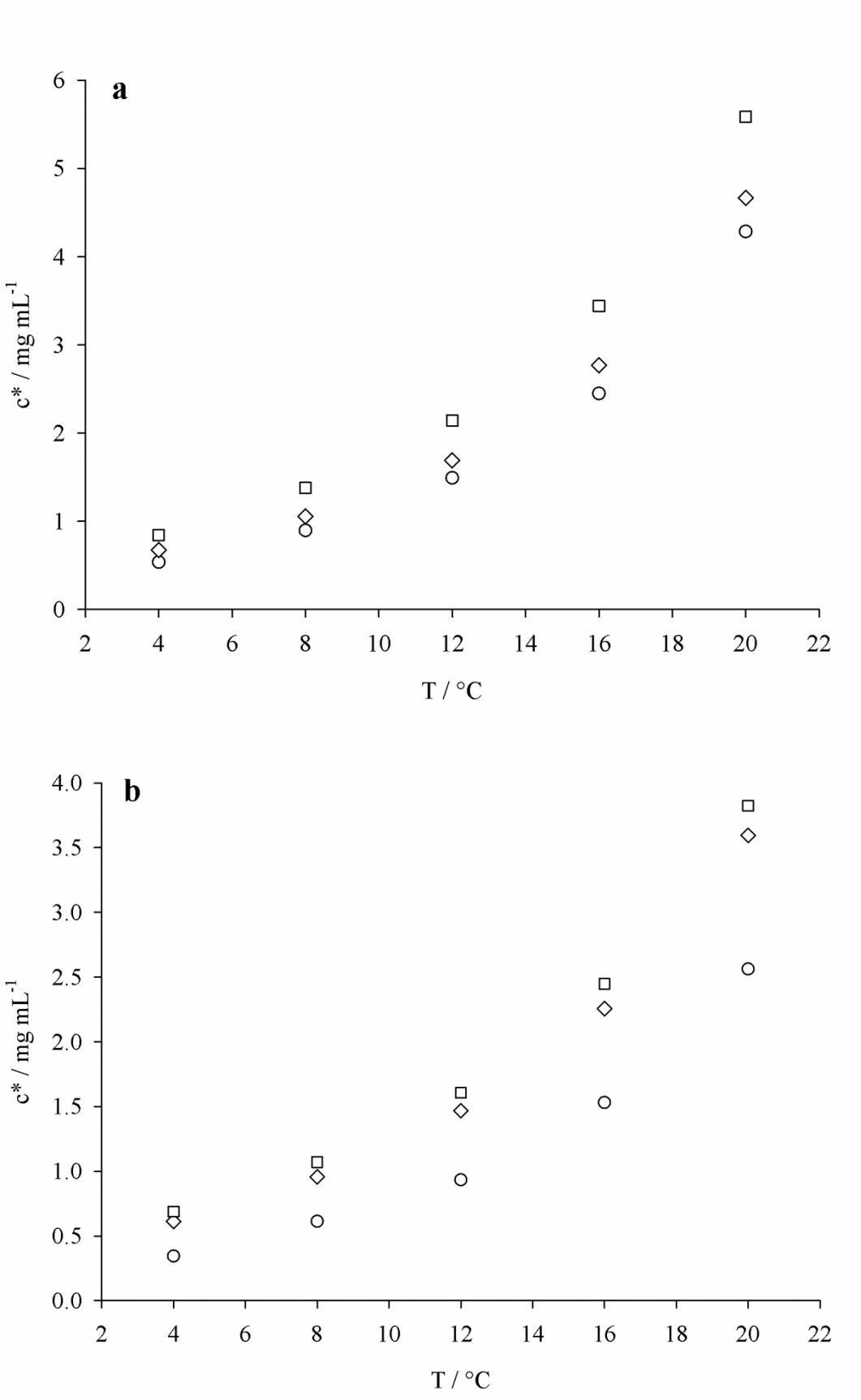
a
b
c* / mg mL-1
T / °C

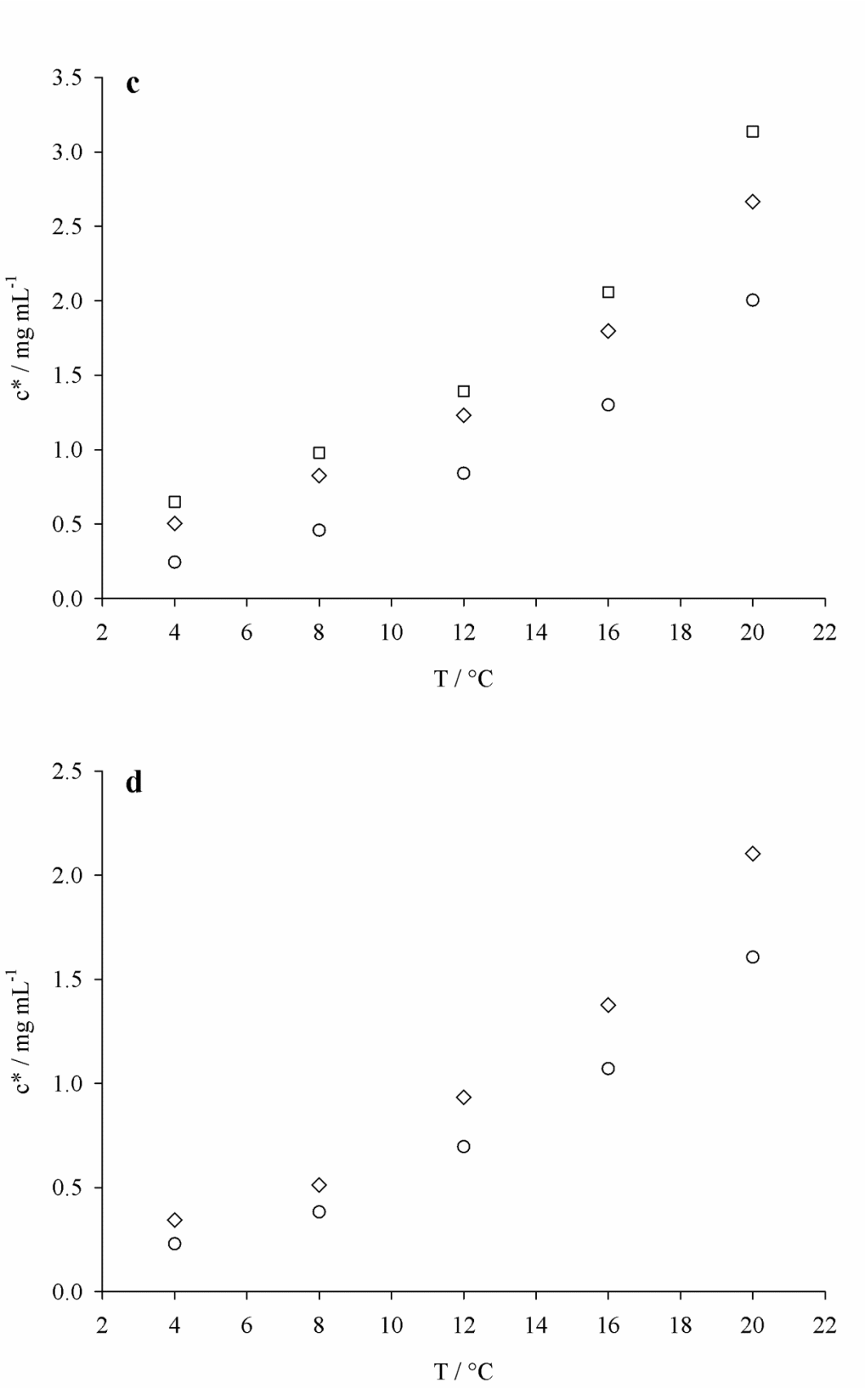

Figure 11: Solubility of tetragonal lysozyme chloride at 8.6 ≤ pH ≤ 10.6 for constant NaCl concentrations (Aldabaibeh 2009). a) 2 %(w/v) NaCl, b) 3 %(w/v) NaCl, c) 5 %(w/v) NaCl, d) 7 %(w/v) NaCl. ○ pH = 8.6, ◊ pH = 9.6, □ pH = 10.6.

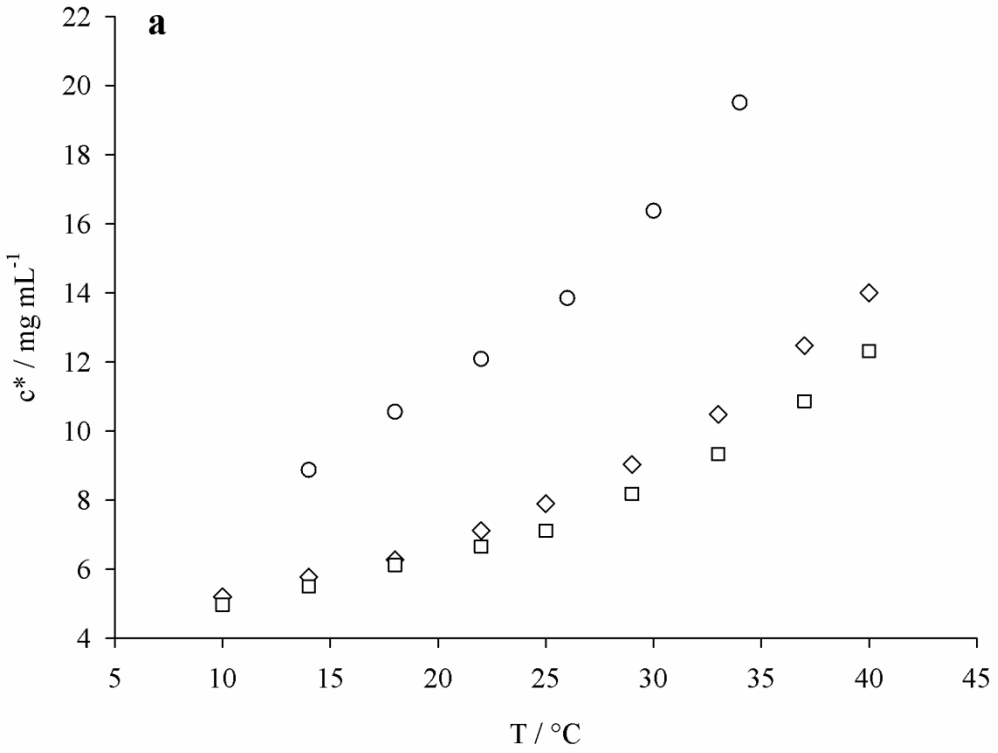
a
c* / mg mL-1
T / °C

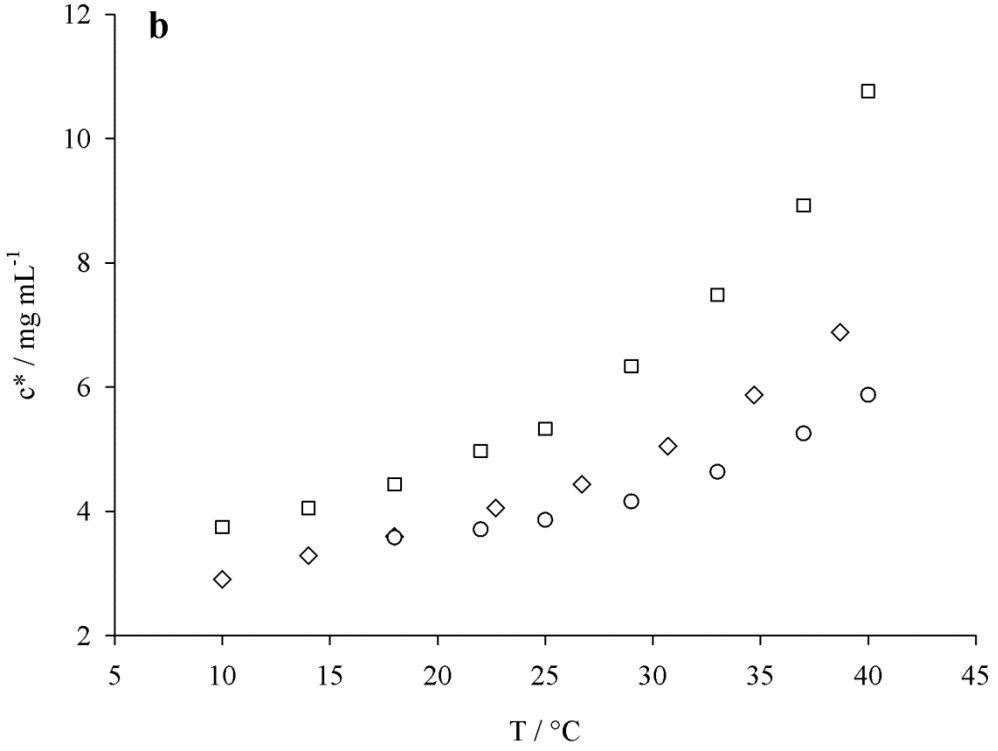
b
c* / mg mL-1
T / °C

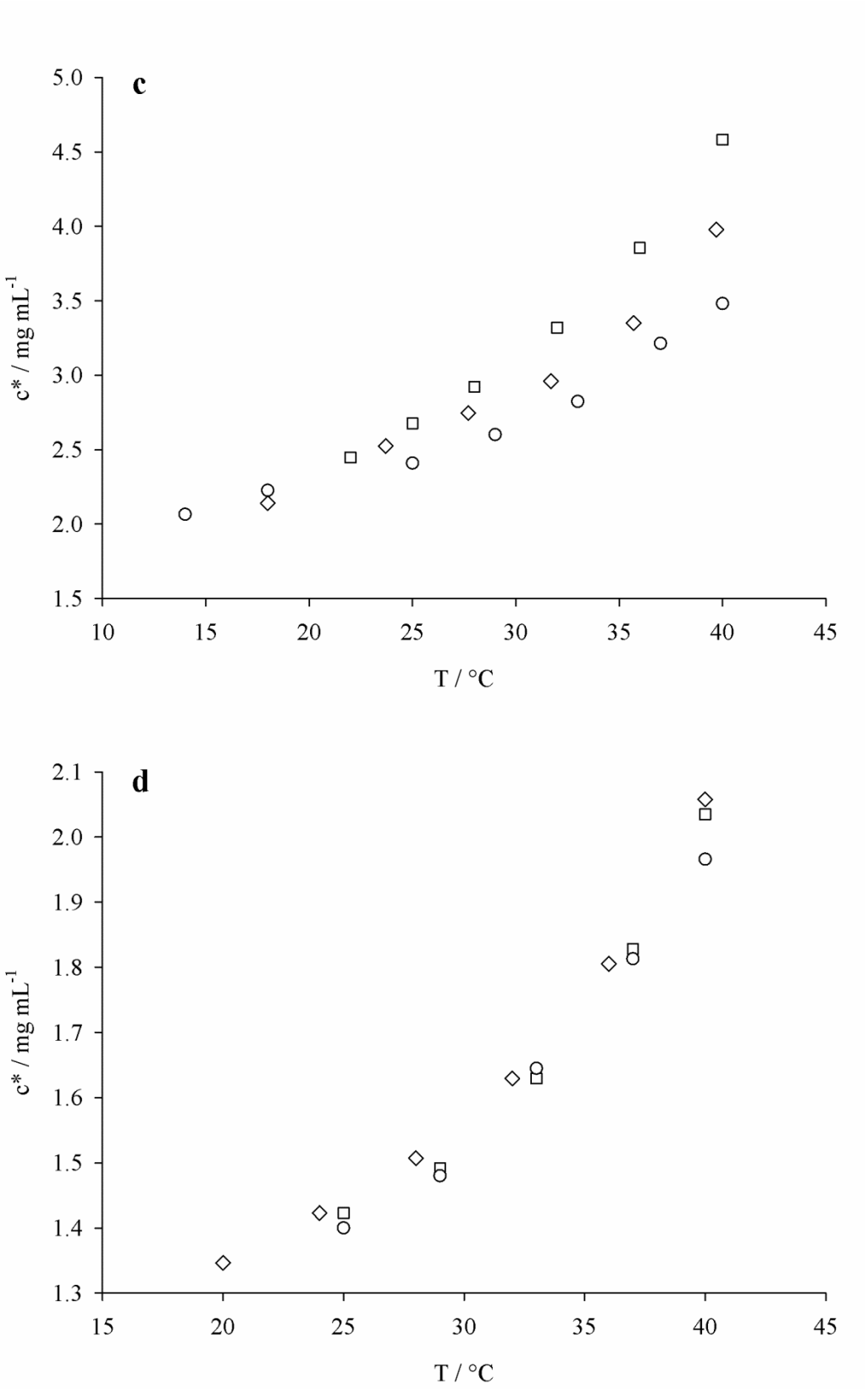

Figure 12: Solubility of high temperature orthorhombic modification of lysozyme chloride at 5.7 ≤ pH ≤ 8.0 for constant NaCl concentrations (Aldabaibeh 2009). a) 2 %(w/v) NaCl, b) 3 %(w/v) NaCl, c) 5 %(w/v) NaCl, d) 9 %(w/v) NaCl. ○ pH = 5.7, ◊ pH = 7.0, □ pH = 8.0.

In contrast to the observations by Howard (Howard 1988) discussed above, the solubility of this crystalline phase does not decrease with increasing temperature, but shows an increase in solubility with temperature, as already observed by Cacioppo (Cacioppo 1991a) at a lower pH of 4.5, indicating that earlier data were an artefact of the equilibration technique used.

Combining the solubility data for both modifications (Figure 13) gives immediate access to transition points in the phase diagram. Figure 13 shows the solubility of both tetragonal and HTO lysozyme chloride as a function of temperature for different salt concentration but at the same pH. Clearly, the speed with which equilibrium is reached in the flow-through column is sufficient to allow the measurement – within limits – of the solubility of a given solid phase in regions of phase space where this solid is metastable. This is most apparent for the lower salt concentrations, where the measured solubility curves intersect for both solid phases and data points extend beyond the intersect, which represents the transition point from one solid phase to the other, into the respective metastable regions. At higher salt concentrations solubility data were not accessible beyond the transition point for the orthorhombic solid phase due to the onset of the transformation to the tetragonal phase. For the higher salt concentrations, the intersect was determined by identifying the intersect of the respective lines fitted through the available data points.

In order to exhibit such an intersecting point in the solubility curves, the tetragonal and HT orthorhombic phases of lysozyme chloride must be related enantiotropically, with the tetragonal modification the stable phase at lower temperature and the orthorhombic modification stable at higher temperature. Interestingly, a closer inspection of the intersects for different salt concentrations and pH values reveals that the transition point is dependent upon both of these concentration variables (Figure 14). At pH = 7.0 the transition temperature appears to be almost constant at low salt concentrations, but drops significantly at high salt concentration.

Investigation of the solubility of the low temperature orthorhombic I modification (LTO) demonstrated that tetragonal modification is metastable with respect to the former under all conditions investigated. As for the other two modifications, the salt concentration range was from 2 %(w/v) – 9 %(w/v) and the pH range studied was from $5.7 \leq pH \leq 10.0$. At the two pH values (pH = 5.7 and 7.0, Figure 15) where data are available for both the tetragonal and the LTO modification, the tetragonal phase has a higher solubility at all temperatures and appears to be monotropically related to the LTO phase, though some ambiguity still exists due to the similarity of measured solubility data at lower temperature for pH = 7.0.

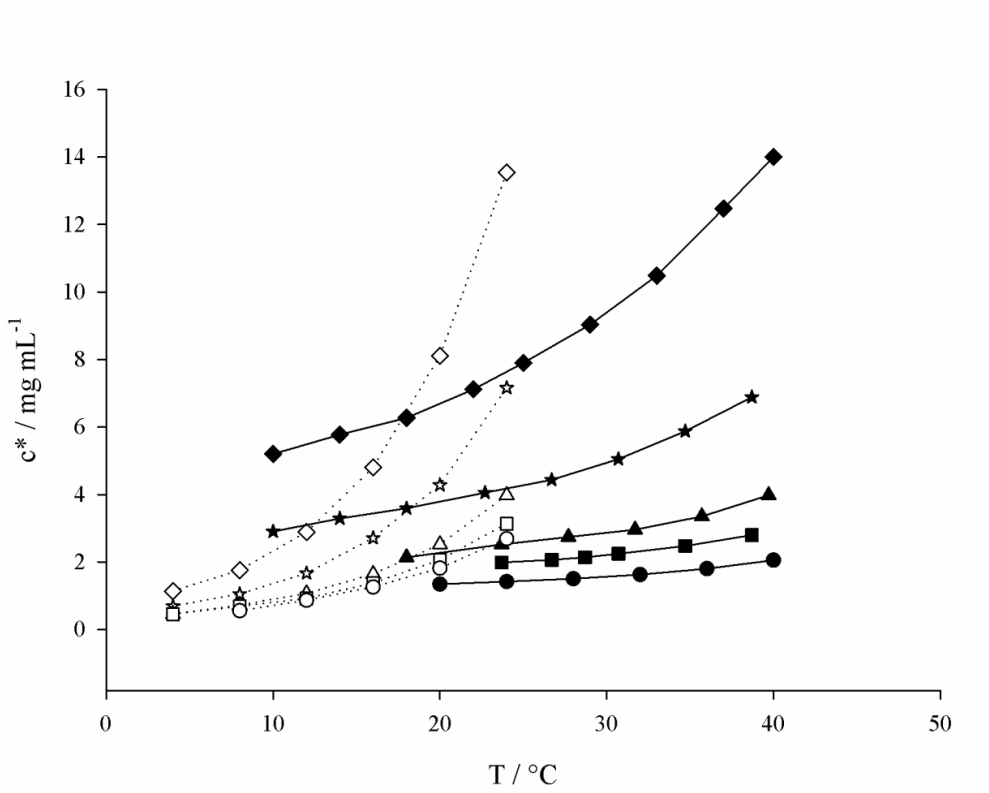

Figure 13: Solubility data for the tetragonal modification (open symbols and dotted line) and the high temperature orthorhombic modification (solid symbols and lines) of lysozyme chloride at pH 7.0 as a function of temperature (Aldabaibeh 2009, Aldabaibeh 2010). ♦ 2 %(w/v) NaCl, ★ 3 %(w/v) NaCl, ▲5 %(w/v) NaCl, ■ 7 %(w/v) NaCl, and ● 9 %(w/v) NaCl.

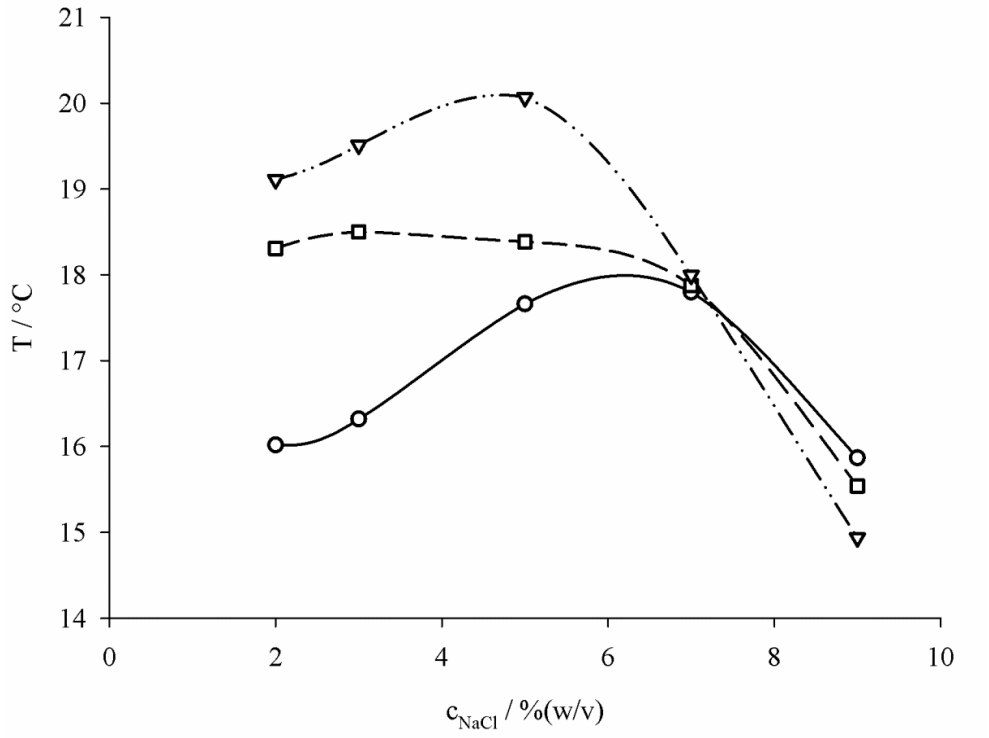

Figure 14: Transition temperature between the region of stability for tetragonal and orthorhombic lysozyme chloride as a function of salt concentration for different pH values (Aldabaibeh 2009). ○ pH = 5.7, □ pH = 7.0, ∇ pH = 8.0. The transition temperature becomes independent of pH at pH = 7.0.

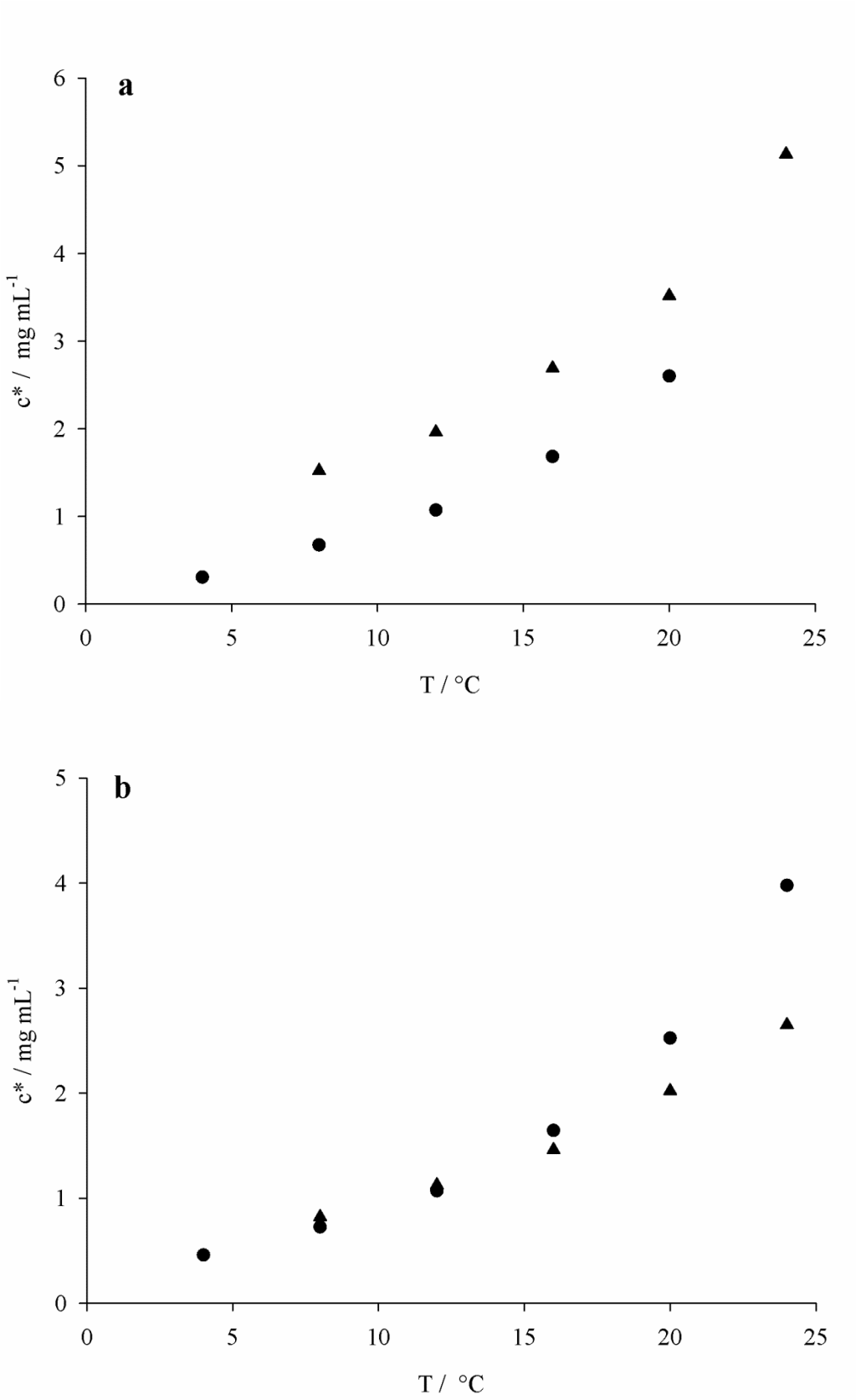

Figure 15: Comparison of the solubility of tetragonal lysozyme chloride to that of the low temperature orthorhombic (LTO) modification at a) pH = 5.7 and b) pH = 7.0 (Aldabaibeh 2010). ▲ LTO, ● tetragonal modification. While the tetragonal modification has a lower solubility at low pH, the solubility of the two modifications differs perceptibly only at temperatures higher than 15 °C at pH = 7.0, where the LTO apparently becomes the stable modification.

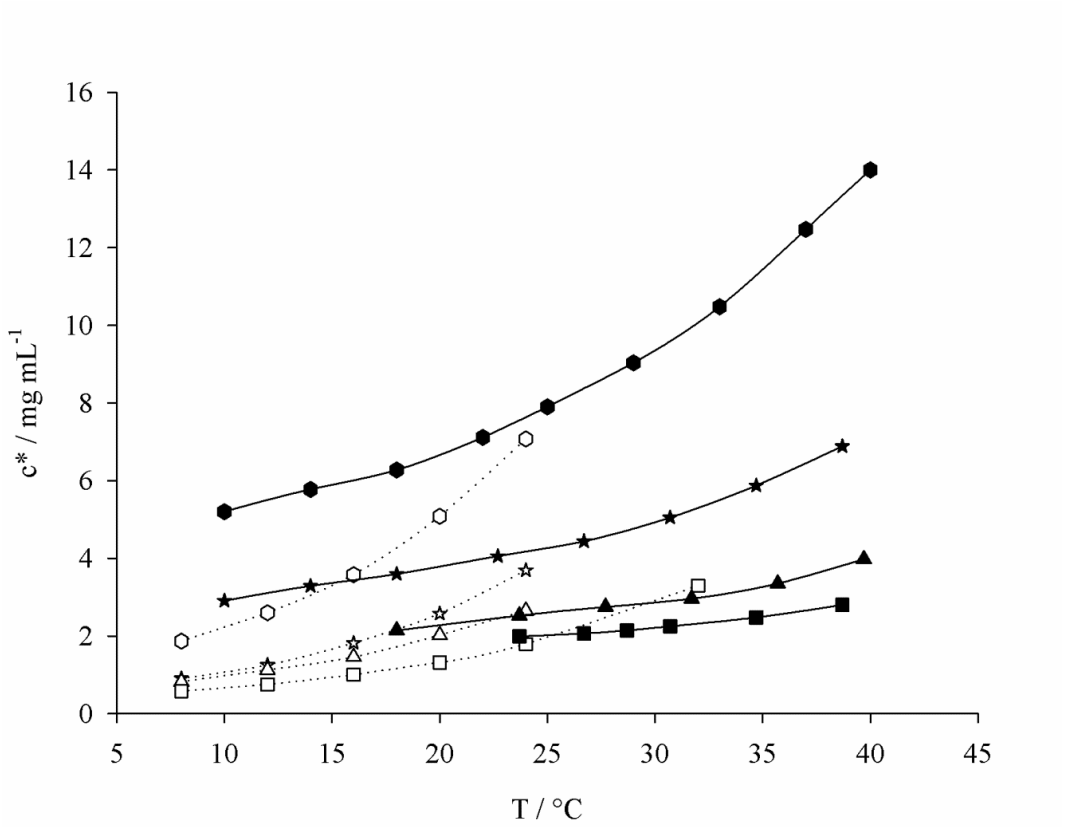

Figure 16: Solubility data for low temperature orthorhombic (LTO) modification (open symbols and dotted line) and the high temperature orthorhombic (HTO) modification (solid symbols and line) of lysozyme chloride at pH 7 as a function of temperature (Aldabaibeh 2009, Aldabaibeh 2010). ♦ 2 %(w/v) NaCl, ★ 3 %(w/v) NaCl, ▲5 %(w/v) NaCl, ■ 7 %(w/v) NaCl, and ● 9 %(w/v) NaCl.

The same procedure for identifying the transition points between the tetragonal and HTO phases can now be carried out for the HTO and LTO crystal modifications. Figure 16 and Figure 17 show the solubility of HTO and LTO lysozyme chloride at pH 8.6 for different salt concentrations and the transition temperatures as a function of salt concentration. It is important to note two conclusions that can be drawn from the data. First, the HTO phase is – kinetically – considerably more stable with respect to the LTO modification than with respect to the tetragonal modification and this is evidenced by the greater extent of the solubility data for HTO into the region of stability of the LTO phase. Furthermore, the transition temperatures between the HTO and the LTO modifications are always higher than those observed for those between the tetragonal and the HTO modification. Assuming that this behaviour also applied at lower pH values (there is no overlap in data available for the transition temperatures of the respective modification, which is, in part due to the distinct crystallization conditions required to generate these modifications, as highlighted by Müller (Müller 2012)), which is a sensible assumption considering that the LTO has been shown to be more stable than the tetragonal modification within the limits of the information available, this has significant consequences for any process to crystallize one or the other modification of lysozyme chloride.

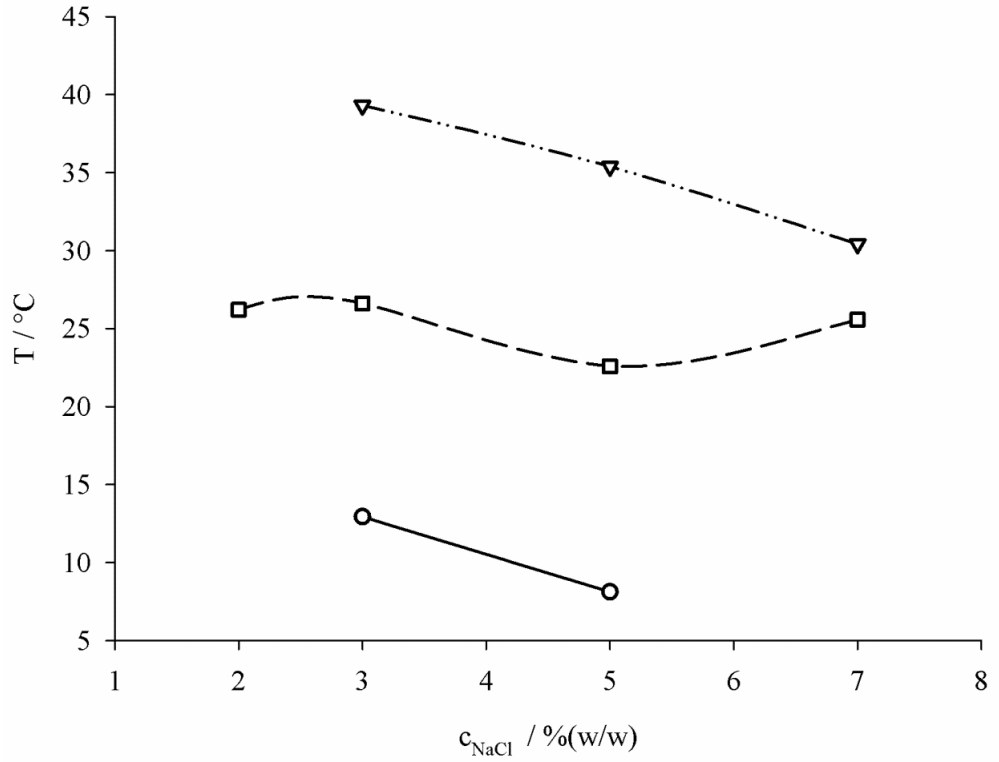

Figure 17: Transition temperature between the region of stability for tetragonal and orthorhombic lysozyme chloride as a function of salt concentration for different pH values (Aldabaibeh 2009). ○ pH = 5.7, □ pH = 7.0, ∇ pH = 8.0. The transition temperature becomes independent of pH at pH = 7.0.

From a purely thermodynamic perspective, a process for the crystallization of tetragonal lysozyme chloride should never exceed a temperature higher than the transition temperature to the HTO modification under given conditions of salt and pH. Since the transition temperature between LTO and HTO is always above that of tetragonal to HTO, there exists a narrow region of temperatures where the LTO modification is more stable than the HTO and any transformation from tetragonal to HTO must necessarily be followed by a transition to LTO. Once the LTO phase has formed, the tetragonal modification can never be recovered if the relationship between LTO and tetragonal lysozyme is indeed monotropic. Of course this cycle ignores the kinetics of phase transformations between different crystalline modifications of proteins, of which what little is currently known will be discussed in the following chapter.
Combining the information discussed above gives rise to a considerably more detailed understanding of the phase diagram of lysozyme chloride and highlights how narrow the respective operating ranges with respect to temperature and solution composition are, with respect to the safe and reproducible crystallization of a given crystal modification. However, though significant new insight has been generated, the phase diagram is far from complete owing, for example, to the lack of data comparing the solubility of the low temperature orthorhombic phase to that of the tetragonal phase at pH < 5.7.
In addition to the tetragonal, HTO and LTO crystal modifications, a fourth modification was observed in the course of the studies discussed above. This modification is called the ‘needle’

phase due to the shape of the crystals. This new solid phase showed solubility behaviour distinct from the other phases discussed in detail and appeared to be stable in a very narrow pH range around pH = 7.0. Since it was not possible to identify this phase form a structural perspective, no further discussion is attempted at this point.

One final observation is worth mentioning with regard to the solubility of the high temperature orthorhombic phase and in relation to the tetragonal phase and its increasing solubility with increasing pH beyond the minimum observed at pH ≈ 8.. Measurement of the solubility of the HTO at low temperatures and in a region of phase space where this modification is metastable also reveals a change of slope of the solubility, though this time not with respect to the pH, but to the temperature dependence. For the solubility curve measured at pH = 9.6 and 7 %(w/v) NaCl and shown in Figure 18, the solubility has a minimum at ca. 20 °C and increases either side of that minimum, *i.e.*, exhibits retrograde solubility with increasing temperature at temperatures below the minimum.

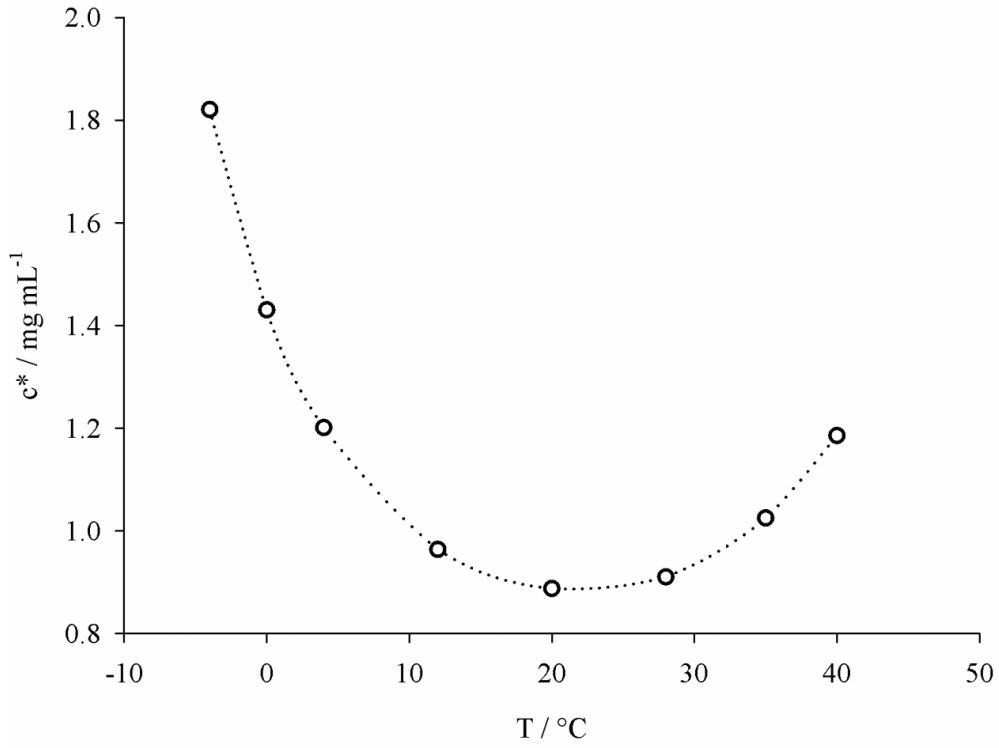

Figure 18: At pH = 9.6 and 7 %(w/v) NaCl the solubility of the high temperature orthorhombic modification of lysozyme chloride exhibits a minimum at 20 °C.

2.5 Analysis of the Solubility of Lysozyme Chloride Modifications in Terms of the Enthalpy and Entropy of Crystallization

The van't Hoff equation (van't Hoff 1898),

$$\boldsymbol{ln\, K = -\frac{\Delta H}{RT} + \frac{\Delta S}{R}} \qquad \textbf{2.5-1}$$

allows the enthalpy ΔH and entropy ΔS of crystallization to be extracted from solubility data. The equilibrium constant K is related to the solubility by the following equation:

$$\boldsymbol{K = a = \left(\gamma \frac{c^*}{c^{\ominus}}\right)} \qquad \textbf{2.5-2}$$

where a is the activity of the solute in equilibrium, γ the activity coefficient, c^* the equilibrium solubility, conveniently expressed as mol fraction x, and $c^{\ominus}$ a suitable chosen standard reference state. Providing the solubility is known as a function of temperature, a plot of $ln\ (x)$ versus the inverse temperature results in a linear representation where the slope of the line represents $-\Delta H/R$ and the intercept is $\Delta S/R$. The results of the analysis of the solubility data for the three crystal modifications of lysozyme chloride are summarised in Table 4 to Table 6.

For the tetragonal modification, crystallization is driven by the strongly negative enthalpy of crystallization. The same behaviour is observed for the low temperature orthorhombic modification, where the standard enthalpy of crystallization is generally greater than that of the tetragonal modification at identical conditions. At the same time the magnitude of the entropy contribution to the Gibbs free energy of crystallization is smaller for the low temperature orthorhombic modification of lysozyme chloride when compared to the tetragonal phase. Although the standard entropy of crystallization is negative for both of these modifications, leading to a positive contribution to the Gibbs free energy, the magnitude of the enthalpy is sufficiently large to compensate for the inherently destabilising effect of the entropy contribution. At high pH, the smaller entropy contribution observed for the low temperature orthorhombic modification results in a more favourable Gibbs free energy and thus greater stability when compared to the tetragonal modification.

For the high temperature orthorhombic modification of lysozyme chloride the standard enthalpy of crystallization has a considerably smaller magnitude than both the tetragonal and low temperature orthorhombic phases. The entropy contribution to the Gibbs free energy, however, becomes positive at higher salt concentrations under all conditions studied and where this is the case, the entropy provides a stabilising contribution to the Gibbs free energy of crystallization. Since the entropic contribution scales with the temperature, this is clearly a contributing factor to the increased stability observed at higher temperature for this crystal modification.

Bergeron *et al.* (Bergeron 2003) investigated the temperature dependence of porcine insulin as a function of precipitant concentration, in this case acetone, and analysed their data in terms of the enthalpy and entropy of crystallization extracted from the data using the van't Hoff

equation (Equation 2.5-1). Here, a cross-over from negative to positive values of the entropy of crystallization was interpreted in terms of water being displaced from the shell of hydration of the protein at higher acetone concentrations. Vekilov *et al.* (Vekilov 2002, Vekilov 2003) investigated the crystallization of human haemoglobin C and also interpreted their data in terms of water restructuring during crystallization. The case of haemoglobin C is particularly interesting since the enthalpy of crystallization is positive and the stabilization of the crystalline solid phase is a result of a large and dominant entropy of crystallization.

Table 4: Standard Enthalpy and Entropy of crystallization for the HTO modification of lysozyme chloride from a fit of the solubility data to the van't Hoff equation (Equation 2.5-1).

pH	C_{NaCl} /% w/v	R^2	ΔH° /kJ/mol	ΔS° / J/molK
5.7	2	0.9965	-28	-37
5.7	3	0.9918	-33	-45
5.7	5	0.9912	-26	-17
5.7	7	0.9886	-22	-1
5.7	9	0.9628	-19	15
7	2	0.9966	-28	-31
7	3	0.9861	-26	-18
7	5	0.9636	-21	0
7	7	0.9921	-20	8
7	9	0.9707	-18	17
8	2	0.9923	-26	-26
8	3	0.9824	-24	-10
8	5	0.9751	-19	9
8	7	0.9848	-14	27

Table 5: Standard Enthalpy and Entropy of crystallization for the tetragonal modification of lysozyme chloride from a fit of the solubility data to the van't Hoff equation (Equation 2.5-1).

pH	C_{NaCl} /% w/v	R^2	ΔH° /kJ/mol	ΔS° / J/molK
5.7	2	0.9925	-98	-278
5.7	3	0.9949	-81	-204
5.7	5	0.9862	-88	-229
5.7	7	0.9961	-76	-189
5.7	9	0.9995	-69	-160
7	2	0.9977	-85	-229
7	3	0.9976	-80	-205
7	5	0.9988	-73	-178
7	7	0.9955	-65	-1146
7	9	0.9929	-63	-140
8	2	0.9966	-87	-235
8	3	0.9971	-77	-196
8	5	0.9983	-87	-226
8	7	0.9979	-70	-163
8	9	0.9980	-65	-148
8.6	2	0.9989	-87	-229
8.6	3	0.9982	-83	-212
8.6	5	0.9940	-89	-165
8.6	7	0.9962	-83	-208
9.6	2	0.9980	-81	-211
9.6	3	0.9993	-74	-184
9.6	5	0.9985	-69	-165
9.6	7	0.9956	-78	-192
10	2	0.9994	-79	-205
10	3	0.9990	-72	-176
10	5	0.9985	-66	-154

Table 6: Standard Enthalpy and Entropy of crystallization for the LTO modification of lysozyme chloride from a fit of the solubility data to the van't Hoff equation (Equation 2.5-1).

pH	C_{NaCl} /% w/v	R^2	ΔH° /kJ/mol	ΔS° / J/molK
5.7	3	0.9967	-58	-134
5.7	3	0.9935	-58	-110
5.7	7	0.9976	-51	-102
7	2	0.9993	-58	-131
7	3	0.9988	-61	-136
7	5	0.9990	-51	-100
7	7	0.9968	-52	-99
8.6	2	0.9997	-77	-185
8.6	3	0.9995	-76	-179
8.6	5	0.9999	-67	-144
8.6	7	0.984	-62	-122
9.6	2	0.998	-71	-165
9.6	3	0.9961	-64	-137
9.6	5	0.9949	-64	-131
9.6	7	0.9933	-58	-108
10	2	0.9953	-64	-136
10	3	0.999	-66	-142
10	5	0.9982	-72	-156
10	7	0.9965	-67	-139

2.6 Nephelometric 'Solubility' Measurement

Nephelometric or turbidimetric 'solubility' measurements have rapidly become the standard method for measuring the solubility of experimental drug products in the pharmaceutical industry (Lipinski 2001, Lipinski 2012). The principle of nephelometry/turbidity measurements is simple. A single-wavelength light source is used to illuminate a sample. The presence of particles in the sample leads to scattering of the light. The difference between classic nephelometry and turbidity measurements to determine 'solubility' is the way in which the scattered light is measured. In nephelometric applications the aim is to quantify the particulate matter in a liquid matrix and the technique measures the scattered light, usually at an angle of 90° from the direction of the incident light beam. In commercial turbidity measurement systems such as Crystallics's Crystal 16 or Electro Thermal's STEM Integrity system, the transmitted light is measured at an angle of 180°, *i.e.*, in transmission. The wavelength used is in these commercial systems is in the near infrared range, as small organic molecules generally do not absorb in this wavelength range when in solution, while

crystalline solids reflect the light. Well defined slurries are heated at a constant heating rate under stirring and the turbidity is measured as a function of temperature. Once all particles in the suspension have dissolved, a maximum in the intensity of the transmitted light is recorded. Strictly, turbidity measurements result in the temperature of dissolution of a given mass of solid suspended in a given mass or solvent at the defined heating rate. Only in the limit of infinitely slow heating rate is this temperature of dissolution equivalent to the solubility of the material. In practice, however, this method has been shown to yield results indistinguishable, within the limits of uncertainty of the methods compared, from those obtained by alternative, analytical chemical methods, providing the heating rate is sufficiently slow and of the order of a few 10^{th}s of a degree per minute. At higher heating rates, lag in dissolution results in increasing temperatures of dissolution, which do not reflect the true solubility of the system.

A major advantage of turbidity measurements is that they not only provide information on solubility, but also on metastable zone widths: the same observations carried out while cooling detect nucleation temperatures and can therefore be used to quantify the metastable zone width, at least at the scale the equipment allows, which is usually restricted to only a few mL of solution.

Recently, the measurement of the solubility and metastable zone width of lysozyme chloride using turbidity measurements has been reported (Maosoongnern 2012) as well as a determination of the phase behaviour of asparaginase II (Liu 2014). In the first publication the solubility of lysozyme chloride is investigated over a temperature range of 20 °C to almost 50 °C with salt concentrations from 3 %(w/v) to 7 %(w/v) and pH values of 4.4, 5.0 and 6.0. Unfortunately, the authors mention neither the nature of the buffer used to define the pH nor the concentration used. In addition, there is no overlap of the lower pH data with ranges already reported in the literature, so that a direct comparison of the value and advantage of this method cannot be made. Nonetheless, they plot their data for higher temperatures together with older literature data from (Forsythe 1999a) and both sets of data fit well to an exponential curve under the same conditions of pH and salt concentration, at least for the two lower pH values investigated. The fit of an exponential function to the higher pH data is not as convincing as for the remaining two data sets and it cannot be excluded that the 'solubility' measured is tainted by the onset of a transition to the high temperature orthorhombic modification, which is stable under the conditions applied. The authors do not provide any detail on the parameters obtained or the quality of the fits to the individual data sets.

Indeed, the nucleation data obtained from cooling the samples illustrate the difficulties in ascertaining that the data measured indeed reflect the properties of one modification or another. An optical microscopy image of the particles obtained immediately after the end of the cooling process for a sample containing 30 mg lysozyme and 4 %(w/v) sodium chloride at pH = 5.0 reveals that the particles are too small for unambiguous identification of the crystalline phase as tetragonal lysozyme chloride by inspection of the morphology alone, and the particles have to be subjected to further cooling at 4 °C for three days in order to obtain an image of larger particles whose morphology is clearly that of the tetragonal phase. The fate of the particles between the first and the second image is unknown.

Similarly, an optical microscopy image of the crystals obtained from a sample containing 40 mg lysozyme at pH = 5.0 and 7 %(w/v) sodium chloride and also subjected to three days additional cooling at 4 °C after completion of the cooling profile clearly shows the presence of orthorhombic lysozyme chloride. This is likely to be the low temperature orthorhombic modification, which is the stable modification under these conditions.
The observations reported by Maosoongnern *et al.* (Maosoongnern 2012) highlight the need for careful characterisation of the solid phase, when present and at the same conditions as those imposed for the measurement, in order to prove the validity of the data.
Apart from the (potential) issues with the 'solubility' data measured, the methodology itself is certainly worth further investigation and is a promising tool for rapid solubility measurements. In addition, there is of course considerable value in the nucleation data reported in this paper. A discussion of this aspect of the publication can be found in chapter 3.

2.7 Second Osmotic Virial Coefficient

Since the observation made by George and Wilson (George 1994) that the second osmotic virial coefficient (B_2) determined by means of static light scattering (SLS) falls into a narrow range of values for protein solutions with a propensity to crystallize, measurement of this solution property has become a popular means of rapidly establishing conditions amenable for crystallization. Over the past 20 years a body of literature has been published (see Table 7) demonstrating the utility of the methodology for a range of proteins under various solution compositions.
It is well known, that the second osmotic virial coefficient correlates with a number of solution properties. For example, in polymer science it is well established, that B_2 correlates with the viscosity of polymer solutions and the swelling of polymers in contact with a solvent (Bruns 1996). Recently a number of research groups have shown that the second osmotic virial coefficient of proteins exhibits a similar temperature and solution composition dependence as their solubility and attempts have been made to correlate the second osmotic virial coefficient to the solubility of a protein (Haas 1999, Ruppert 2001, Franco 2013). While the second osmotic virial coefficient can be related to the solubility via a suitable interaction potential, the resulting equations are straightforward to evaluate only for the simplest of potentials.
Expressing the osmotic pressure Π of a single solute species A in a single solvent under conditions of constant temperature and chemical potential as a virial expansion yields the polynomial expression

$$\boldsymbol{\Pi_{T,\mu} = RT \left[\frac{c_A}{M_A} + B_2 \left(\frac{c_A}{M_A} \right)^2 + B_3 \left(\frac{c_A}{M_A} \right)^3 \ldots \right]} \qquad \textbf{2.7-1}$$

where R and T take their usual meaning and c_A is the molal concentration of the solute and M_A its molar mass. B_2 is the second osmotic virial coefficient, B_3 the third, *etc.*. The second

osmotic viral coefficient is generally interpreted as a measure of pair-wise interactions and strictly incorporates non-ideal solution behaviour due to solute-solute and solute-solvent interactions. Using a suitable thermodynamic framework and a statistical mechanical approach, the second osmotic virial coefficient can be related to the potential of mean force *U(r)* between pairs of solute molecules in the field of the solvent and other solute molecules

$$\boldsymbol{B_2 = \frac{4\pi N_A}{2m^2} \int_0^\infty \left[1 - e^{-\frac{U(r)}{k_B T}}\right] r^2\, dr} \qquad \textbf{2.7-2}$$

N_A is the Avogadro number, m the mass of the particle, k_B Botzmann's constant and T the temperature. In this equation the second osmotic virial coefficient becomes a functional of the potential of mean force of a pair of (solute) particles at a distance r from each other and is therefore a measure of their interaction alone. All other interactions are implicit and subsumed into the potential energy function. The interaction between pairs of solute molecules is repulsive if B_2 is positive and attractive if negative.

A range of experimental techniques can be employed to measure the second osmotic virial coefficient. Amongst these are membrane osmometry, static light scattering, self-interaction chromatography and sedimentation analysis. Due to the relative ease of measuring B_2 and the fact that it can be used to characterise the interaction between solute molecules, B_2 is considered a viable alternative measure to protein solubility for determining those ranges of solution compositions where a protein is likely to crystallize.

George and Wilson (George 1994) first suggested that the second osmotic virial coefficient obtained from static light scattering may be used to define a 'crystallization slot'. Studies on a selection of proteins, amongst others, lysozyme, canavalin, concanavalin A, bovine serum albumin and ovalbumin, all with known crystallization conditions, studied under different solution compositions both suitable and unsuitable for crystallization, established a narrow range of B_2-values for those solutions that produce a crystalline solid.

$$\boldsymbol{-2 \cdot 10^{-4} \leq B_2 \leq -8 \cdot 10^{-4}\ mol\, mL/g^2} \qquad \textbf{2.7-3}$$

This range has since been cited extensively as generally applicable for the crystallization of any protein and has even been equated with the solubility, which is problematic, as will be discussed below. In the original paper, George and Wilson (George 1994) clearly state that their observations are merely qualitative and based upon a limited number of model systems and observations and that a universal validity of their proposed 'crystallization slot' can only be established by extending the amount of data available. Since this initial study, literature has been published describing investigations employing different experimental techniques to determine the behaviour of the second osmotic virial coefficient under varying solution conditions for a number of different proteins. Table 7 provides an overview of a selection of proteins investigated together with pertinent references. In all cases values are found that lie within the crystallization slot proposed by George and Wilson (George 1994), not all demonstrate clearly that crystallization actually takes place under those conditions that produce B_2 values within this range.

Table 7: Selected literature reporting measured second osmotic virial coefficients for different proteins. The methods employed are static light scattering (SLS), self-interaction chromatography (SIC) and membrane osmometry (MOS).

Protein investigated	Method	References
Lysozyme	SLS	(George 1994, Rosenbaum 1996a, Curtis 1998, Velev 1998, Neal 1999, Tessier 2002a, Valente 2005, Velev 2005, Espitalier 2009, Liu 2011, Wanka 2011)
	SIC	(Valente 2005, Dumetz 2008)
Proteinase K	SLS	(Liu 2011)
Concanavalin	SLS	(George 1994, Liu 2011)
α-chymotrypsinogen	SLS	(George 1994, Velev 1998, Neal 1999, Tessier 2002a, Liu 2011)
	MOS	(Rosenbaum 1996b, Pjura 2000)
Ovalbumin	SLS	(George 1994, Demoruelle 2002)
	SIC	(Curtis 1998, Dumetz 2007, Dumetz 2008)
Equine Serum Albumin	SLS	(Demoruelle 2002)
Catalase	SIC	(Dumetz 2007, Dumetz 2008)
β-Lactoglobulin (A and B)	SIC	(Aymard 1996, Dumetz 2008)
Ribonuclease A	SLS	(George 1994)
	SIC	(Tessier 2003a, Dumetz 2007, Dumetz 2008)
Calcium and integrin binding protein	SIC	(Berger 2005a)
Enfurvitide (therap. Peptide)	SIC	(Payne 2006)
Bovine Serum Albumin	SLS	(George 1994, Asanov 1997, Dumetz 2007, Wanka 2011)
	SIC	(Tessier 2002b)
Cytochrome C	SIC	(Dumetz 2007)
α-Lactalbumin	SIC	(Dumetz 2007)
Myoglobin	SIC	(Tessier 2002b, Dumetz 2007)
Glucose Isomerase	SIC and SLS	(Gillespie 2014)
Bacteriorhodopsin	SIC	(Berger 2005b, Berger 2006)
Canavalin	SLS	(George 1994)
Ovostatin	SLS	(George 1994)
Subtilisin	SLS	(Pan 2003)
Recombinant human interleukin-1 receptor agonist	SLS and MOS	(Alford 2008a, Alford 2008b)
Apoferritin	SLS	(Petsev 2000, Petsev 2001)

While the measurement of the second osmotic virial coefficient may well present an interesting alternative to knowledge of the supersaturation of a given solution as a guide to establishing suitable crystallization conditions for proteins, it should not be interpreted as a measure for the equilibrium composition for several reasons. First and foremost, the osmotic pressure is a solution property and the virial expansion used as the starting point for defining B_2 is valid only for dilute solutions. Whether or not a solution in equilibrium with a solid fulfils the requirements for a dilute solution in its thermodynamic treatment is a matter of debate. Furthermore, the virial expansion assumes a single solute species and while, in the case of a dilute solution, a single solute species may well be present at a low concentration far from equilibrium, sedimentation analysis and dynamic light scattering have clearly demonstrated the formation of dimers or higher order clusters (Wills 1980, Mikol 1989b, Wilson 1990, Bolanos-Garcia 1998, Tessier 2003b, Pan 2007) at high solute concentrations. Solubility, on the other hand, is a property of a solution in contact and in equilibrium with a defined solid and as such depends upon the crystal modification present. Whereas the presence of a solid and the precise knowledge of its nature is a prerequisite for defining solubility, this solid phase has no relevance when considering a dilute solution property. Therefore, any claim that the second osmotic virial coefficient and solubility are equivalent evidently must be treated with caution. Clear experimental evidence to this effect is provided by Velev *et al.* (Velev 1998), where the B_2 for lysozyme was determined as a function of pH-values covering a range incorporating both regions of stability for the tetragonal and the low temperature orthorhombic chloride. On crossing the boundary between the regions of stability for the respective phases the solubility exhibits a discontinuity. In contrast, the second osmotic virial coefficient reported by Velev *et al.* (Velev 1998) appears to be a monotonic function of the pH and does not exhibit a discontinuity as could be expected if B_2 were strongly correlated with the solubility. This notwithstanding, the weaker claim that B_2 exhibits similar behaviour to the solubility, based upon observed experimental trends, is of course a helpful one. Measurement of B_2 for a range of potential crystallization conditions, though by no means trivial, is considerably less involved than systematic experimental screening for suitable crystallization conditions or the measurement of a solubility phase diagram for a given protein. However, it has yet to be shown that the so-called crystallization slot is universally applicable, and doubts have even been raised as to whether the second osmotic virial coefficient derived from light scattering data even represents B_2 correctly. Based upon marked differences in second osmotic virial coefficients derived from sedimentation equilibrium measurements and those obtained from static light scattering or osmometry under otherwise identical conditions, where the former returns positive values and the latter two techniques return negative values, Deszczynski *et al.* (Deszczynski 2006, Winzor 2007) argue that sedimentation analysis measures protein self interaction alone, while SLS and osmometry incorporate non-ideality due to protein-cosolute interactions and that therefore these techniques do not truly reflect the second osmotic virial coefficient. However, this is, as the authors themselves state, a subtle matter of interpretation that should not detract from the diagnostic value of the quantity derived from SLS and equivalent techniques for determining

parameter ranges suitable for crystallization. On the other hand, the question posed in these papers as to what the techniques actually measure is closely related to the question discussed in chapter 2.3 as to the nature of the crystallizing species and the need to understand in more detail the nature and composition of the protein crystal itself.

Despite the reservations expressed in the paragraph above regarding the equivalence of B_2 and solubility, it is worth examining the literature on this topic. Haas *et al.* (Haas 1998, Haas 1999) derived a simple relationship between the solubility and the second osmotic virial coefficient assuming an isotropic square well potential (Equation 2.7-4), which contains a single variable parameter:

$$\boldsymbol{B_2 = \left(\frac{4}{M\rho}\right)\left[1 - A\left\{(c^*/n)^{-\left(\frac{2}{z}\right)} - 1\right\}\right]} \qquad \textbf{2.7-4}$$

Here, M is the molecular mass of the protein, ρ the density of the protein crystal, z the number of nearest neighbours in the crystal and $n = M/18\,\rho$ represents the number of water molecules that can be placed in the volume occupied by a protein molecule. The solubility of the protein is c^*, and the variable parameter A accounts for anisotropy in the interaction potential not captured by the square well potential employed to derive Equation 2.7-4. Haas *et al.* (Haas 1999) plot experimental solubility data for lysozyme taken from the literature together with the solubility/B_2 correlation given by Equation 2.7-4 assuming a value for A of 0.01 showing a reasonable qualitative agreement of the theory with the experimental data. For equine serum albumin and ovalbumin, the agreement of the simple correlation with experimentally determined data for the second osmotic virial coefficient and solubility is less than convincing (Demoruelle 2002). In neither of these two publications do the authors provide residuals as a measure of the quality of the fit of the model to the experimental data. As a result a quantitative evaluation of the goodness-of-fit is not possible.

Haas *et al.* (Haas 1999) also consider an alternative potential energy function commonly employed in colloid science, the Yukawa potential. The Yukawa potential is also a symmetric potential, but decays exponentially with increasing distance between the interacting molecules. The resulting relationship between the solubility and the second osmotic virial coefficient (see (Haas 1999) for details) is more complex than Equation 2.7-4 and must be evaluated by numerical integration. Qualitatively, the behaviour of the solubility as a function of B_2 is similar to that of the square well potential and overall it exhibits a stronger dependence upon the anisotropy and range of the interaction as well as the coordination number z than on the exact shape of the potential energy function.

In an alternative approach, Ruppert *et al.* (Ruppert 2001) derive a relationship between the solubility of a protein and its B_2 that is independent of any statistical thermodynamic model. In its functional form the expression is similar to Equation 2.7-4 above and it is therefore not surprising, that a comparison of the model to experimental data, again for lysozyme, is qualitatively similar to the results reported by Haas *et al.* (Haas 1999).

Katsonis *et al.* (Katsonis 2006) employed Monte Carlo simulation to study the phase behaviour of protein solutions in terms of corresponding states laws and using potential

energy functions of varying shape and range. While the focus of this study is to demonstrate the applicability of the corresponding states approach for protein solutions, one observation made is that there is a significant difference between the dependence of B_2 upon reduced temperature and that of the solubility upon reduced temperature. The implication of this observation is that solubility cannot be predicted based upon corresponding states laws. The wider consequence of this statement is that there is no straightforward relationship between the solubility and B_2 of protein solutions.

Allahyarov *et al.* (Allahyarov 2003) carried out a molecular dynamics study focussing upon the relationship between salt concentration and second osmotic virial coefficient. In this study, two charge models were considered. The 'smeared charge model' (SCM) assumes that the total charge is uniformly distributed over the protein – assumed to be globular and represented in the simulations as an idealised sphere – whereas the second, 'discrete charge model' (DCM) assumes discrete charges distributed over the surface of the sphere. The results of the simulations are also compared to results obtained using DLVO theory (Israelachvili 2011). Though not directly related to the discussion on the relationship of the solubility to the second osmotic virial coefficient, the findings presented in this paper are instructive as they clearly demonstrate that simple, isotropic potential energy function do not capture fully the subtleties of such complex systems as protein solutions. For the DCM model the authors find a marked non-monotonic behaviour of the second osmotic virial coefficient as a function of salt concentration and interpret the observed variation in terms of salting-in and salting-out effects (thus implicitly invoking solubility). Neither the SCM nor the DLVO model, both isotropic, can reproduce this behaviour, and result in a monotonic decrease of the second osmotic virial coefficient with increasing salt concentration. This observation highlights the importance of capturing anisotropic interactions when calculating thermodynamic functions of protein solutions.

Clearly, measurement of the second osmotic virial coefficient has benefits if the problem it is meant to address is merely concerned with the identification of conditions suitable for crystallization. Where the task at hand is the design of crystallization processes, the second osmotic virial coefficient is of limited value. In this case, a good understanding of phase equilibrium as a function of composition of the solution and knowledge of metastable zone width as well as some understanding of nucleation and growth kinetics are required. In light of the discussion above, this means that one cannot easily circumvent the task of measuring solubility data as accurately as possible and for as many solution compositions and temperatures as necessary and the technique discussed in this chapter represents a big step in the direction of establishing technologies that are capable of delivering the requisite data within a short period of time and with reduced material requirements.

3. Kinetics of Protein Crystallization

3.1 Nucleation

Prior to discussing nucleation of protein crystals, it is important to recall that the term 'nucleation' covers a number of distinct processes. The accepted classification distinguishes three general types of process (see, for example, chapter 5, (Mullin 2001)). The first is primary, homogeneous nucleation, also called spontaneous nucleation, which is a stochastic event depending upon the physical properties of the solution and the particles generated. Primary, heterogeneous nucleation is distinct from homogeneous nucleation in as much as heterogeneities in the solution, for example foreign particles, liquid-liquid or even liquid-vessel interfaces serve to promote the nucleation event. Finally, secondary nucleation describes the formation of new crystals from existing crystals, for example by attrition. Seeding of a supersaturated solution is frequently observed to induce secondary nucleation. As a rule, primary homogeneous nucleation is an improbable event since solutions are rarely free of impurities such as atmospheric dust particles, even with meticulous preparation. Heterogeneous nucleation is generally the more likely primary nucleation process. In industrial mass crystallization from solutions, secondary nucleation is generally the dominant nucleation mechanism, especially at low supersaturation (Garside 1980).

Nucleation of protein crystals is perhaps the most poorly studied aspect of protein crystallization, though an increase in research activity has become evident in recent years (Vekilov 2011). Much of this interest has been driven by the observation of liquid-liquid phase separation prior to nucleation from the dense liquid phase. This has led to the proposition of a two-step mechanism for nucleation, where the formation of two liquid phases, one enriched and one depleted in protein, is followed by nucleation in the protein rich phase, which in turn is followed by crystal growth and depletion of both phases until equilibrium is reached and a single liquid phase restored.

Classical Nucleation Theory (CNT) based upon the work of Gibbs and Vollmer (Gibbs 1928, Vollmer 1939), in contrast, treats nucleation as a stochastic process where the rate of nucleation is a measure of the probability of forming a particle sufficiently large, that the addition of a further 'building block' leads to a stabilisation of that particle. CNT assumes random collisions of particles, but does not require the prior formation of a distinct, dense liquid phase prior to nucleation.

The excess Gibbs free energy of a particle in solution is the sum of the excess surface Gibbs free energy and the excess volume Gibbs free energy. Assuming that the particle forming is a sphere, the former is a function of the square of the radius of that particle and the latter a function of the third power of the radius. Since the excess surface Gibbs free energy and the excess volume Gibbs free energy have opposite signs in a supersaturated solution, the total excess Gibbs free energy of the growing particle is initially positive, where the positive surface term dominates, reaching a maximum at a characteristic, supersaturation-dependent

size, after which the negative volume term begins to dominate the total excess Gibbs free energy. A particle possessing this maximum in energy is called the critical nucleus, since either the addition or removal of a 'building block' (atom, ion, molecule or smaller aggregate) will decrease its energy. Upon addition of a building block, the negative slope of the excess free energy with respect to the size will, however, ensure a greater likelihood for further growth rather than dissolution. The critical nucleus is generally assumed to be spherical and is characterised by its radius, the critical radius r_{crit}.

The probability of reaching such a critical nucleus is given by the Arrhenius-type rate equation:

$$J = A\, e^{-\frac{\Delta G}{kT}} \qquad \textbf{3.1-1}$$

Where the pre-exponential factor A is a kinetic factor and ΔG is the work required to generate the new interface between the solid and the liquid. For homogeneous nucleation, assuming a spherical nucleus, and employing the Gibbs-Thompson equation for a non-electrolyte, one arrives at the expression:

$$J = A\, e^{-\frac{16\,\pi\,\gamma^3 v^2}{3\,k^3 T^3 [ln\,S]^2}} \qquad \textbf{3.1-2}$$

where γ is the interfacial energy of the particle in the solution and v is the volume of the 'building block' in the solid. The kinetic factor A and the interfacial energy can be extracted from nucleation rate measurements at defined temperature and supersaturation. Expressions for the kinetic factor can be derived and vary somewhat depending upon the assumptions made in the derivation of A. A commonly used expression (Vekilov 2010) for A is:

$$A = v^* Z n \qquad \textbf{3.1-3}$$

Where v^* is the frequency of attachment of building blocks to the nucleus, Z the Zeldovich factor and n the number density of (solute) molecules in solution. The Zeldovich factor accounts for the width of the free energy in the vicinity of its maximum.

The dependence of the nucleation rate upon $exp(-1/[lnS]^2)$ results in a rapid increase in the nucleation rate with increasing supersaturation. Herein lies one of the difficulties in measuring nucleation rates – as a rule (and in contrast to precipitation, which requires only low supersaturation for the generation of particles and where, as a result, nucleation and growth processes compete for the available supersaturation, resulting in a mass of very small crystals), nucleation requires significantly higher supersaturation than crystal growth. Since any nucleus exceeding the critical radius will immediately grow, and grow rapidly at high supersaturation, the resulting depletion of the solution will have a profound impact on the nucleation rate and this coupling is difficult to overcome in a bulk solution. Furthermore, particles only become detectable at sizes considerably larger than that of the critical nucleus, adding a further difficulty to the measurement of nucleation rates.

In addition to this, and as alluded to above, the difficulties in measuring nucleation rates for primary, homogeneous nucleation lie in ensuring the absence of factors that may lead to heterogeneous nucleation, such as the presence of dust particles and other interfaces that may promote heterogeneous nucleation, as well as counting the nuclei themselves and in sufficient number in order to generate reliable and statistically relevant rate data. Heterogeneous nucleation may likewise be analysed in terms of Equation 3.1-2. In this case, the interfacial tension and the pre-exponential factor will reflect the influence of the heterogeneity at which nucleation occurs.

3.1.1 Early Protein Nucleation Studies

Perhaps the earliest study of protein crystal nucleation was presented by Schlichtkrull (Schlichtkrull 1957a), who investigated the nucleation and growth kinetics of bovine insulin using a large-scale (4 L) crystallization process, which was sampled and characterised in terms of the concentrations of insulin present in solution, in the crystalline phase as well as in any amorphous solids. For this study, Schlichtkrull exploited the rhombohedral shape of the crystals, allowing changes in size to be characterised by a single length variable. By counting the number of crystals observed for given crystallization conditions as a function of time and measuring their size, characteristic nucleation rates are derived employing geometric arguments and the assumption of a single, common growth rate for all crystals.

Almost 30 years later Ataka and Tanaka (Ataka 1986) presented a comprehensive study of nucleation and crystal growth for both tetragonal and high-temperature orthorhombic lysozyme with the aim of identifying conditions for growing few but large crystals suitable for physical characterisation. Induction times were measured as a function of protein, precipitant and proton concentration (in the absence of buffer salts) and the general trends agree with those observed for small molecule crystals. With increasing supersaturation, the induction times decrease rapidly, those solutions with lowest supersaturation and concentrations close to the solubility curve fail to nucleate even within the experimental time-scale of one year. The appearance of crystals was monitored optically. Since the magnification used was low, crystals were not visible until they reached a significant size (ca. 50 μm). As a consequence, the induction times necessarily include a growth period, biasing the true nucleation kinetics. Nonetheless, a double-logarithmic plot of the induction time vs. the supersaturation (variable protein concentration, constant salt concentration) shows a linear dependence which is in agreement with classical nucleation theory and suggests that crystal growth rates do not depend strongly upon the crystallization conditions in the range investigated.

Interestingly, the number of crystals counted appeared to depend not merely upon the absolute supersaturation, but seemed to show a weaker dependence upon the protein concentration than upon the precipitant concentration, though the numbers reported are unlikely to be statistically significant.

A further observation reported in this paper (Ataka 1986) which is worth noting, is that all crystals observed were attached to the surface of the vials used for the crystallization experiments, suggesting a heterogeneous nucleation process.

3.1.2 Pre-Nucleation Particle Aggregation

From the late 1970s onwards a steady succession of light scattering studies of protein solutions has been published. Some have already been discussed above in chapter 2.8. Others, mainly concerned with understanding pre-nucleation aggregation of protein molecules in solution in order to characterise the nucleation process without having to resort to involved experimental procedures to decouple nucleation and growth and avoiding tedious counting of crystals, are discussed here.

One of the earliest studies employing quasi-elastic light scattering (also known as dynamic light scattering (DLS in the following) or photon correlation spectroscopy) as a means for studying protein crystal nucleation was published by Kam *et al.* (Kam 1978). With the aid of suitable models for the system under investigation, DLS allows information on the structure and dynamics of this system to be extracted. The major advantage is therefore the relative ease and speed at which information on nucleation can be obtained when compared to other methods such as those described below.

Kam *et al.* (Kam 1978) focussed upon characterising solutions of lysozyme at different levels of supersaturation, in order to identify conditions that would either lead to crystallization or the formation of amorphous precipitates. The model employed assumes that nuclei grow by a stepwise mechanism involving the addition of a single lysozyme molecule in each step. The formation of crystals is favoured, if the nuclei formed are densely packed, whereas amorphous precipitates are likely to be generated if this is not the case. The packing of the lysozyme molecules determines the shape and relative surface area of the aggregates and thus the response of the system to irradiation by monochromatic light. The frequency distribution of the scattered light is a function of the size distribution of the aggregates and relates to their translational diffusion coefficients. Larger aggregates diffuse more slowly than smaller aggregates and lead to a narrower spectral width. It is therefore expected, that the line width of the scattered light in terms of the frequency distribution will narrow at higher lysozyme concentrations, where aggregates in the solution are likely to be larger. This assumption is confirmed by the observations reported. In the derivation of the model, it is assumed that a steady-state of the size distribution of the aggregates is reached rapidly and in a considerably shorter time frame than that required for nucleation of lysozyme.

From their data, Kam *et al.* (Kam 1978) extract critical nucleus sizes for different lysozyme concentrations ranging from 8 molecules at the highest reported concentration of 5 %(w/v) lysozyme to 23 for a concentration of 2 %(w/v).

Later studies on lysozyme nucleation (Mikol 1989b, Kadima 1990, Kadima 1991, Pusey 1991, Georgalis 1993, Sibille 1994, Georgalis 1997a, Georgalis 1997b, Georgalis 1998, Umbach 1998, Moreno 2000) extend the approach described by Kam *et al.* (Kam 1978) by

investigating further crystallization conditions and additional proteins. Only a selection of these publications will be discussed in the following.

Mikol *et al.* (Mikol 1989b) studied the time-dependent evolution of the solution structure, initially cooling a solution of defined composition to a predefined supersaturation. The data are analysed in terms of the Stokes radius of the scattering aggregates. In the initial stages of the experiment and during cooling, the Stokes radius is observed to increase and the growth of the Stokes radius continues long after a constant supersaturation is reached. At some time t, denoted t_{max}, a maximum in the Stokes radius is reached, after which this radius begins to decrease. After a period of time $t_{cryst} > t_{max}$, diffraction of the forward scattered intensity is observed and ascribed to the presence of sufficiently large crystals.

The results are interpreted in terms of the generation of clusters of lysozyme followed by growth of critical clusters to macroscopic crystals and subsequent reduction of the supersaturation, which in turn leads to a decrease of the cluster size in solution and hence the reduction in Stokes radius observed. Interestingly, the authors note that the maximum in the Stokes radius does not correspond to the critical nucleus since a higher supersaturation leads to an increase in this value, which is contrary to nucleation theory, where the critical nucleus size is expected to decrease with increasing driving force.

While Kam *et al.* (Kam 1978) provide convincing arguments for their assumption of rapid attainment of quasi-equilibrium with respect to the distribution of cluster sizes in the supersaturated lysozyme solution, the results presented by Mikol *et al.* (Mikol 1989b) appear to contradict this assumption, showing that the Stokes radius continues to increase for several hours after the final temperature of their solution is reached.

Pusey (Pusey 1991) casts doubt on another assumption made by Kam *et al.*, analysing light scattering data from lysozyme solutions in terms of a model assuming formation of lysozyme clusters by aggregation of larger clusters rather than a model considering monomer-only-addition. A better agreement with the data is found for the cluster-aggregation model, though clusters no greater than tetramers are considered in the analysis.

Pre-crystallization aggregation of the jack bean storage protein canavalin was studied by Kadima *et al.* (Kadima 1990) and compared to insulin in a later paper (Kadima 1991). Three distinct regions are observed for the size of aggregates as a function of protein concentration and constant pH and salt concentration (NaCl in this case). Initially the cluster size increases linearly with concentration and the polydispersity – a measure of the distribution of clusters with different sizes – is low. At a concentration of 0.12 %(w/v) canavalin, the curve changes slope and the aggregate size continues to increase linearly but with a much steeper slope until, at a concentration of 0.20 %(w/v), the cluster size appears to level off. In this concentration range, the polydispersity also increases, indicating the formation of a range of different clusters. At higher protein concentrations large scatter in the cluster sizes is observed with no clear protein concentration dependence, while the polydispersity remains high. Structural considerations led to the conclusion, that the first domain contained only monomers of canavalin, while in the second domain the average Stokes diameter of the aggregates increased, reaching a maximum at the upper concentration limit of this domain. In the first

domain, no solid formation was observed even after an extended period of time, while irregular particles precipitated from the second domain. Crystallization occurred only in the third domain and the authors concluded, again using structural arguments, that it is only towards the upper concentration limit of the second domain that the correct type of aggregate required for crystallization is formed.
For insulin crystallized from zinc sulfate solutions (Kadima 1991), in contrast, the only species observed in solution was the insulin hexamer. Nonetheless, crystallization occurred, despite the lack of evidence for the formation of larger aggregates. The authors offer perhaps the only sensible explanation for the absence of larger aggregates, namely that the formation of crystalline particles in this system is likely to be governed by heterogeneous nucleation at the vessel walls and not detectable using their particular experimental set-up.

3.1.3 Induction Time Measurements

More traditional approaches to studying crystal nucleation involve counting of crystals generated under given crystallization conditions. As discussed above, one of the limits to obtaining reliable nucleation kinetics is the ability to decouple nucleation from crystal growth and generating sufficient data for these to be statistically meaningful.
Galkin and Vekilov (Galkin 1999) described an experimental set-up which allows the nucleation and the crystal growth kinetics to be decoupled to the greatest possible extent. By reducing the liquid volume in which nucleation takes place to the nL range, rapid and homogeneous cooling and heating of the droplets can be achieved. Droplets are initially cooled to a high supersaturation for a pre-defined period of time in which nucleation is likely to occur and then heated to a lower supersaturation, at which nucleation is unlikely, but crystal growth will still occur. Effectively, this method determines the nucleation rate at fixed induction times. By allowing the crystals to grow at a lower supersaturation after the induction period, the particles generated can be observed and counted by optical microscopy. In order to ensure statistical relevance of the experiments, well-plates containing 400 identical droplets are used. In order to avoid evaporation of solvent and undesired nucleation at the air-liquid interface, the droplets are suspended in an inert oil. Using this experimental set-up, Galkin and Vekilov (Galkin 1999) characterised the nucleation of lysozyme chloride from a well-defined supersaturated solution and analysed their observations in terms of Poisson-statistics and classical nucleation theory, extracting interfacial energies for the protein nuclei and demonstrating that even with this set-up and carefully prepared solutions, heterogeneous nucleation cannot be avoided, which is not surprising considering the presence of a liquid-liquid interface between the droplets and the inert oil used to isolate them.
Microfluidics have been employed to similar effect by several research groups (Chen 2005, Shim 2007, Selimovic 2009, Ildefonso 2011, Ildefonso 2013). Chen *et al.* (Chen 2005) employed a device containing sinusoidal channels to study the nucleation of thaumatin with sodium potassium tartrate as precipitant. Droplets containing spatially separated aliquots of protein solution and precipitant solution were generated by controlled injection of the two

solutions into a water-immiscible carrier fluid and the separation of the two solutions in the droplets was ensured by injecting a thin layer of a protein- and precipitant-free buffer solution between the other two. The sinusoidal channels of the microfluidic device exert a folding motion on the droplets as they are transported through the device, leading to the successive formation of protein-precipitant solution interfaces and mixing of the two solutions by means of chaotic advection. The results of the study are discussed qualitatively and the results are as expected for such a set-up: the nucleation rate depends upon the lifetime and total area of the interfaces generated by the device (Chen 2005). For high flow rates of the carrier fluid, the creation of the interfaces is rapid but their lifetime is comparatively short. The time required to reach a fully mixed state is therefore shorter than for a slower flow rate. As a consequence, the nucleation rate is smaller in the rapidly mixed samples and fewer crystals are observed in the individual droplets. In those droplets where mixing is slower, fewer interfaces exist over a longer period of time, compared to rapid mixing, which results in higher local supersaturation at the interfaces due to diffusion across the protein solution-precipitant solution interface. Shim *et al.* (Shim 2007) describe a microfluidic device capable of generating and storing 500 nL-droplets. Unlike the device described by Galkin *et al.* (Galkin 1999), the degree of supersaturation is not controlled by rapid heating or cooling, but rather by rapid changes in chemical potential. The storage wells of the device are separated from a reservoir by means of a semi-permeable membrane which is permeable only for water and low molecular weight organic solvents while remaining impermeable to precipitants or protein. A single reservoir serves 100 wells and by changing the solution in the reservoir, or even by introducing dry air, the concentration of the droplets can be manipulated. The authors claim that the low thickness of the membrane ensures rapid concentration changes, thus allowing nucleation and crystal growth to be decoupled as in Galkin's device. In a later paper from the same group (Selimovic 2009), this device is used to study the nucleation rate in the manner employed by Galkin and Vekilov (Galkin 1999); droplets of defined protein and precipitant concentration are generated and the supersaturation is initially increased by reducing the water content of the droplets and, after an induction period, increased again by increasing the water content via the semi-permeable membrane. These two studies highlight the difficulties in comparing results from subtly different experimental approaches to nucleation rate measurements. Although the critical nucleus interfacial energy broadly agrees with previous studies (Vekilov 1996), it is found to be significantly higher than the value of Galkin and Vekilov (Galkin 1999). In addition, the nucleation statistics do not follow the Poisson equation, and the authors discuss several potential sources of error, including the change in droplet size (and therefore surface area) during the experiment, the change in concentration imposed upon the drops as well as possible interactions with the inert oil enclosing the droplets. One further factor that may be important but is not discussed by the authors is the use of surfactants to modify the surface tension of the oil and allowing better control of the droplet formation. It is not only conceivable, but also likely, that this surfactant will diffuse into the nano-drop and modify the solution physical properties.

Ildefonso *et al.* (Ildefonso 2011, Ildefonso 2013), also employ a microfluidics device to study nucleation of lysozyme chloride and analyse their experiments in terms of classical nucleation theory. Again, their results are in broad agreement with the studies discussed above, but the authors refrain from claiming that they observe homogeneous primary nucleation, rather discussing their observations in general terms. Interestingly, they employ devices manufactured from distinct polymers and two different inert oils – one for each device - and observe differences in the nucleation rates of the systems, a clear indication that both the device and the continuous fluid employed have an impact on the observed nucleation rates.

3.1.4 Calorimetric Studies of Nucleation

Calorimetry can be employed to study the evolution of supersaturated solutions via the heat signature of aggregation events. In combination with fluorescence quenching and light scattering experiments, Sibille and Pusey (Sibille 1994) used calorimetric measurements to study the nucleation of lysozyme chloride. In this concise report, the authors only briefly discuss their observations, stating that the heat of anion binding, that is the initial reaction of added chloride ions with the protein, dominates the initial heat signature after mixing. The accompanying fluorescence quenching studies reveal that the number of chloride ions binding with lysozyme depends upon the salt concentration in the solution and reaches a maximum value of 21 – 23 chloride ions per lysozyme molecule. These numbers agree well with results obtained from potentiometric titrations reported earlier (Tanford 1954). Providing the heat of adding a chloride ion to lysozyme is of similar magnitude to the heat of aggregation of two lysozyme molecules, it is obvious that the heat evolved by the ion-binding will be significantly larger than the heat of aggregation for small aggregates. Nonetheless the authors observed a long-term evolution of heat in their calorimetric signal which was ascribed to aggregating lysozyme.

Georgalis *et al.* (Georgalis 1997b) also combined calorimetric experiments with light scattering to investigate lysozyme chloride nucleation. Using a stirred sample chamber in an isothermal micro calorimeter and thermal pre-equilibration of the freshly mixed samples prior to commencing the experiments, a clear exothermic peak is observed after a given time period. This peak is ascribed to nucleation of lysozyme crystals. Experiments were carried out for constant lysozyme concentration and varying salt concentration, as well as for solutions with constant salt concentration and varying lysozyme concentration. In both series, the induction time observed was dependent upon the respective concentration variables and decreased with increasing concentration, as expected. However, these nucleation exotherms were only observed in agitated samples and were not observed in unstirred samples.

3.1.5 Turbidity Measurements

As already mentioned above in chapter 2.6, nephelometric studies have been reported for the characterization of metastable zone widths of supersaturated lysozyme solutions (Maosoongnern 2012). Liquid-liquid separations may lead to false measurements when observing nucleation, as any liquid droplets present in the solution will scatter – in addition to any particles - and, as a consequence, a reduction in the transmitted light intensity will result, even in the absence of crystalline particles. Some caution is therefore necessary when making these measurements and additional controls are required to distinguish between nucleation and liquid-liquid separation. Maosoongnern *et al.* (Maosoongnern 2012) briefly mention the possibility of liquid-liquid separation in the context of nucleation from protein-rich droplets, but fail to draw the full consequences and at no point is it made clear that an independent verification of the occurrence of nucleation was carried out. Moreover, several identical experiments were performed, each using fresh solutions of identical composition, resulting in a very small experimental error with respect to the cloud point temperatures determined, which strongly suggests that the authors indeed observed liquid-liquid separation rather than nucleation: the former is a thermodynamic event and must occur at the same temperature for solutions with identical composition, whereas the latter is a stochastic event, for which larger variations should be expected.

Moreno *et al.* (Moreno 2000) use turbidity information derived from DLS data and extract qualitative information on growth mechanisms of a number of proteins from these data. The increase in turbidity is expected to be linear with concentration of either protein or precipitant, providing the growth of aggregates proceeds via a random process, *i.e.*, different sized aggregates coalesce with other, randomly sized aggregates. The turbidity is expected to follow a parabolic curve if growth occurs via a regular, stepwise addition of molecules to the clusters. The data presented appear to exhibit more complex behaviour than expected from these two growth modes, yet for some of the proteins approximately linear or quadratic behaviour is indeed observed. For others, random changes of turbidity with concentration are interpreted as characterising solution conditions not conducive to crystallization, as confirmed by independent crystallization experiments.

3.1.6 Generalised Solution Phase Diagram

The following two chapters discuss trends in crystal nucleation research, which appear to call into question classical nucleation theory. Prior to discussing these trends, it is instructive and useful to review the theoretical phase behaviour of solutions, as illustrated in Figure 19. It must be stressed that this diagram is, of course, a simplification as it contains merely one concentration variable. For simple solutions containing a single solute and a single solvent this is of course sufficient. For more complex solutions, as are typically found encountered in the case of protein crystallization, this concentration variable must be viewed as a generalisation of the concentrations of the individual solutes influencing the solubility of the

protein, that is all components of the protein crystal as well as any electrolytes, such as buffer salts and acids/bases, that are not components of the protein crystal itself, but modify the solubility.

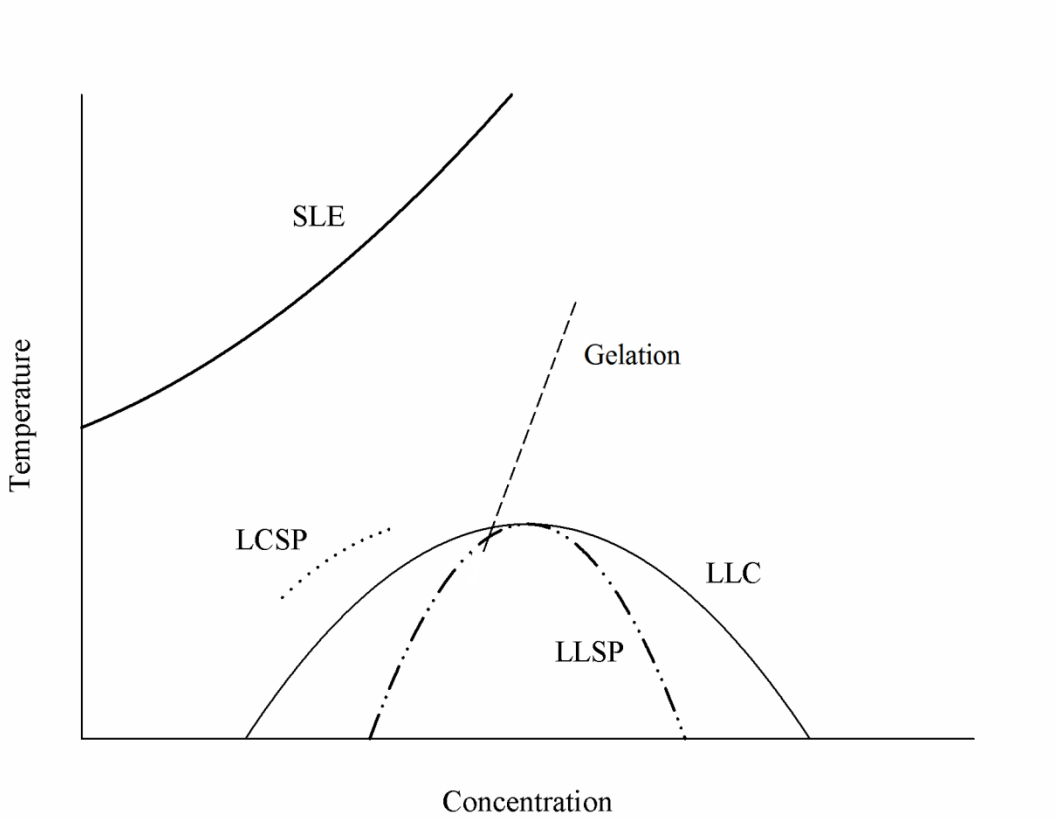

Figure 19: Generalised phase diagram for protein solutions. The thick solid line (SLE) represents the solid-liquid equilibrium, the thin solid line (LLC) the liquid-liquid coexistence line where two liquids with distinct compositions coexist. The dot-dashed line (LLSP) is the liquid-liquid spinodal where energy barrier for the separation of the two liquid phases vanishes. In analogy to this line in the phase diagram, Vekilov (Vekilov 2010) defines the liquid-crystal spinodal (LCSP, dotted line), as those points where the energy barrier for nucleation vanishes. The dashed line represents the boundary for gel formation.

Figure 19 depicts the behaviour of a generalised solution phase diagram as a function of concentration according to Vekilov (Vekilov 2010). It contains only one equilibrium line, namely the familiar solid-liquid equilibrium denoted SLE. At the concentrations and temperatures specified by this line a crystalline solid is in equilibrium with the, saturated, solution.

Above the SLE, the solution is undersaturated, below it is supersaturated and metastable. As soon as crystalline particles of the solute are introduced into the solution in the metastable region, be it by nucleation or by seeding, these will grow as long as the solution is supersaturated. This leads to a depletion of amount of solute in solution until equilibrium is achieved. As discussed above, according to classical nucleation theory, the probability of – primary – nucleation occurring, and with that the nucleation rate, will increase with increasing supersaturation.

A second curve, denoted LLC, represents a submerged liquid-liquid phase separation. Above this curve the solution is stable with respect to liquid-liquid separation, *i.e.*, only one liquid phase is possible for a given solution composition and temperature. Below the curve, however, the solution is metastable with respect to a liquid-liquid phase separation and will separate into two distinct liquids of differing composition, except at the upper consolute temperature T_c, or critical point, where the two liquids have identical composition. Since the submerged LLC curve lies beneath the solubility curve, once it has been traversed and the region of metastability of the solution to liquid-liquid separation has been reached, the solution can return to equilibrium by one of two paths. The first involves direct nucleation of the crystalline solid, the second involves two nucleation steps, first nucleation of liquid droplets of a dense liquid phase followed by nucleation of the crystalline solid in either of the liquid phases, as both remain supersaturated and are thus metastable with respect to crystallization. Considering CNT, nucleation of the solid phase will be more likely in the dense liquid due to the higher supersaturation compared to the dilute liquid. Curve 2 is characterised by a vanishing partial first derivative of the Gibbs free energy of mixing ΔG^{mix} of the solution components with respect to concentration (expressed as molar fraction x), *i.e.*:

$$\frac{\partial \Delta G^{mix}}{\partial x} = 0 \qquad \textbf{3.1.6-1}$$

The third, dashed curve represents those points in phase space, where the curvature of ΔG^{mix} with respect to concentration changes vanishes, *i.e.*, this partial second derivative of the Gibbs free energy of mixing vanishes. This curve is called the spinodal and below it the solution becomes labile and separates spontaneously as a result of density (concentration) fluctuations at the molecular level. At the upper consolute temperature the LLC and the spinodal coincide. In contrast to the metastable regions in phase space, where density fluctuations are compensated for by means of 'down-hill' diffusion, *i.e.*, the diffusion coefficient is positive and diffusion of a species is towards those regions in space which are relatively poorer in that species, the diffusion coefficient in the labile region is negative and a density fluctuation leads to diffusion in the direction of increasing concentration. As a consequence, a phase separation occurs without a nucleation barrier. This type of phase separation is called spinodal decomposition. The result, in any case, is the formation of continuous regions in space which are enriched or depleted with respect to a given chemical species, all the while remaining supersaturated with respect to crystallization. Once inside the phase space delimited by the spinodal, the system will ultimately relax by forming two liquids with compositions defined by the two intersects of the isotherm containing the initial composition of the single liquid phase with the spinodal. Again, providing the thermodynamics of the system are of the type shown in Figure 19, all liquid-liquid phase separations lead to new phases that are metastable with respect to the solid-liquid equilibrium and must, eventually, relax to the state corresponding to the equilibrium at the given conditions of composition, temperature and pressure. It is only natural to expect that those regions richer in the solute should show enhanced formation of solid particles.

Two further curves are shown in Figure 19, neither of which represents a true phase transition. The first of these, the gelation line, delimits that region in phase space, where the formation of a gel is observed. Gel formation is characterised by a rapid increase in the viscosity of the solution, due to the formation of an extended network of solute molecules leading to a dynamically frustrated state, while the structural characteristics of a liquid are maintained. Such 'transitions' are frequently observed in concentrated protein solutions.
The second of these additional curves is the so-called 'crystallization spinodal'. This line is defined by a critical nucleus size of 1 molecule, which effectively means that the thermodynamic barrier for crystallization vanishes. This phenomenon will be discussed more fully in chapter 3.1.8, below.

3.1.7 Liquid-Liquid Phase Separation as a Precursor to Nucleation

It has been noted on several occasions in the past, that protein solutions frequently exhibit a liquid-liquid phase separation prior to nucleation. Alber *et al.* (Alber 1981) reported the crystallization of a new crystal modification of yeast triose phosphate isomerase from poly(ethylene glycol) where the solution undergoes a liquid-liquid phase separation prior to nucleation in the dense, discontinuous phase. Careful analysis of the two liquid phases reveals that the protein is found exclusively in the dense liquid yielding a concentration 2.5 times higher than in the initial, homogeneous solution. The PEG concentration as well as the amount of water in both phases was found to be similar, though the uncertainty in determining these concentrations was estimated to be high.
Liquid-liquid separation of aqueous solutions of bovine γ-crystalline, a lens protein, was studied by Thomson *et al.* (Thomson 1987) using light scattering and chemical analysis of the phases. Light scattering provides easy access to the temperature of phase separation, which is taken as the average value of measured cloud and clear points for a solution of given composition which is cooled and heated, respectively. In order to determine the chemical composition of the separated phases, solutions were rapidly quenched to a temperature below the coexistence line and the two liquids were allowed to separate. The protein concentration in the respective solutions were determined and found to agree with the phase separation temperature determined previously. Using a mean-field approach, the critical point of the coexistence curve was calculated from the available data. The spinodal for the system could only be estimated from light scattering data since the liquid-liquid phase separation interfered with the measurements.
A consequence of liquid-liquid separation prior to nucleation is that, after the separation has occurred, there are two new phases of different composition within which nucleation can occur, one depleted in protein with respect to the single liquid phase and one rich in protein. The former generally presents as the continuous phase and the latter as the discontinuous phase. Providing that the entire liquid-liquid binodal lies under the solubility curve, both of these phases are supersaturated with respect to nucleation of the crystalline solid and as such, nucleation can occur in either of the two phases, while the nucleation rate will be higher in the

dense phase due to the increased supersaturation. It is therefore no surprise that nucleation was observed in the dense liquids in the above studies.

3.1.8 Two-Step Nucleation Model

The observation of liquid-liquid separation in protein solutions followed by crystallization in the dense liquid phase has resulted in a critical re-evaluation of classical nucleation theory, with some researchers going as far as suggesting that liquid-liquid separation is a necessary prerequisite for crystal nucleation (Gliko 2005, Heijna 2007). A recently proposed two-step nucleation model (Galkin 2000a, Vekilov 2004, Kashchiev 2005, Vekilov 2005, Vekilov 2012a) is frequently cited in this context. In this section, this two-step model is discussed with the aim of dispelling some common misunderstanding surrounding the model and its use to justify the view that liquid-liquid separation (or even spinodal decomposition) is a necessary prerequisite to nucleation.

Whereas CNT is based on the premise that the building blocks of an ordered crystalline solid initially aggregate randomly from the homogeneous, metastable solution, the two step model explicitly requires two order parameters to describe the nucleation process (Vekilov 2005). Specifically, these order parameters describe the transition along a concentration (density) coordinate and along a coordinate characterising the structural ordering of the solute molecules. The use of two order parameters in the two step model allows the overall formation of crystalline nuclei to be separated into two processes. The first is the formation of dense liquid clusters, the second process is the establishment of structural order within these cluster. Using two order parameters to characterise the liquid-solid transition, first promulgated by Landau and Lifshitz (Landau 1996), remedies a weakness in Gibbs's work on the thermodynamics of phase separations (Gibbs 1928), where only one order parameter is required, which may suffice for fluid-fluid phase transitions, but is indeed questionable for the liquid-solid phase transition.

The two-step model was developed as a consequence of the following experimental observations:

1. Evidence from dynamic light scattering suggests the existence of large clusters with a correlation time several orders of magnitude larger than that for molecular diffusion.
2. Plots of the nucleation rate vs. the logarithm of the supersaturation reveal a discontinuity.
3. For a solution of constant composition, the nucleation rate exhibits a maximum with decreasing temperature.

The first step of the two-step model, the formation of dense clusters, serves to explain the observation mentioned in point 1 above. DLS measurements on protein solutions (Georgalis 1997a, Follmer 2004, Poznanski 2005) appear to reveal two processes in the solution with correlation times that differ by several orders of magnitude. The first process corresponds to Brownian motion of the individual protein molecules. The correlation time of the second

process, while independent of the protein concentration, does depend upon the protein under investigation and ranges from a few μs for lysozyme and haemoglobin (Onuma 2007, Pan 2007) to several seconds for lumazine synthase (Gliko 2005).
The amplitude of the feature in the inverted DLS data that is associated with this second process is concentration dependent and increases with increasing protein concentration. It was observed, that the second feature appears rapidly and within a few seconds of generating the solutions. This behaviour was interpreted as evidence for the formation of dense clusters of solute, also called dense liquid droplets, in the solution. The clusters were estimated to contain of the order of 10^6 solute molecules and have a density closer to that of the crystalline solid than that of the bulk liquid. (It should be noted that the solutions investigated, in the case of lysozyme, had protein concentrations of around 30 - 80 mg mL^{-1}, while the clusters were estimated to have protein concentrations of the order of 300 mg mL^{-1}. Crystalline phases of lysozyme have concentrations of between 760 and 950 mg mL^{-1}.) While the size of these clusters does not vary over time, their number increases with increasing bulk protein concentration, explaining the concentration-dependent amplitude.
It must be noted, that the formation of clusters is not a classical thermodynamic phase separation process, but rather a meso-scale density fluctuation, a dynamic feature of the solution. Although their formation appears to be instantaneous, the correlation time obtained from DLS can be (and indeed is, see (Georgalis 1997a, Galkin 2007, Onuma 2007, Pan 2007, Li 2011)) interpreted as a life-time for these clusters. Since they form and decay, they cannot represent a thermodynamically stable phase with respect to the bulk liquid. Indeed, they are observed in the metastable single-liquid region of the phase diagram. Evidence for the existence of these clusters in the stable, undersaturated liquid, above the SLE, has been reported (Gliko 2007). The comparatively long correlation time of the clusters has led to their description as metastable dense liquid droplets, which might lead to considerable confusion were these droplets interpreted as a distinct liquid phase.
Since the process of cluster formation is rapid, it is not rate-determining. The rate determining step for the formation of the crystalline solid according to the two-step model is the structural ordering within the dense clusters. Vekilov proposes the following rate equation (Vekilov 2012b) for this process:

$$J = \frac{k_2 c_1 T}{\eta(c_1,T)\left[1+\frac{U_1}{U_0}\, exp(\frac{\Delta G_c^0}{k_B T})\right]}\, exp(-\frac{\Delta G_2^*}{k_B T}) \qquad \textbf{3.1.8-1}$$

The energy barrier for nucleation within the dense clusters is ΔG_2^* and it is this quantity which is used to define the 'crystallization spinodal' already mentioned in chapter 3.1.6 above. The pre-exponential factor is determined by the concentration of solute in the cluster c_1, a scale factor k_2, the viscosity of the clusters $\eta(C_1, T)$, the ratio of the rate of decay U_1 and the rate of formation U_0 of the clusters and the excess Gibbs free energy ΔG_c^0 of the solute molecules in the cluster with respect to the Gibbs free energy of that same molecule in the bulk solution. This excess Gibbs free energy is estimated to be of the order of 10 $k_B T$, where k_B and T take their usual meaning.

The slope of the nucleation rate vs. the logarithm of the supersaturation can be employed to derive the size of the critical nucleus. Any discontinuity in the relationship between rate of nucleation and supersaturation implies a change in the critical nucleus size. Nucleation rate measurements for lysozyme chloride (Galkin 2000b, Galkin 2001) reveal such a discontinuity (point 2, above). Depending upon the composition of the solution, the critical nucleus is initially constant with increasing supersaturation and the nucleation rate increases with increasing supersaturation. However, for the highest precipitant concentration studied by Galkin and Vekilov (Galkin 2000b, Galkin 2001) the nucleation rate exhibits a discontinuity with respect to the supersaturation and remains constant after this point and the critical nucleus size becomes one. As a consequence, the energy barrier for nucleation vanishes and it is this point that Vekilov uses to define a 'crystallization spinodal'. The term 'spinodal' is used in analogy to the liquid-liquid spinodal discussed above, where the barrier for nucleation of liquid droplets in a metastable liquid phase disappears. It does not, however, imply any other mechanistic or even thermodynamic similarity of the liquid-to-solid phase transition to the liquid-liquid spinodal decomposition. In fact, the nucleation rate of the crystalline solid remains finite below the 'crystallization spinodal' and the only significance of the vanishing energy barrier for nucleation is that the rate of nucleation is then governed solely by the pre-exponential factor once the crystallization spinodal has been crossed. Furthermore, the 'crystallization spinodal' does not imply or even require a liquid-liquid phase separation of any type. Quite the contrary, it is reported to lie within the metastable single liquid region of the phase diagram for the case of lysozyme and thus within a region of phase space where a thermodynamic liquid-liquid separation is not possible.

The temperature dependence of the nucleation rate (point three) is explained in terms of the viscosity of the clusters. Whereas the viscosity of the bulk solution varies only weakly with temperature in the temperature range studied, it is surmised, that the viscosity of the clusters is significantly higher than that of the bulk liquid and that their viscosity exhibits a considerably stronger temperature dependence. These assumptions are sensible, considering the estimated density of the clusters and a strong increase in viscosity with decreasing temperature would have a noticeable effect upon the nucleation rate. In addition, the cluster size is assumed to decrease with decreasing temperature. The second term within the bracket of the denominator of the rate Equation 3.1.8-1 represents the inverse of the volume fraction of clusters in the solution. Vekilov (Vekilov 2011) states that the cluster volume fraction decreases with decreasing temperature, an effect that then contributes to the decrease in nucleation rate.

A further, quantitative argument against classical nucleation theory is given by Vekilov (Vekilov 2010), which concerns the magnitude of the nucleation rate observed for protein solutions. With reference to measurements first published by Galkin and Vekilov (Galkin 2000b) and already mentioned above, and estimating the magnitude of the variables determining the pre-exponential factor A (Equation 3.1-2), the experimental nucleation rate is found to be 10 orders of magnitude lower than that estimated from CNT. In contrast, an estimate based upon the estimated concentration, viscosity and volume fraction of the clusters, results in a closer match of theory to experiment.

While the two-step nucleation model is interesting, it leaves a number of open questions. First and foremost one must ask the question whether the model in fact presents anything new, or whether it merely represents a different perspective on one and the same phenomenon. Formally and qualitatively, the rate equation presented for the two step model is equivalent to that derived from classical nucleation theory, even if differing with respect to the physical variables that appear in the respective models. Starting from this point of view, one can question whether the main difference is merely subtle and a consequence of the rapid formation and long life time of the clusters observed, which, as a result, requires a change of reference state from the homogeneous, dilute solution, to the denser clusters. One must not forget that the formation of clusters is an integral part of CNT, as the nucleation rate is controlled by the stability of the clusters while the dynamics of formation and decay are not explicitly addressed.

In addition, the observations of dense clusters in a few protein solutions is not sufficient to claim universality of the two-step mechanism and too little evidence from other crystallizing solutions has been provided in order to generate confidence in the model proposed. The nature of the clusters observed in DLS measurements is intriguing and merits further investigation, in particular with respect to their internal dynamics. High viscosity within the clusters is of course a convincing argument for the slowing of the nucleation rate with decreasing temperature, but such arguments have been presented previously for viscous melts, where a similar phenomenon has been observed, and quantitative analysis of experimental nucleation rates from viscous fluids has been reported using variations of CNT incorporating an additional viscosity term (see for example (Mullin 2001) and references therein). Clearly, a new theory is not necessary to explain the experimental observations, while its premises are certainly sensible and worth further experimental qualification. Obviously, a deep, molecular-level understanding of crystal nucleation is still a somewhat distant prospect.

3.2 Crystal Growth

Investigation of the growth of protein crystals has been a very active research area, driven to a large extent by the need to understand those factors influencing crystal growth that also have an impact upon the diffraction quality of single crystal in order to control these effectively.

Since crystal growth is a complex process the literature is broad and individual contributions generally – and necessarily – focus upon a particular aspect of the process or upon specific techniques for the investigation of growing crystals. Due to the size of protein molecules, they are uniquely suited for investigations by imaging techniques such as atomic force microscopy, yielding valuable information on mechanistic aspects of protein crystal growth. Only few studies are available on overall growth rates and the growth properties at scales and under conditions relevant to mass crystallization and, despite the breadth of studies mentioned above, the vast majority or publications is concerned with the model protein lysozyme.

This chapter is not intended to provide an overview of crystal growth theory. There exists a plethora of primary and secondary literature the reader may refer to (see for example (Ohara

1973, Myerson 1993, Saito 1996, Mullin 2001, Mutaftschiev 2001) and references therein) and this aspect of crystallization is too broad to cover adequately in anything other than a dedicated monograph. Rather, an overview of the recent literature concerned with protein crystal growth will be provided and discussed with regard to its relevance to large-scale mass crystallization of proteins.

3.2.1 Growth Rate Measurements

Prior to discussing growth rate measurements, it is important to recall that different measures for crystal growth can be defined. The growth of a crystal can be viewed as the result of the growth of individual crystal faces. In the absence of external factors resulting in growth rate dispersion (Tavare 1985, Ulrich 1989, Judge 2010), symmetry-equivalent crystal faces will have identical growth rates while crystallographically distinct faces will exhibit different growth rates due to the differences in their surface chemistry. Indeed, the different growth rates for distinct crystal faces result in the characteristic crystal habits in the case of stable growth.

The growth of a single crystal face can be defined by means of a linear growth rate $v_{(hkl)}$. This growth rate will depend upon the local supersaturation at the crystal-liquid interface and thus the temperature at which growth takes place. Generally the linear growth rate can be expressed by a simple correlation with the supersaturation:

$$\boldsymbol{v_{(hkl)} = K\,\Delta c^{g'}} \qquad \textbf{3.2.1-1}$$

where K is the growth rate, Δc the supersaturation and g' the growth exponent.

Measuring a face growth rate is straightforward and can be carried out by simple observation of the propagation of a given face of an otherwise immobilised crystal with time under defined conditions of supersaturation.

While interesting, this measure of growth is of little relevance to industrial mass crystallization as it does not provide useful information for a population of crystals, even for highly symmetric crystals with no or few crystallographically distinct faces. Factors such as local compositional inhomogeneity or growth inhibition due to the presence of impurities and their interaction with the crystal surfaces result in a distribution of growth rates for crystallographically identical crystal faces in a population of crystals. This distribution of growth rates is the previously mentioned growth rate dispersion.

In order to define the growth characteristics of a population of crystals, statistically significant, averaged face growth rate data would be required, which to obtain is unfeasible with individual face growth rate measurements. However, two other measures of crystal growth are available, which are (comparatively) easy to obtain employing simple batch crystallization experiments. The first of these is the overall linear growth rate G, which is defined as:

$$G = \frac{m_i^{1/3} - m_f^{1/3}}{(\alpha \rho N)^{1/3}\, t} \qquad \textbf{3.2.1-2}$$

Where m_i and m_f ate the initial and final masses of a defined number N of crystals, ρ their density and α a shape factor. The mass deposition rate R_G is defined via the differential equation:

$$R_G = \frac{1}{A}\frac{dm}{dt} = K_G \cdot \Delta c^{g''} \qquad \textbf{3.2.1-3}$$

i.e., the rate of change of the mass of a population of crystals with time, normalised to the surface area of the initial population of crystals. Equation 3.2.1-3 neglects the change in surface area with progression of the growth process and corrections to account for the growth-dependent surface area are available (Mullin 2001). The mass deposition rate can be expressed in a manner equivalent to the linear growth rate, Equation 3.2.1-1 above, while the rate constant and exponent are not the same as those for linear growth, as indicated by the use of subscript and primes to distinguish the mass deposition parameters from the linear growth parameters.

Both the overall linear growth rate and the mass deposition rate can be determined using suitable experimental procedures using, for example, fluidised beds or batch crystallization methods.

3.2.1.1 Overall Linear Growth Rates

As for crystal nucleation discussed in chapter 3.1 above, Schlichtkrull provided perhaps the earliest systematic study on protein crystal growth as part of his series of papers on insulin (Schlichtkrull 1957a, Schlichtkrull 1957b, Schlichtkrull 1957c).

In (Schlichtkrull 1957a) the nucleation and linear growth rates of rhombohedral bovine zinc insulin are investigated and discussed. The author extracts growth information from large scale (4 L) crystallization experiments (described in detail in (Schlichtkrull 1956)) both by measuring the time-dependent desupersaturation of the solution and by counting and analysing the size and size distribution as well as volume and surface area of the crystals in samples taken from the crystallizing solution. In order to avoid continuing growth of the insulin crystals after the samples have been taken, the crystallization is arrested and insulin solubility is reduced by adding a suitable buffer solution. In analysing the data the assumption is made, that the linear growth rate is the same for all crystal sizes present and the applicability of this assumption is demonstrated for different size classes and for the later stages of the crystallization process. In the early stages of crystallization deviations are observed. Since there is no seeding in the process, one may assume that the differences observed are caused by nucleation.

The growth rate is found to be proportional to the square of the difference between the actual concentration of insulin at the point of sampling and the final concentration of insulin. While it is reasonable to assume that this concentration difference represents the supersaturation

with respect to insulin, Schlichtkrull himself (Schlichtkrull 1957a) expresses uncertainty as to whether this is the case due to evidence from auxiliary experiments that suggests that the final insulin concentration may not represent the equilibrium concentration or solubility. Interestingly, porcine insulin growth appears to be a function of the cube of the 'supersaturation' or difference between the actual concentration at the time of sampling and the final insulin concentration at the end of the experiments (Schlichtkrull 1957c).

In the sixth paper of the series on insulin crystallization (Schlichtkrull 1957b) investigates the face growth rate of porcine insulin. Porcine insulin crystallizes as rhombohedral crystals under the conditions of composition and temperature employed. The growth experiments are carried out in two steps. In the first step small crystals are allowed to grow in a solution containing a dye, which is incorporated into the protein crystal. In the second step, the stained crystals are allowed to continue to grow in one of two solutions. The first is identical to the initial solution with the exception that the dye is absent and the second has a different overall composition. Although no numerical values for the growth rate are given, the face growth rate reported to follow the same 'supersaturation'-dependence as the overall linear growth rate. Interestingly, the stained seed crystals are all observed to lie at one of the vertices of the final crystals after the second growth phase. This clearly demonstrates that the space group representing the crystal structure is polar and that the respective faces of the rhombohedron are not symmetry-equivalent. In fact there exist two sets of three equivalent faces, of which one set of three grows with a considerably greater rate that the second set. If the six faces of the rhombohedron were to grow with the same or similar rates, the stained seed crystal should be observed in the centre of the final crystal and not at one of the vertices.

Almost four decades later Judge *et al.* (Judge 1995) presented a study of bulk crystal growth of ovalbumin using a 1 L batch crystallizer. With the benefit of more refined analysis techniques and a better, *a priori,* knowledge of the solubility and metastable zone of ovalbumin than that available to Schlichtkrull (Schlichtkrull 1957a) when studying insulin earlier, the influence of nucleation could be minimised by seeding the crystallising solutions thus allowing a better quantitative understanding of crystal growth. The crystallizing solutions are analysed in terms of desupersaturation, change of protein content in the solid phase and size distribution, which is measured by means of laser light scattering. The cumulative size distributions obtained for different crystallization times reveal a parallel shift towards larger sizes with increasing time. On the one hand this indicates that little to no nucleation, primary or secondary, takes place during the crystallization process. On the other hand, aggregation and agglomeration can also be deemed negligible. Overall growth rates are extracted from the spatial propagation of the distribution functions with time. The growth rate thus determined is relative to the change in volume of the crystals, which can be converted to linear growth rate using appropriate geometric conversion factors derived from the observed shape of the crystals.

The growth of ovalbumin determined in these experiments was found to follow a second order rate law, as was the case for bovine insulin described above. The face growth rate was found to be of the order of $1.67 \cdot 10^{-7}$ m/s when converted to an overall linear growth rate.

Interestingly, the growth rate was found to be relatively insensitive to the concentration of the precipitant – in this case ammonium sulfate – while the pH had a profound effect upon crystal growth, increasing the rate constant by a factor of 10 when the pH was decreased by a factor of less than one. This suggests a linear dependence of the growth constant on the proton concentration.

3.2.1.2 Face Growth Rates

The major focus of protein crystal growth studies has been on face growth rates and atomistic growth mechanisms. The latter will be discussed in the next chapter, 3.2.1.3.
Several publications have reported investigations of the face growth rates of tetragonal lysozyme chloride (Forsythe 1994, Nadarajah 1995, Gorti 2005). This crystal modification of lysozyme possesses only two forms, namely {110} and {101}. The form {101} contains four symmetry equivalent crystal faces that form a square prism, which is capped at either end by four of the eight symmetry equivalent faces of the form {110}. Consequently, only one of the symmetry equivalent faces in each of the two forms has to be considered when discussing face growth rates, conveniently the faces (110) and (101). These two faces have different growth rates due to their differing surface chemistry, and the supersaturation-dependence of these growth rates also differs, which leads to a pronounced dependence of the morphologies of tetragonal lysozyme upon the growth conditions while the crystal habit remains constant (Figure 20).

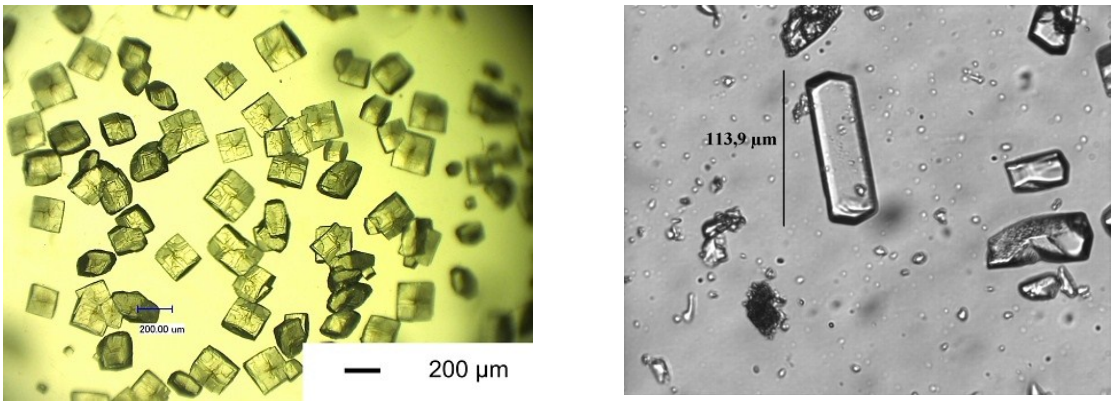

Figure 20: Growth morphology of lysozyme chloride. Left: crystals obtained at pH = 4.4 in the presence of 4 %(w/v) NaCl (image generated by V. Diaz Borbon) . Right: crystals obtained at pH = 5.0 and 2 %(w/v) NaCl (image generated by N. Aldabaibeh). The two forms are evident. In the left hand image the {101} form dominates, which caps the prism generated by the {110} form, leading to equant crystals. In the right hand image the {110} form dominates, leading to elongated crystals. While the habit remains constant, the aspect ratio depends upon the growth conditions.

Forsythe and Pusey (Forsythe 1994) quantified this behaviour in their investigation of the face growth rates of the two crystallographically distinct faces of tetragonal lysozyme chloride as a function of temperature and precipitant (NaCl) concentration. A modified version of the apparatus previously described by Pusey and Naumann (Pusey 1986) was employed. At constant salt concentration, the growth of both faces is protein concentration and temperature

dependent and for all temperatures studied the growth rate increases with temperature and with protein concentration. At constant temperature, the growth rate therefore increases with increasing supersaturation. However, at the same supersaturation, the growth rate decreases with decreasing temperature and the authors interpret this seemingly unexpected result in terms of the solution properties and assuming that the growth unit for tetragonal lysozyme chloride is not the protein monomer, but rather a pre-structured aggregate. Providing the formation of these aggregates is a rate limiting step in the growth kinetics, the lower growth rate would suggest a lower rate of formation of these clusters in solution at lower temperatures. This, however, is to be expected, as the supersaturation is a relative measure and obscures the fact, that the absolute concentration can be vastly different for the same supersaturation if a strong temperature dependence of the equilibrium concentration exists.
The precipitant concentration dependence of the face growth rates observed for the (101) and the (110) faces appears to be negligible. A plot of the growth rate of both faces as a function of supersaturation for two different salt concentrations shows little effect from the salt concentration at constant temperature. However, the curvatures and the slopes of the growth curves for the two faces differ significantly. This asymmetry is the cause for the pronounced effect of the crystallization conditions on the morphology of the crystals as discussed above and the driving force for the morphology change is clearly the supersaturation.

3.2.1.3 Mechanistic Studies

The greater size of protein molecules in comparison to small organic molecules and inorganic salts results in a greater size of features on the surface of a crystal resulting, for example, from dislocations or from the deposition of clusters of solid formed in solution. This makes the surfaces of protein crystals amenable to visualisation techniques such as atomic force microscopy (AFM), enabling the study of crystal growth mechanisms at the atomic level. Several research groups have recognised this and have exploited AFM to gain a better understanding of the growth mechanisms governing protein crystal growth.
Since the atomistic mechanism of crystal growth has a direct bearing on molecular discrimination and therefore the purification effect of a crystallization process, it is of interest to discuss the results of some selected studies briefly.
Although tetragonal lysozyme chloride has been employed as a model system for AFM studies of crystal growth mechanisms in protein crystals (Durbin 1993, McPherson 1999), a number of other proteins such as porcine α-amylase (Astier 2001), bovine pancreatic trypsin (Plomp 2001) and porcine insulin (Gliko 2003) have also been investigated.
A common result in these studies is that protein crystal growth follows the same mechanistic principles already established and accepted for small molecule growth. At low supersaturation growth occurs at step dislocation in accordance with the BCS growth theory and the steps have a spiral topography resulting from screw dislocations. At moderate to high supersaturation a 2D surface nucleation mechanism (also known as Birth and Spread) takes over from step growth, where larger clusters of solute formed in solution are deposited on the surface and integrated into the crystal structure.

4. Crystallization Process Technology – Applicability to Protein Products

One obvious choice of process for the crystallization of proteins based upon the discussion of the thermodynamics of protein crystallization in chapter 2 above is batch salting-out (or, alternatively or even in combination, applying a pH-shift or using an 'antisolvent', see chapter 4.2) crystallization from solution. Why this is not necessarily a sensible choice will be discussed in the following, together with a number of alternative approaches and technologies that have been shown to be useful for protein crystallization.

4.1 Solution Crystallization

With the clear dependence of protein solubility upon pH and precipitant concentration as discussed in chapter 2 above as well as in the literature cited, it is only natural to assume that salting-out of the protein from a solution, perhaps in combination with a pH-shift, is the straightforward choice of process. Such a process could be isothermal, or if sufficiently large yield improvements were expected from known solubility data at different temperatures, polythermal in nature.

Indeed, crystallization of proteins – or to be more precise, precipitation – has been used as a method of separation for more than a century. Osborne and Campbell (Osborne 1900) for example, first described the fractionation of proteins from egg white using various dilutions of ammonium sulfate and acidification of the successive filtrates, a process later re-investigated in some detail by Sörensen and Young (Sörensen 1934, Young 1937). Osborne and Campbell (Osborne 1900) identified four major protein fractions in his work, at least one of which was visibly crystalline. Two decades later Fleming (Fleming 1922) identified lysozyme as a component of egg white and other tissues and physiological fluids and purification methods were subsequently developed (Meyer 1936, Roberts 1937, Abraham 1939, Alderton 1945), of which that proposed by Alderton *et al.* (Alderton 1945) was based upon crystallization of this particular enzyme. Warner (Warner 1954) later summarised the then state-of-the-art in egg protein knowledge, including separation methods. This review contains a detailed flow chart illustrating the steps for isolating the proteins from egg white known at that time.

Protein crystallization is indeed employed industrially, though very little has been published in the scientific literature. The manufacture of insulin, for example, a polypeptide used for the treatment of diabetes, can include a crystallization operation (Barfoed 1987, Brader 2000, Strube 2011), though this process step is not used for purification of the peptide, but rather for form-giving and particle shape and particle size control.

Judge and co-workers (Judge 1995) pointed out the potential of bulk crystallization for the isolation and purification of proteins in their study of ovalbumin. Based upon the procedure described by Warner (Warner 1954) a detailed investigation of the crystallization process at a

scale of several 100 mL and in terms of nucleation, growth kinetics and purification efficiency was reported. It is not known to this author, whether any industrial implementation of this process exists and in view of the fact that ovalbumin itself is of little value, deemed unlikely.

In his paper entitled 'Crystallization of Proteins is an Exacting Task but can be Successfully Applied in Industry', Visuri (Visuri 2000) discusses the general requirements for protein crystallization on an industrial scale and also provides an example of a real process for the purification of glucose isomerase implemented at Genencor's production facility in Hanko, Finland. Although the process is not discussed in great detail, an interesting comparison of economics and efficiency of the crystallization process compared to a chromatographic purification also considered in the development process is provided, and makes a compelling case for the use of crystallization rather than a chromatographic process. The crystallization process itself is described in a patent (Visuri 1987).

A later publication co-authored by Visuri (Vuolanto 2003) gives a detailed account of development work towards a scalable and reproducible seeded cooling crystallization process for the isolation of xylose isomerase from *Streptomyces rubiginosis*. The authors use magnesium sulfate as precipitating salt and avoid nucleation by seeding the supersaturated solution. Seeding also serves the purpose of controlling crystal size and size distribution in the product. Although the process described was rationally designed, the starting material used was previously purified xylose isomerase and not the fermentation broth it was derived from and as a result no conclusions can be drawn as to the applicability and performance of the method when applied to a more realistic manufacturing problem.

As discussed above, the vast majority of proteins manufactured on an industrial scale are produced for their enzymatic activity. It is therefore surprising that one discussion has been conspicuously absent from the literature, namely the effect of processing parameters upon the enzymatic activity. The activity must be considered as one of the primary product specifications, in addition to yield, purity and particle properties, as any deactivation of an enzyme diminishes its commercial value.

Enzymatic activity was initially highlighted as an important quality parameter by Jones and Ulrich (Jones 2005) and considered in detail in the studies carried out by Weber *et al.* (Weber 2008b, Weber 2008c). The work described in these papers is concerned with a solution crystallization process for the enzyme urease from jack beans (*canavalia ensiformis*). This particular enzyme was selected as much for historic reasons as well as for the challenges posed in extracting it from the raw material and then crystallizing the enzyme directly from the extracts, considering that the jack bean meal contains less than 0.1 % (by mass) urease.

Urease was the first enzyme to be crystallized (Sumner 1926b) and this work served to prove that enzymes are catalytically active proteins, earning Sumner a share in the 1946 Nobel Prize in Chemistry. The method used for isolating urease from jack beans has remained essentially unchanged since the first report. In contrast to the processes discussed above, the urease process consists of extraction of the enzyme (along with other proteins and non-proteinaceous soluble compounds) from dried bean meal using a binary solvent consisting of water and acetone with subsequent crystallization from the extract. Interestingly, the crystal structure of

jack bean urease was not published until 2010 (Balasubramanian 2010). The work described in the following aimed at investigating the effect of changing process parameters in the extraction and crystallization process upon the crystals obtained.

4.2 Case Study I: Extraction and Crystallization of Urease from Jack Bean Meal

The crystallization process as described by Sumner (Sumner 1926b) is simple. De-fatted jack bean meal is extracted with five volumes of an 'ice cold' acetone-water solvent containing 31.6 % (vol/vol) acetone. The meal-solvent slurry is stirred for a few minutes and then filtered. The filtrate is cooled to approximately 2 °C and left overnight, the crystals formed are centrifuged and the sediment is blot-dried with filter paper. Finally, the partially dried sediment is suspension-washed in fresh acetone-water solution and again separated from the solvent by centrifugation and blot-dried. While the initial paper does not consider alternative processing conditions, in a note published later the same year (Sumner 1926a) and prompted by a successful attempt at re-crystallizing the enzyme, Sumner provided additional consideration complementing the original publication and suggesting the extraction temperature should be raised to 28 °C to improve the extraction of urease while at the same time reducing the amount of other proteins extracted from the jack bean meal. It was also noted that the initial extract is slightly acidic with a pH = 6.1.

Noting that Sumner's method was not always successful, either as a result of the variability of the raw material, as already noted by Sumner (Sumner 1928b), or due to the extreme sensitivity of the enzyme to impurities such as metal ions (Sumner 1928a), the methodology was later re-examined, amongst others by Gorin, Hanabusa and Conway (Gorin 1960, Hanabusa 1961, Conway 1966). However, none of these took a systematic approached based upon processing parameters.

Starting from the initial method, Weber *et al.* (Weber 2008a, Weber 2008b, Weber 2008c) re-investigated the process by studying the impact of changes of the extraction solvent and its composition, the extraction temperature, solid-liquid separation, crystallization conditions such as cooling rate and the influence of additives. The influence of these and other parameters was characterised in terms of yield and purity as expressed via the activity and specific activity of the resulting enzyme crystals, respectively.

Urease catalyses the decomposition of urea to ammonium ions and carbon dioxide and its activity is easily quantified by measuring the amount of NH_4^+ generated under well-defined conditions according to the method described by Weatherburn (Weatherburn 1967). Although a standard unit of enzyme activity is defined as a derived unit (mol s^{-1}) in the SI system of units (the katal, see (BIPM 2006)), the unit "U" expressed as μmol min^{-1} is still commonly used as a measure of enzymatic activity. Irrespective of the unit used, it is always a function of the conditions under which it is measured, and these have to be specified. In the specific case of urease activity, a separate unit of activity is still in use and this is the so-called

'Sumner Unit' (S.U.), which is defined as the amount of enzyme which in five minutes produces, at 20 °C, 1 mg of ammonia nitrogen from a 3 % urea solution in a 9.8 % neutral phosphate buffer containing 2 % gum arabic (Sumner 1928a). In the following discussion the unit of activity used is 'U'. For the sake of comparison with older literature data, it should be noted that 1 S.U. ≅ 3.22 U.

The activity of an enzyme can be used as a measure of quantity and can therefore be used to assess, indirectly, the yield of protein from a process. Assessing the purity of the enzyme, however, is another matter. SDS-PAGE (Laemmli 1970) is a suitable but time consuming quantitative protein assay, which is also useful for providing a visual indication of the type and quantity of other proteins present in a given solution. A perhaps more useful and more rapidly assessed quantity for assessing enzyme purity is the specific activity, which is defined as the activity divided buy the total protein quantity present. Several colorimetric assays are available for measuring total protein content (Sapan 1999).

In this case study, both activity and specific activity were used to assess quantity and purity of urease extracted.

4.2.1 Extractions from Jack Bean Meal

Extractions were initially carried out from commercial jack bean meal provided by Fluka (94280), later from material imported from the USA (A.L. Jowitt, 612 Runaway Bay Drive, Bridgeport, 76426 Texas, USA). The four main extraction solvents investigated were (a) de-ionised water, (b) a binary solvent consisting of 32 % (v/v) acetone in de-ionised water, (c) a 0.1 M phosphate buffer at pH = 7 and finally, (d) 32 % (v/v) acetone in 0.1 M phosphate buffer at pH = 7. A series of three successive extractions, each with fresh solvent using the same aliquot of bean meal results in the activities of urease in the extracts shown in Figure 21. Clearly the amount of urease extracted in successive operations decreases for all solvents investigated. Interestingly, the 'Sumner-solvent' acetone-water is by far the least effective solvent for extracting urease, while pure de-ionised water performs best, both when comparing the first extraction and the overall amount of active urea extracted from the meal. However, the specific activity, which measures the purity of the protein, reveals a different picture, as seen in Figure 22. Here it becomes clear that the purity of urease suffers significantly, when other solvents are used. The highest specific activity is achieved with the classic 'Sumner-solvent' and the extract from water has a significantly lower specific activity. This behaviour clearly indicates that while solvents (a), (c) and (d) extract considerably more urease than the 'Sumner-solvent', they are also more efficient at extracting other proteins present in the bean meal.

Figure 23 shows a typical SDS-PAGE gel. Lane 4 in this gel shows that a large number of different proteins over the mass range 0 – 100 kDa are extracted using acetone-water. The urease band at 91 kDa is barely visible in this lane as it overlaps with several other proteins in the same mass range. In contrast, the crystals obtained from this extraction solvent show a clear and dominant urease band.

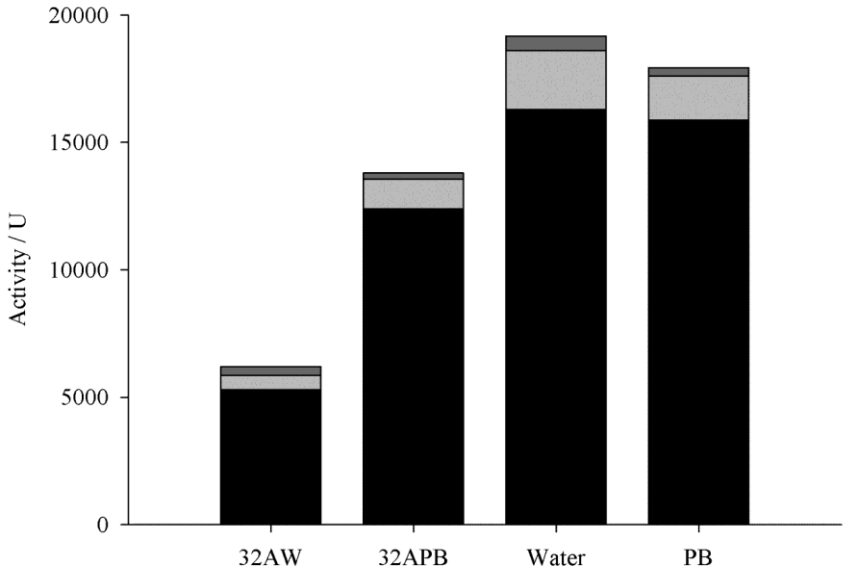

Figure 21: Cumulative urease activity obtained with three successive extractions of bean meal from different solvents. Black: first extraction, light grey: second extraction, dark grew: third extraction. The solvents are: 32 %(v/v) acetone in water (Sumner solvent, 32 AW), 32 %(v/v) acetone in aqueous phosphate buffer (32APB), Water, and phosphate buffer (PB). The same amount of bean meal is used for each solvent and for each extraction the same aliquot of meal is employed. Water extracts the largest amount of urease from the meal in each extraction step, while the Sumner solvent performs worst, extracting the least amount of urease.

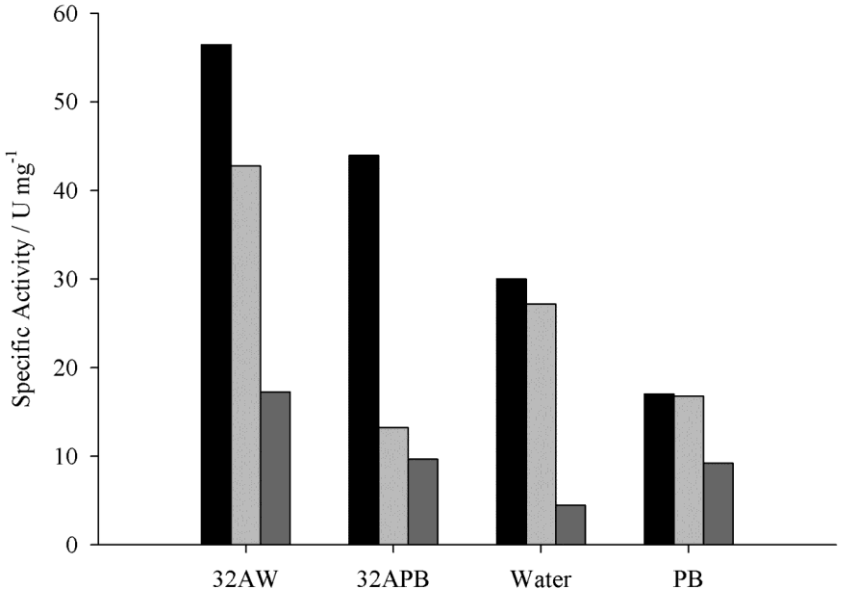

Figure 22: Specific activity of urease obtained with three successive extractions of bean meal from different solvents. Black: first extraction, light grey: second extraction, dark grey: third extraction. As in Figure 21 the solvents are: 32 %(v/v) acetone in water (Sumner solvent, 32AW), 32 % acetone in aqueous phosphate buffer (32APB), water, and phosphate buffer (PB). While the Sumner solvent extracts the least amount of urease, it is highly selective, resulting in the highest specific activity. Based upon this measure the phosphate buffer performs worst, *i.e.*, it extracts other proteins equally well as it does urease, resulting in a low specific activity.

The urease purity estimated from the optical density of the bands in this gel is of the order of 50 % and there are no major impurities. In comparison, the purest available commercial urease (Sigma-Aldrich, U0251) shows a similar degree of purity and contains one major impurity in approximately equal amount as urease. It is suspected that much of the impurity in the crystallized urease stems from mother liquor adhering to the crystals, as no suitable washing method for the crystal slurry was available (see chapter 4.2.3.5 below).

In order to better understand the role of acetone in the extraction solvent, two further experimental series were devised with the rationale of increasing both the active urease yield and purity. For this purpose the extraction from the meal was carried out in solvent (a) or in solvent (c) (high yield according to Figure 21) adding acetone to the extract after separation from the solids and to the same concentration as in solvents (b) and (d) (high purity, Figure 22). This process resulted in an intermediate precipitate after acetone addition. Interestingly, process modification resulted neither in increased yield nor improved purity when compared to the 'Sumner-solvent', but demonstrated that the main role of acetone in the latter is to modulate the solubility of precanavalin, a precursor to canavalin, which has a molecular mass of 49 kDa (Smith 1982).

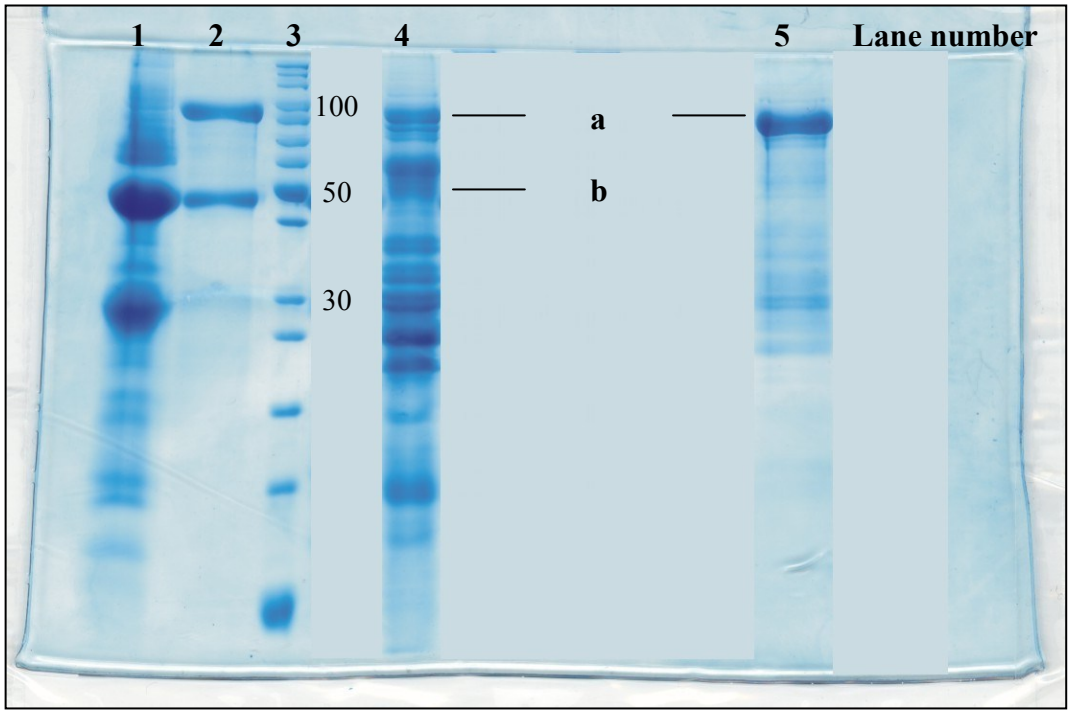

Figure 23: SDS-PAGE for different stages of the urease extraction and crystallization process. Lane 1: extract from bean meal using water as solvent. Lane 2: commercial urease (Sigma-Aldrich, purchase number U0251). Lane 3: reference proteins (Fermentas PageRuler #SM0661). Lane 4: extract from bean meal using acetone-water as solvent. Lane 5: crystallized urease. The urease band (a) is barely visible in the water extract, where precanavalin (b) is the major protein extracted. The molecular masses (in kDa) of three reference proteins are shown to the right of lane 3.

While the precanavalin content in the initial extracts is high, it is significantly reduced after addition of acetone and removal of the precipitate. Nonetheless, the amount of this protein and other proteins remaining in the extract after acetone addition is significant.

Variation of the acetone content in the binary system acetone-water showed that a reduction in the amount of organic solvent present results in an increase of urease activity – consistent with the observations made for the solvents (a) and (c) – while the specific activity decreases, whereas an increase in acetone content leads to a decrease of both activity and specific activity.

Poly(ethylene glycol) (PEG) was investigated as a replacement for acetone in the extraction solvent (Weber 2008c). PEG is a commonly used material in the crystallization of proteins and is known to be an effective crystallizing agent for large proteins (Vivares 2002). Here, the effect of two PEGs were studied, one with a mean molecular mass of 6000 g/mol and the other with a mass of 4000 g/mol. In addition to varying the concentration of the respective PEGs (Figure 24), pH variation was also investigated (Figure 25). It was found, that the presence of the polymer in fact reduces the amount of urease extracted and this reduction is greater at higher PEG concentrations for both molecular masses, as shown in Figure 25. In contrast, the specific activity in the extract initially increases and reaches a maximum at 7.5 %(w/v) for both PEGs, after which it decreases again.

Similarly, the specific activity of the precipitate from these extractions reaches a pronounced maximum at this PEG concentration, while remaining considerably lower than for the traditional acetone-water extraction. As can be seen in Figure 25, a variation of pH at constant PEG concentration leads to a clear increase in the urease activity, independent of the PEG molecular mass, while the specific activity exhibits a maximum at pH = 6, which is more pronounced for PEG6000 than for PEG4000.

Selected additives were also investigated as to their effect upon the product when present in the extraction. It has been noted previously, that urease is easily deactivated, particularly so in the presence of certain metal ions (Sumner 1928a, Gorin 1960). For this reason small amounts of ethylenediamine tetraacetate (EDTA) were added to extraction solvents in the expectation that complexation of metal ions in the solution by EDTA may increase the activity of urease. The opposite effect was observed (Weber 2008b).

Since Nickel is an integral part of the enzyme (Alagna 1984), the addition of $NiSO_4$ was investigated in order to assess whether the presence of Nickel in the solution increases urease activity. It was found, that the addition of $NiSO_4$ significantly reduces the activity of urease.

The final additive examined was 2-mercaptoethanol. In earlier publications (Conway 1966, Lynn 1967), an increase in urease activity was noticed in the presence of 2-mercaptoethanol. A systematic study (Weber 2008a) revealed, that the increase in activity was dependent upon the concentration of the additive, with an optimum value of 0.1 M. At this concentration the activity of the crystalline enzyme recovered from the extraction solvent more than doubles, compared to the ‘Sumner-solvent’. Based upon the evidence available, the additive appears to reduce the amount of urease extracted while at the same time significantly increasing its propensity to crystallize, presumably by lowering the solubility, and significantly increasing the yield and the purity of the solid obtained.

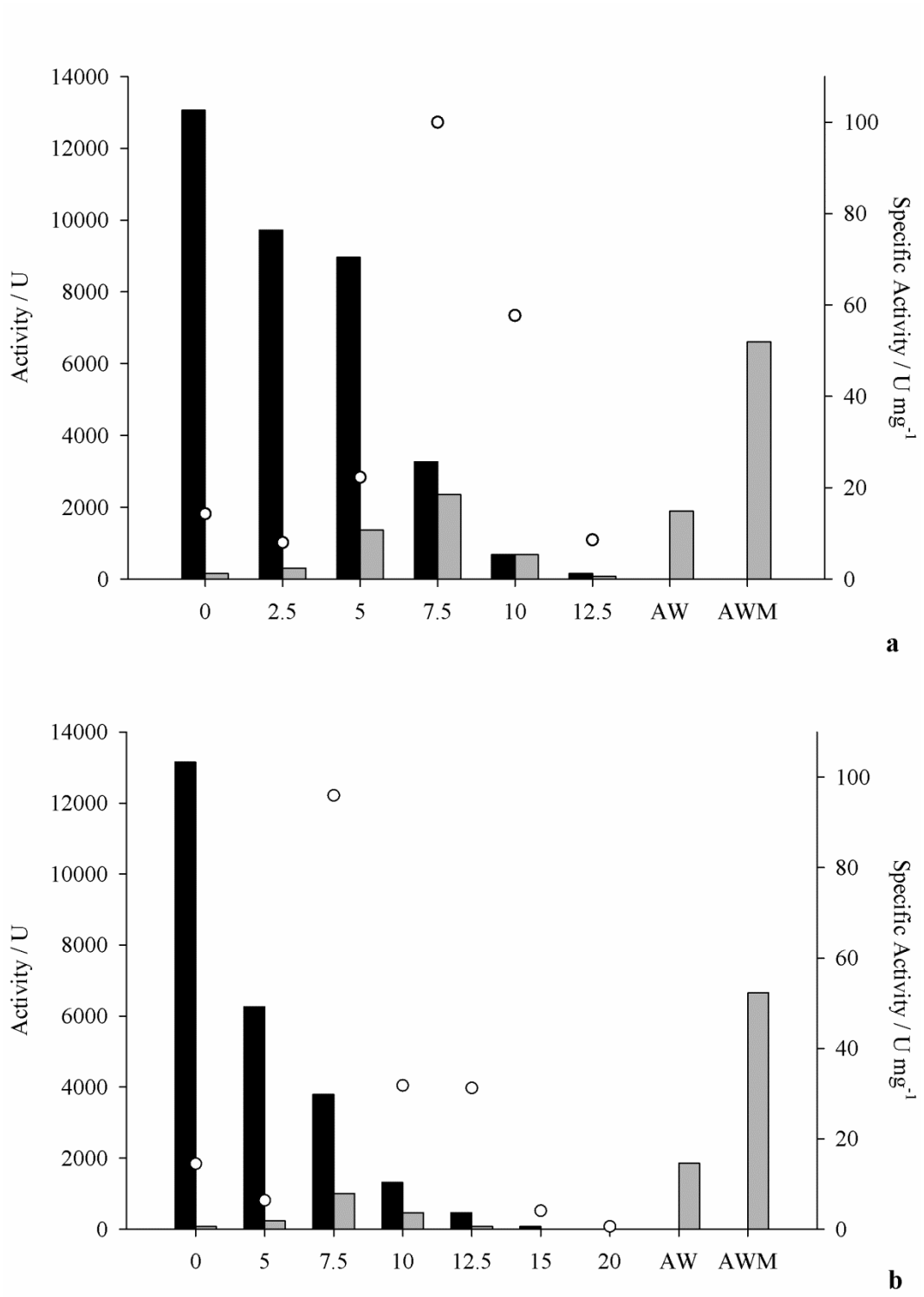

Figure 24: Total and specific urease activities for extraction with aqueous poly(ethylene glycol) (PEG) solutions as a function of PEG concentration (a, PEG6000; b, PEG4000). For the purpose of comparison the total activity of the precipitates obtained from acetone-water extracts with (AWM) and without (AW) 2-mercaptoethanol as described in chapter 4.2.1 is also shown. The black bars represent the activity in the extract, the grey bars the activity in the precipitate while ○ represent the specific activity in the precipitate.

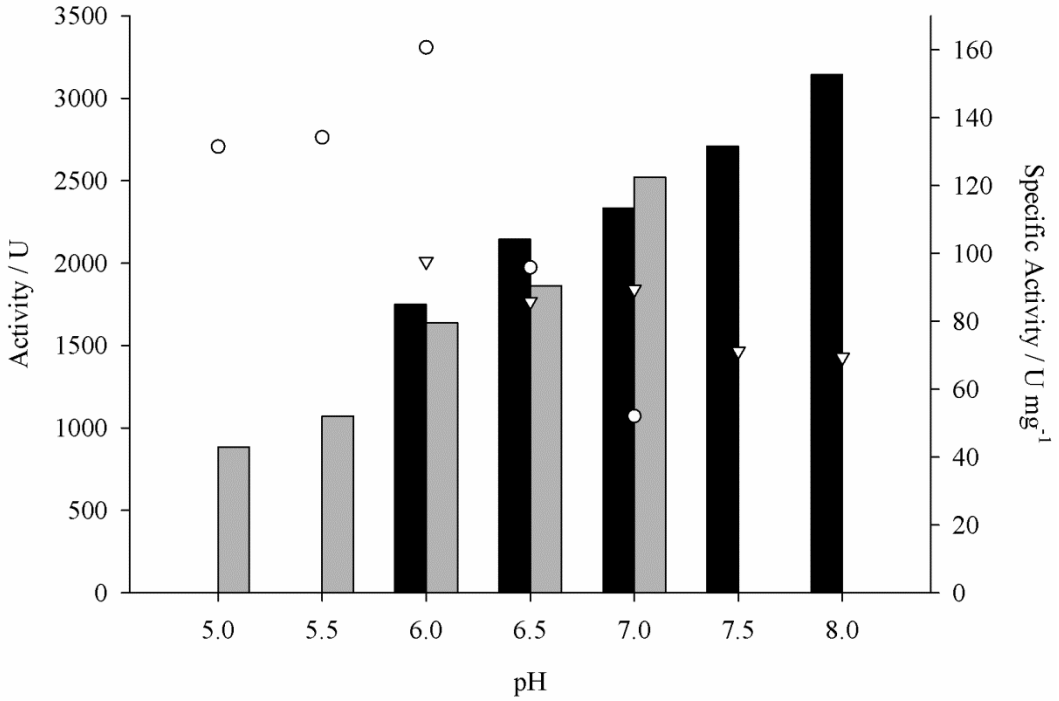

Figure 25: Total and specific urease activities for extraction with aqueous poly(ethylene glycol) (PEG) solutions as a function of pH. The activities obtained from extractions with 7.5% PEG 6000 (grey bars total activity, o specific activity) and PEG 4000 (black bars total activity, ∇ specific activity) are shown.

A similar investigation was carried out for the extraction solvents containing PEG rather than acetone and the results here were that the additive has a negative effect upon both the extraction and the crystallization and significantly reduced urease activities were observed in all cases.

Although non-protein matter extracted was not investigated, the evidence clearly suggests that the solvent composition as well as the manner in which the final solvent composition is achieved has a significant impact upon the purity and activity of urease crystals later harvested from the solvent (Weber 2008a).

4.2.2 The Influence of Process Parameters on Extraction and Solid-Liquid Separation

As mentioned above, and in addition to variation and modification of the solvent composition, the variation of process parameters such as extraction temperature and duration, intensity of mixing during extraction as well cooling rate during crystallization and parameters pertaining to solid-liquid separation were investigated.

4.2.2.1 Extraction Duration and Mixing Intensity

The investigation of the effect of extraction duration upon extract activity, *i.e.*, extraction yield, was carried out in combination with varying mixing intensities as defined by impeller tip speed. Based upon the dynamic viscosity of the slurry, which was measured and revealed

non-Newtonian, dilatant behaviour (Weber 2008a), an approximate range of impeller speeds were calculated based upon work described elsewhere (see, for example (Zogg 1993)), and covering the range of suspension behaviours from just suspended to homogeneous suspension. Experimentally, the lowest impeller speeds employed led to incomplete suspension, while the highest led to significant vortex formation and foaming. The former results in poor extraction, while the latter detrimentally affects the quality of the extracted proteins, as these may denature at liquid-gas interfaces (Noskov 2014). Both vortex formation and foaming increase the surface area of the liquid-gas interface and should therefore be avoided.

Overall, the duration of extraction and the impeller rate were not found to have a significant influence on the extraction yield within the constraints mentioned above. While the results of the individual experiments show a variation of 16 % with respect to the specific activity measured, this was ascribed predominantly to inhomogeneity of the raw material. Indeed, the major part of urease extractable was seen to go into solution within the first three minutes of the process.

The above study was carried out in a baffle-free reactor. The use of baffles to improve mixing had a significant negative impact upon the process, leading to a specific activity reduction of 50 % when compared to a reference process without baffles. This behaviour was explained by the observed retention of the solids by the baffles, leading to incomplete extraction of urease (Weber 2008a).

Solid-liquid separation post-extraction was also investigated. Both centrifugation and filtration were considered and again the specific activity was used to quantify differences in the process caused by changing process parameters.

In the case of centrifugation, the efficiency of the separation depends upon the centrifugal force applied, the duration of the process as well as the particle size distribution present. A range of durations and speeds, corresponding to different relative centrifugal forces, were employed. A slight trend was observed, with the specific activity increasing with increased centrifugal force and longer duration of the process, but the variation in specific activity was deemed insignificant, as it was only slightly greater than the estimated experimental error (Weber 2008a).

Filtration experiments were generally not successful, irrespective of the method and filter medium used. Filter papers with pore sizes of 2.5 µm and 8 µm as well as a cellulose membrane filter with a pore size of 0.2 µm clogged immediately both during pressure filtration and vacuum filtration. Using a filter paper with a larger pore size did allow filtration of a limited amount of material but here, too, clogging necessitated a change of filter medium. The behaviour observed was ascribed to the compressibility of the bean meal. In view of the fact that the later product is likely to have a particle size considerably smaller than the pore size – or at most will be of the order of the pore size of the media employed (Sumner 1926b) – filtration appears to be an unsuitable method for solid-liquid separation in this case.

4.2.3 Variation of Crystallization Conditions

4.2.3.1 Solvent Composition

Since the crystallization process is carried out directly from the extraction solvent, the compositions studied are identical to those already discussed above. The effect of the extraction solvent is, naturally, mirrored in the product quality, namely the activity (yield) and specific activity (purity) of the urease crystals. Nonetheless, additional observations with regard to the properties of the crystals are worth mentioning.

The first observation worth highlighting concerns the crystallization of urease from extracts to which acetone was added after extraction. The effect of this process has already been discussed in chapter 4.2.1 above. In contrast to the observed differences in the extract, the overall purity and yield of urease does not seem to be affected by the procedure. However, a significant increase in crystal size was observed for urease crystallized from phosphate buffer solutions with subsequent acetone addition (Figure 26). While the crystal size observed from other extraction procedures never exceeds 10 µm, this process yields crystals approaching diameters of 40 µm, an 8- to 9-fold increase in size (Weber 2008a).

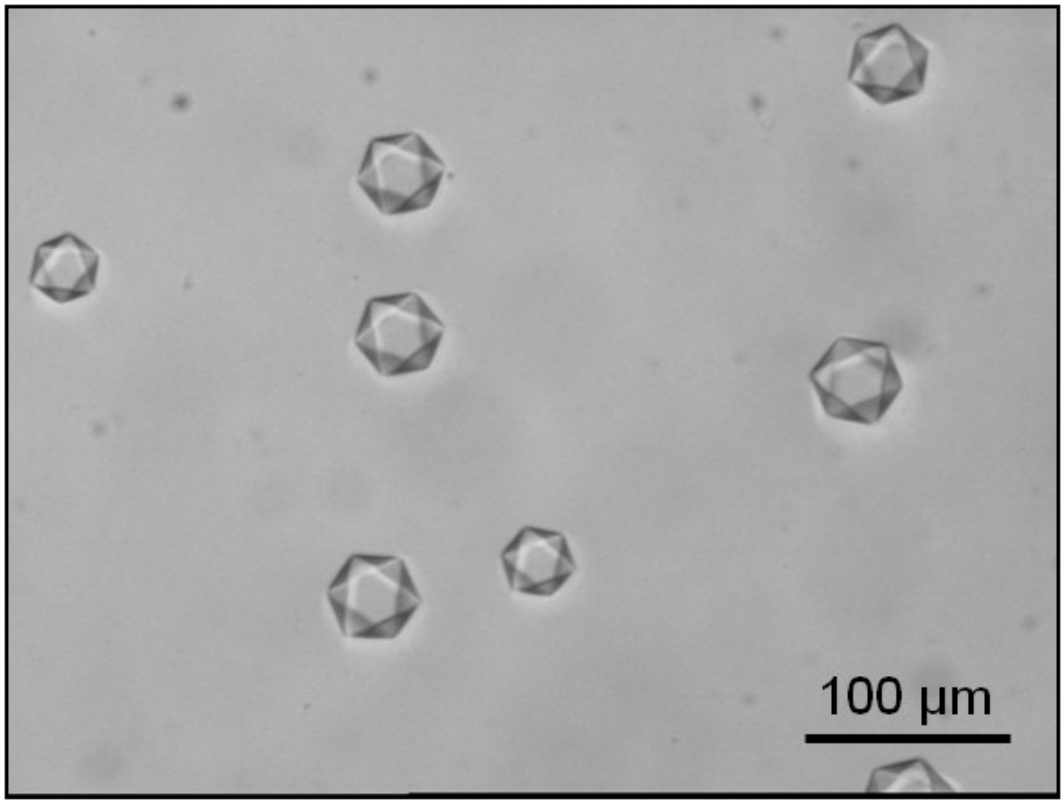

Figure 26: Large urease crystals obtained from extractions with water where acetone was added subsequently. In terms of their linear dimensions, these crystals are almost one order of magnitude larger than those obtained from the conventional extraction procedure using a binary acetone-water solvent (Weber 2008a).

The second observation worth mentioning concerns the crystals obtained from solutions containing 2-mercaptoethanol. The addition of 2-mercaptoethanol to the extraction solution

leads to a significant increase in urease activity not only in the extracts, but also in the crystals produced. It was surmised that the effect observed during extraction was due to modulation of the solubility of urease as well as that of other proteins in the presence of the additive. The most compelling evidence that this is the case was later delivered by a set of experiments, where extractions were carried out in the absence of 2-mercaptoethanol and the extracts were divided into two equal portions after clarification, which were allowed to undergo an initial crystallization, before adding 2-mercaptoethanol to just one of the two fractions. The results from these experiments strongly suggest that the additive indeed reduces the solubility of the enzyme, since the yield in the fraction containing the additive was approximately 30 % higher than that from the additive-free fraction. Moreover, a study of the crystal size distribution provides further evidence for solubility reduction by the additive. A comparison of crops of crystals derived from three solutions that were allowed to crystallize under otherwise identical conditions, but differed in solvent composition, reveals the following. For a solution containing no additive, the majority of crystals (70 %) is found in the size range of between 5 and 7 Å, while only 30 % are smaller and none are observed with larger linear dimensions. This indicates that nucleation of the crystals takes place more or less simultaneously and all crystals have a similar time-span available for growth before the supersaturation becomes so low that growth effectively ceases. If 2-mercaptoethanol is added to the extraction solution, the same size ranges are observed as for the extraction from acetone-water, but the maximum of the solution is shifted to the size fraction between 3 and 5 Å. This can be explained by a greater number of nuclei generated as a result of greater supersaturation in the initial extract. Providing the total amount of urease extracted is not greater than in the first case, more crystals are competing for the same amount of dissolved urease and a distribution shifted to a lower mean size would be expected. In contrast to these two extracts, the extract where 2-mercaptoethanol was added after an initial crystallization period of 2 day shows a distinct increase in the crystal size. Here, an additional fraction in the size range 7 – 9 Å was identified, which is again consistent with a lowering of solubility leading to additional crystal growth over and above that observed in the additive-free extract (Weber 2008a).

4.2.3.2 Temperature

While the effect of the solvent with regard to the product is largely determined by its extraction properties, the temperature the solution is subjected to during crystallization and the nature of cooling profiles has a profound effect upon the product quality.

Natural cooling with end-point temperatures ranging from 18 °C to -2 °C with a constant process duration of 48 hours appeared to have no impact upon the crystal size of the product. However, a clear influence both on the activity of the product and its specific activity was observed. The urease activity was seen to decrease with increasing end-point temperature. Normalising the results to the activity measured at 4 °C, Weber (Weber 2008a) observed that the activity at 20 °C was only about 75 % that of the activity at the reference temperature. In clear contrast to this, the specific activity initially increases with increasing temperature and appears to reach a plateau at between 4 °C and 8 °C. Visual inspection of the solid obtained at

lower temperature suggests that the amount of solids generated at lower temperature is larger than at higher temperature, consistent with a solubility increase with increasing temperature, while optical microscopy reveals the presence of particles that do not match the characteristics of urease crystals suggesting the concomitant crystallization of other protein components from the extract. Controlled cooling using a cubic time profile (see p. 425 (Mullin 2001)) is detrimental to the product activity, presumably due to the increased time at higher temperature.

The duration of the crystallization process appears to have no impact upon the activity of the final product over and above the expected changes with increasing amount of product crystallized. Crystallization is essentially complete within 24 hours, as established by measuring the activity of urease in the supernatant, which remains unchanged within the accuracy of the activity assay after that period of time. An assessment of size distribution, however, reveals significant changes in the crystal sizes observed with larger particles only emerging several days after the solution activity reaches its limiting value.

4.2.3.3 Mixing

In chapter 4.2.2.1 it was stated, that any change in extraction duration and impeller tip speed within a range that leads to good suspension of the meal but avoids excessive vortex formation and foaming of the slurry has no impact upon the activity of urease in the extract. This is no longer true when considering the specific activity of the crystals obtained from the respective extracts. Figure 27 illustrates the specific activity obtained from several extracts generated using extraction times from 3 min – 9 min and impeller tip speeds from 0.4 m s^{-1} to 1.4 m s^{-1}. All crystals were separated from their respective mother liquors using centrifugation and under identical conditions. A clear correlation of the specific activity with the process conditions is apparent. While the activity and the total protein content remain essentially constant in the extracts, the specific activity in the crystalline phase decreases for all mixing intensities for extraction times beyond five minutes. For extraction times lower than five minutes, the specific activity increases with increasing impeller tip speed, with a maximum at a tip speed of 0.79 m s^{-1} for 5 minutes extraction duration and at 1.44 m s^{-1} for 3 minutes extraction duration. Various factors contribute to the behaviour observed and it is not trivial to discern the main cause for these observations. At low extraction times and low mixing intensity the homogeneity of the suspension as well as the kinetics of extraction of the proteins from the meal will have a major impact. In view of the fact that extraction of urease is generally complete after five minutes, the explanation for the observed decrease in specific activity for greater extraction durations is likely to be found in the level of solid impurities in the precipitate. However, whether the amount of impurity proteins present is governed by changing thermodynamics due to changes in composition for different extraction times, due to changing crystallization kinetics or even both, cannot be stated with certainty.

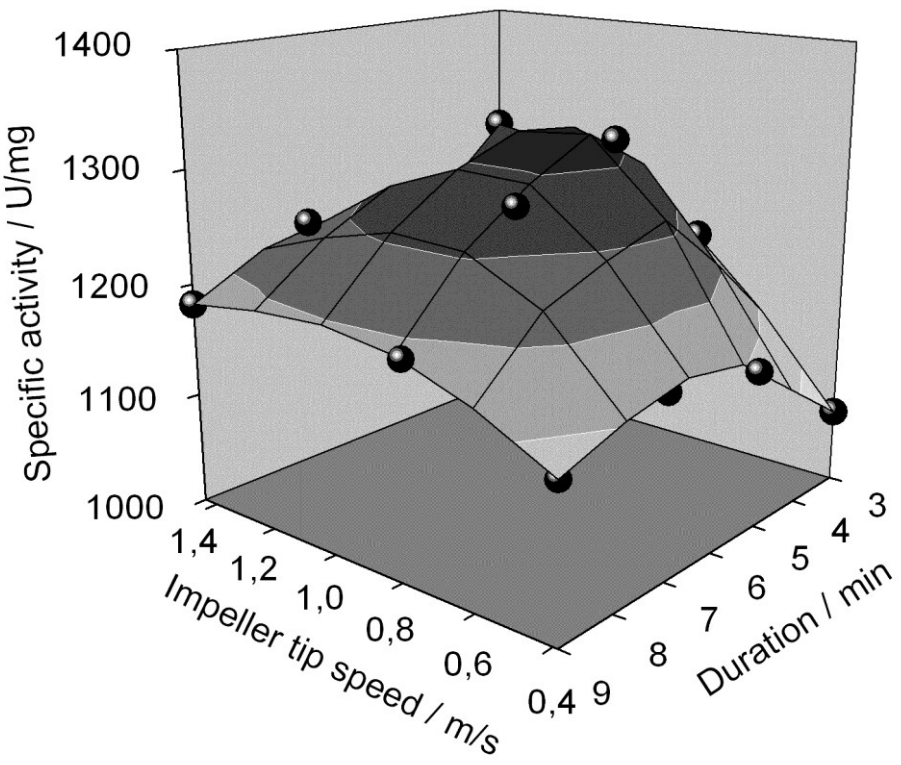

Figure 27: Specific urease activity as a function of extraction duration and mixing intensity (represented by the impeller tip speed) during extraction (Weber 2008a). The experimental data are represented by the black spheres, the correlation surface was obtained using the Renka-Cline gridding method available in OriginPro (OriginLab).

4.2.3.4 Solid-Liquid Separation

Similar to the mixing conditions imposed during the extraction step, solid-liquid separation by centrifugation was seen to have little impact upon the extract quality, even though a slight trend was observed. Again, when considering the specific activity of the crystalline product after separation from the mother liquor by centrifugation, the process parameters have a significant impact, as illustrated in Figure 28, which shows normalised specific activities as a function of duration of the centrifugation and the applied relative centrifugal force. All specific activities were normalised to the average value of the activity on the day the experiments were conducted.

Clearly, the relative centrifugal force applied does not have a significant influence upon the normalised specific activities, while the duration of the operation has a clear effect. A small reduction of the specific activity was observed for the shortest centrifugation duration of 1 min and the lowest relative centrifugal force of 5000 *g*, suggesting that not all the urease had settled in this time. At higher centrifugal forces the specific activity is essentially constant for this process duration. The largest activity at all centrifugation intensities was observed for a process duration of 5 minutes, after which the specific activity significantly decreases to as

little as 70 % of the average specific activity. Since no duration between 1 min and 5 min was investigated, the optimum centrifugation time may well fall within this short time period.
As the particle size of impurity solids is considerably lower than that of the urease crystals (the maximum size of particulate impurities was 2 μm), this behaviour can be ascribed directly to the sedimentation of non-urease protein solids present in the crystallization slurry.

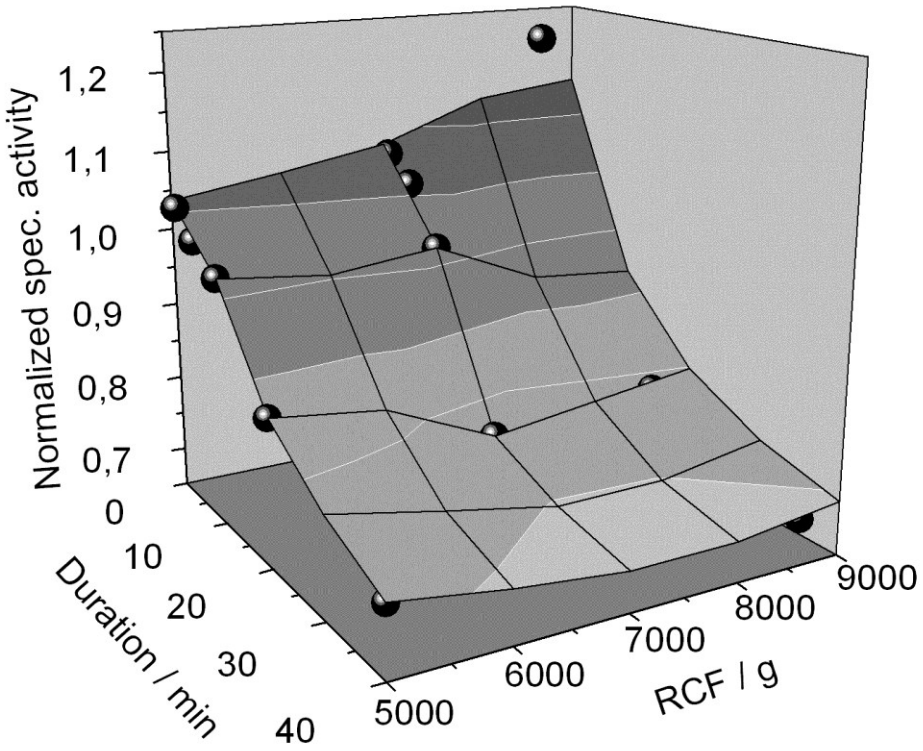

Figure 28: Normalized specific urease activity of the urease extract after centrifugation as a function of the relative centrifugal force *g* at the centrifuge tube bottom and the duration of the process (Weber 2008a). The experimental data are represented as black spheres, the surface was obtained using the smoothing correlation gridding method available in OriginPro (OriginLab).

4.2.3.5 Post-Crystallization Treatment: Washing and Recrystallization

Identifying a suitable solvent for washing protein crystals is a difficult task. Not only must the protein be essentially insoluble in the solvent while the solvent should be capable of dissolving any other solid impurity present, the solvent must, in addition, not have a detrimental impact upon the product properties. These simple conditions exclude the vast majority of solvents for washing. Proteins in general have non-negligible solubility in aqueous solvent and in addition, distinct proteins may have similar solubility in similar solvent compositions precluding any significant additional purification in the washing process. Organic solvents, with some exceptions already mentioned, generally lead to degradation of proteins and cannot be used for this reason.
As already discussed above, aqueous poly(ethylene glycol) solutions as well as lithium sulfate solutions were shown to be reasonable solvents for extraction and crystallization of urease,

though not as effective as the 'Sumner solvent' acetone-water with 32 % (v/v) acetone. These solvent systems were therefore also investigated as potential wash solvents, together with the modified 'Sumner solvent' with added 2-mercaptoethanol. In all but one case (Weber 2008a) washing resulted in a significant reduction of yield and specific activity of the urease crystals. The only case where the specific activity increased significantly, despite measureable losses of urease in the process, was when the crystals were washed with the system acetone-water-2-mercaptoethanol, providing further evidence of the activating effect of 2-mercaptoethanol upon urease.

Recrystallization experiments were also of limited success. The method reported by Dounce (Dounce 1941) was investigated at a larger scale and characterising the solutions and product crystals in the manner used in the previous studies. The method itself consists of dissolution of crystalline urease in a suitable amount of aqueous citrate buffer followed by antisolvent crystallization with acetone. The activity measurements revealed both significant urease loss as well as deactivation, as evidenced by the substantially reduced specific activity.

4.2.3.6 Summary of Urease Case Study

The detailed investigation of the separation of urease from jack bean meal with the express aim of understanding the influence of process parameters upon both the quantity and quality of the product obtained demonstrates the complexity of separation process for natural products. In this specific case, as undoubtedly in the majority of materials recovered from renewable resources, a good choice of process conditions can be found based upon rational variation of individual process parameters. It becomes clear, however, that a systematic investigation is both time consuming and, to a great extent, a matter of trial and error. In the case of urease extracted from jack bean meal, it is clear that the optimum process will necessarily consist of a set of unit operations and associated processing conditions that lead to a product which is essentially a compromise between high activity, *i.e.*, urease yield, and high specific activity, *i.e.*, product purity. It cannot be excluded that solvent systems not investigated and described here might deliver a superior product than those investigated here, but, in view of the complexity of the raw material and the number and quantity of extractable proteins alone, a detailed solvent search will be tedious and time consuming.

Nonetheless, a rational approach to process design is capable of delivering improvements to existing processes as demonstrated in the above discussion.

4.3 Case Study II: Combined Solid Layer Melt Crystallization and Solution Crystallization

4.3.1 Introduction

The previous section focussed upon identifying process and product critical factors in the extraction of a protein from a natural source and its subsequent crystallization from solution. Essentially, this section is also concerned with solution crystallization and the example considered is the salting-out of lysozyme. However, the main point of attention here is the novel method by which supersaturation is generated.

As already discussed above and as a result of the properties of proteins and protein solutions, salting-out and antisolvent crystallization are the main methods for crystallizing these macromolecules. However, both salting-out and antisolvent crystallization, when applied on a large, manufacturing scale, require the addition of the salt or the antisolvent to a protein solution (or vice versa, as the case may be). The unavoidable consequence of the addition of a concentrated salt solution or of a neat antisolvent is the immediate generation of extreme supersaturation at the interface between the two solutions at their point of contact. While the level of supersaturation can be moderated either by dilution of the salt solution or antisolvent, this is undesirable as it leads to dilution effects and either product loss or loss in process economy as a result of increased process equipment scale or reduced through-put, increased energy requirements for cooling/heating, a requirement for larger volumes of solvent and other chemicals and the inevitable cost of treatment and disposal of increased amounts of waste.

A diligent choice of mixing conditions may also moderate the impact of immediate and high supersaturation in the initial stages of mixing of the two solutions, one must be aware, however, that proteins tend to precipitate as amorphous solids under extreme conditions, which may lead to the irreversible loss of desired properties due to structural degradation. The effect of antisolvent addition was demonstrated in the case of lysozyme crystallization where the protein immediately precipitates in the vicinity of a drop of salt solution entering the protein solution. In the initial stages of salt addition the precipitate dissolves in the process of mixing and dispersion of the locally supersaturated region into the reactor and its accompanying dilution, in the later stages, where the bulk solution is significantly saturated or even supersaturated, dissolution no longer occurs. In the case of lysozyme, this leads to a pronounced decrease in activity.

Concentration of the solution by means of solvent evaporation, even if accelerated by the presence of a concentrated salt reservoir in indirect contact with the protein solution, as practiced in the case of hanging drop/sitting drop crystallization for generating diffraction-quality crystals, is unfeasible at a scale of even just a few mL. Low pressure distillation of the solvent is conceivable, but has, to the best of this author's knowledge, not been investigated and is unlikely to be a viable option as the boiling point of water can be reduced to at best 24 °C at 3 kPa, which is a common lower pressure limit achievable by standard displacement

pumps. More expensive solutions are necessary to reduce the pressure even further, and in the presence of salt and protein, the vapour pressure will be lower than for pure water due to the ebullioscopic effect.

Two obvious alternatives are to freeze-out the solvent, which is the subject of this section, and membrane-based separation operations (Curcio 2003, Di Profio 2003, Curcio 2005, Di Profio 2005a, Di Profio 2005b, Curcio 2006, Gugliuzza 2009, Di Profio 2010), which are not discussed here. Specifically, the combination of solid layer melt crystallization with solution crystallization is addressed here. Two melt crystallization technologies are commonly used for industrial separations, one is solid layer melt crystallization and the other is suspension crystallization. While both employ cooled surfaces to reduce the temperature of a melt to below the temperature of solidification of the material to be purified, a major distinction between the two is that the solid layer method allows the product to grow on the heat transfer surface, whereas in the suspension crystallization the product crystals are generated in the melt. This leads to significant differences in the way the processes are operated and the quality of the product obtained (see, for example, (Ulrich 2003, Ulrich 2004)). Solid layer crystallization has the advantage that, in the simplest implementation, no moving parts are required in the equipment. In addition, solid-liquid separation is comparatively straightforward, the surplus and depleted liquor is simply drained from the crystallizer by gravitational action, after which the product can be recovered by melting and draining. For organic solids in particular, growth of the solid crystalline layer on the walls of the heat exchanger leads to a progressively increasing heat transfer resistance and due to their poor heat transfer coefficients and the increase in solid layer thickness with time. In practice, the reduction in heat transfer due to the increasing layer thickness is compensated by applying a decreasing temperature to the cooled surface to compensate for the decrease in heat transfer and to ensure effective heat dissipation.

Since the temperature gradient across the solid-liquid interface largely determines the growth mechanism of the solid layer, and this temperature gradient must be smaller than the gradient of the solidus in the vicinity of the interfacial temperature in order to ensure smooth surface growth and minimisation of inclusions. Once the temperature gradients at the solid-liquid interface exceed the gradient of the solidus, the change in composition of the liquid layer in front of the solid layer due to solute rejection may lead to constitutional supercooling, where the solution is supercooled despite possessing a higher temperature than the solid surface (Tiller 1953). Constitutional supercooling leads to unstable growth of the solid surface, often observed as dendritic growth, which itself leads to increased liquid inclusion in the solid layer and a concomitant reduction in its purity. Clearly, the temperature gradient across the interface is an important control parameter for a solid layer melt crystallization process. In practice, smooth interface growth is rarely achieved and fast growth rates more than compensate for increased impurity levels, which can be mitigated by post-crystallization treatments such as washing and sweating. In fact, sweating, that is partial melting of the crystal surface, is an attractive post-crystallization purification step due to the behaviour of impurity inclusions during crystallization. As a result of the temperature gradient, impurity

rich liquid inclusions tend to migrate towards the warmer surface of the growing crystal (Burton 1953, Wilcox 1968, Scholz 1993, Henning 1997), equivalent to the behaviour of impurities in zone refining. As a consequence, impurity concentrations are expected to decrease from the surface layer towards the cooling surface and in fact this is generally observed. Partial melting of the outermost layer of the crystal is therefore an effective post-crystallization purification step.

Suspension crystallization does not suffer from the heat transfer issues common in solid layer crystallization, providing the surfaces of the heat exchanger exposed to the melt are regularly scraped clean, a commonly implemented technical solution. Since suspension crystallization is not considered in the following, no detailed discussion is provided here. The interested reader may refer to the following literature for more information (Ulrich 2003, Ulrich 2004).

The rational of the process discussed below is to create sufficient supersaturation for nucleation and growth of protein crystals in solution by removing the solvent by solid layer melt crystallization and at the same time minimising the amount of precipitating agent employed, hence the coupling of solid layer melt and solution crystallization.

For the purpose of removing the solvent and concentrating an aqueous protein solution including a suitable precipitant, solid layer melt crystallization is the method of choice, since the solvent removed adheres to the surface of the heat exchanger and does not form a suspension with the liquid phase. Providing the heat exchanger is not a fixed part of the equipment, it can be removed from contact with the solution, together with the frozen layer of water, allowing easy analysis of the crystalline solvent layer. Once a sufficient amount of solvent has been removed from the solution to generate a sufficiently large degree of supersaturation with regard to the protein to be crystallized, nucleation can be allowed to occur or the solution may be seeded for controlled growth of crystals. A number of prerequisites have to be fulfilled with regard to the physical properties of the system and the process conditions imposed thereon for this procedure to be successful:

- The solvent to be frozen out (in this case water), must not form a solid solution or a compound containing a significant amount of one or more of the solution components under the conditions selected.
- None of the components solidify at a temperature higher than that of the solidification temperature of the solvent under the given thermodynamic conditions.
- The layer growth process has to be controlled carefully to avoid constitutional undercooling of the liquid in close proximity to the solid interface, in order to avoid liquid inclusions due to unstable, dendritic growth of the solid layer.
- The protein crystals must not form by epitaxy on the solid ice layer, as this would necessitate a mechanical removal of the product from the solidified solvent.

The first prerequisite has to be investigated on a case to case basis, preferably by studying the phase diagram of the system. In the case of crystallization of lysozyme chloride from an aqueous NaCl solution, there is no known risk of forming a solid phase containing water and the precipitant until temperatures lower than ca. -20 °C, where sodium chloride solidifies as a

dihydrate together with ice, or for salt concentrations greater than 30 %(wt/wt), where again, at temperatures below 0 °C sodium chloride dihydrate is formed (Korolev 1939). The incorporation of protein into the solid water layer was subject to investigation in the study discussed below.

The second point is fulfilled, as long as all solution components that are solid at the temperature of operation of the process are present at concentrations below their respective saturation concentrations. At the salt concentrations employed, this is the case for sodium chloride, the buffer concentrations are also sufficiently low so as not to become supersaturated and merely the lysozyme concentration is such, that crystallization should occur, and this, indeed, is desired. More importantly, the crystallization must not occur epitaxially on the ice layer (point 4) as this would lead to the need for additional, mechanical separation of the crystals, providing they have not been encased by the propagating ice layer.

Point 3 is the most important prerequisite and a key point of investigation in the case study presented.

One major advantage of the combination of melt and solution crystallization is that the process is subject to low temperatures at all times, reducing the risk of protein degradation due to extended exposure to high temperatures. Furthermore, raw materials can be limited to absolute minimum amount necessary, as the concentration change with respect to the protein and the dissolved precipitating agent can easily be calculated as a function of the water removed. As a consequence the amount of saline waste-water produced can be reduced. In order to demonstrate the suitability of the process, the fate of the protein generated in the process has to be investigated, considering the quality parameters already introduced in the study on urease.

4.3.2 Application of Combined Solid Layer Melt and Solution Crystallization to the Manufacture of Lysozyme Chloride

The case study described in the following builds upon two PhD theses (Ryu 2010a, Diaz Borbon 2013a). The first of these is mainly concerned with the proof-of-concept together with preliminary investigations of the effect of the ice growth rate on product loss by inclusion and the effect of the estimated degree of supersaturation upon the product quality, while the second takes up this work and demonstrates the purification effect achieved in the presence of an impurity protein.

4.3.2.1 Experimental Set-Up

The implementation of a solid layer melt crystallization coupled to a solution crystallization at the laboratory scale. The simplest possible heat exchanger providing a surface for solid layer growth is used, namely an internally cooled tube, colloquially called a ‘cold finger’. This is immersed into the solution from which the solvent is to be withdrawn and the solute, in this case lysozyme, to be crystallized. The solution is contained in a standard double-walled reactor provided with its own temperature control. Two thermostats are therefore necessary,

one to provide cooling to the cold finger, the second to control the temperature of the solution in the reactor. The reactor and the tubing transporting the cooling liquid from the thermostats to the equipment and back are insulated to prevent the build-up of ice on the cold surfaces exposed to the atmosphere. The experimental set up is shown in Figure 29.

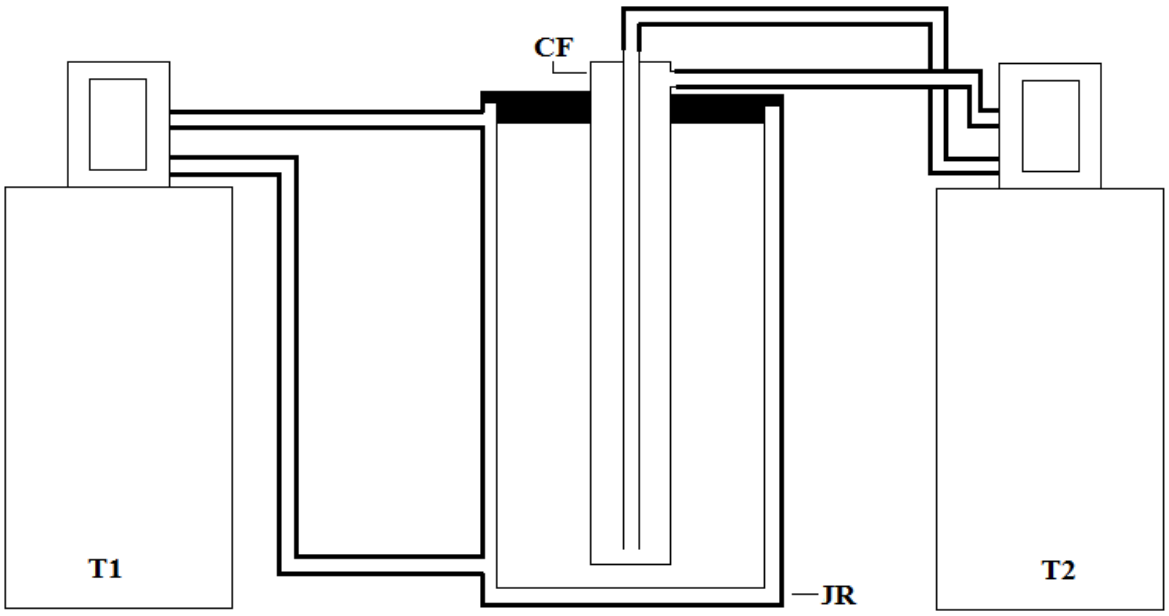

Figure 29: Schematic representation of the equipment used for solvent freeze out experiments. The protein solution is contained in the jacketed reactor JR, thermostatic bath T1 provides the temperature control for the reactor. The cold finger CF is immersed in the protein solution and cooled by the thermostatic bath T2. The temperature of the solution is monitored using a thermocouple (not shown).

When operating the equipment, the reactor jacket is kept at a constant temperature, usually close to the melting temperature of water. The solution is not stirred, and the process is therefore operated as a static solid-layer melt process as far as the solidification of the solvent is concerned. In this mode of operation, the temperature gradient across the solid ice-liquid interface is determined by the temperature of the cooled surface of the cold finger.

4.3.2.2 The Effect of the Ice Growth Rate on Protein Loss

The quality of a solid produced by solid layer melt crystallization depends upon the ability of the propagating layer to reject impurities back into the solute. This can only be achieved effectively, if the surface growth is sufficiently slow to be lead to a smooth surface and for impurities to diffuse into the solution and away from the growing crystal surface. Generally, this situation is fulfilled only if the temperature gradient across the solid liquid interface is sufficiently small to avoid constitutional undercooling, which is accompanied by unstable growth of the solid surface.

In the case where a solid layer melt crystallization is employed to generate supersaturation of a second component in the solution, which subsequently crystallizes in the remaining liquid, it is desirable to avoid any inclusion of the desired product in the solid solvent layer. On the one

hand inclusion of protein leads to product loss, on the other it diminishes the level of control over the process, in particular if the magnitude of inclusion is not reproducible from batch to batch.

Ryu, in her proof-of-concept study (Ryu 2010b), investigated the effect of process parameters, in particular changes in driving force/growth rate of the solid ice layer, upon solute inclusion. For this purpose, either different driving forces were applied for constant process durations, or a constant, cold-surface temperature was applied for varying process durations, effectively providing a diminishing driving force for crystallization with increasing process duration.

Figure 30 illustrates the change of concentration of protein inclusions with process duration and changing driving force with time. The observed effect is most pronounced for the highest lysozyme solution concentration, where the amount of protein included decreases substantially with increased process duration. This decrease is not quite so obvious for the lower initial protein concentration. The effect appears to be independent of the initial protein concentration, since the absolute amount of protein detected in the ice layer scales approximately with the initial lysozyme concentration. Since the cooling rate applied to the cold finger was the same in all experiments, the results are consistent with decreasing driving force and consequently decreasing ice growth rate with increasing time. Although the time dependence of the growth rate was not determined, an average growth rate was calculated from the process duration and the ice layer thickness at the end of the process.

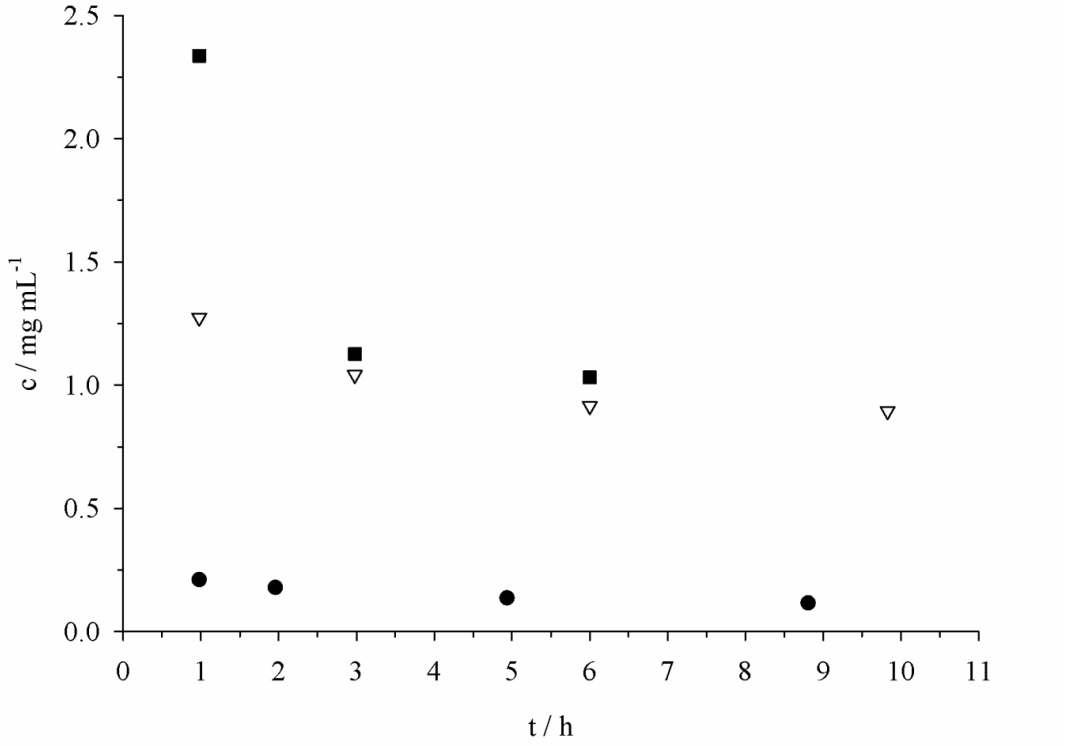

Figure 30: Inclusion of protein in the ice layer as a function of process time for different protein concentrations. The solution contained 5 %(w/v) NaCl and the pH was adjusted to pH = 4.4. The protein concentration was ■ 4 mg mL^{-1}, ∇ 2 mg mL^{-1}, and ● 0.3 mg mL^{-1}. The cooling rate applied to the cold finger was 0.1 K/min.

Not quite unexpectedly, Figure 31, which shows the protein concentration in the ice as a function of the distance from the cold surface for different cooling rates applied to the cold finger, reveals that protein inclusions accumulate in the vicinity of the solid-liquid interface. The amount of protein found in sections of the ice layer is greater for the higher cooling rate applied and is consistent with the greater driving force and hence ice layer growth rate this implies. For the lower cooling rates there is little difference in the absolute ice concentrations detected in different ice layers, but the trend is the same as for the highest cooling rate.

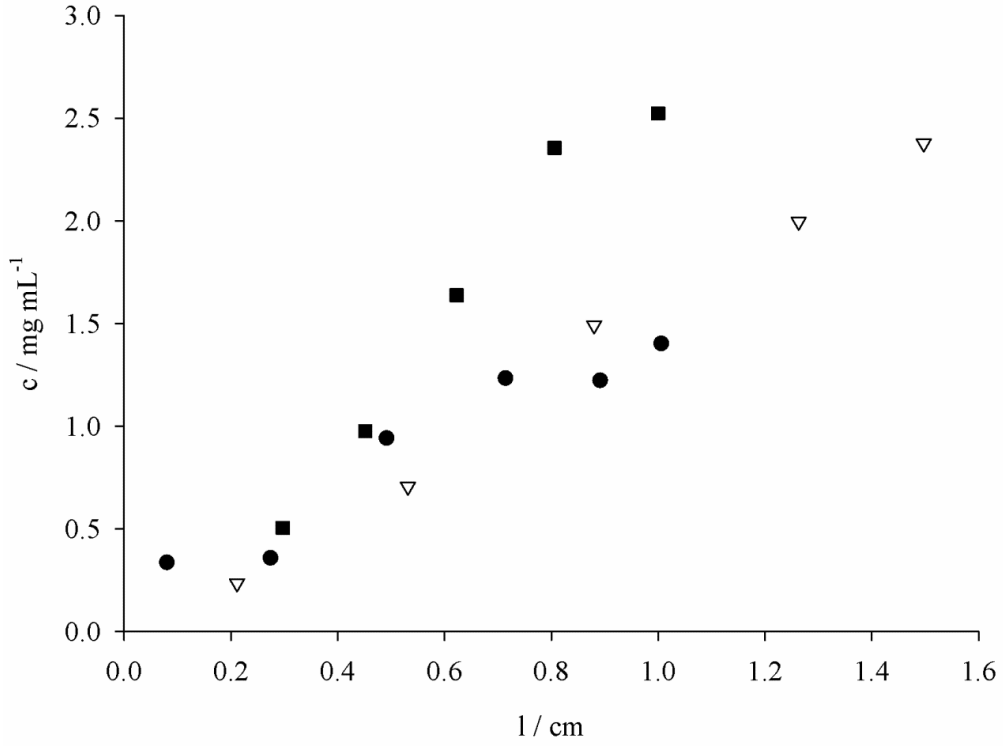

Figure 31: Loss of protein to the ice layer as a function of ice layer thickness for different cooling rates. ■ 0.4 K/min, ●, 0.1 K/min, ∇ 0.05 K/min. The data were obtained from a protein solution with a protein concentration of 4 mg mL^{-1}, 5 %(w/v) NaCl and pH = 4.4.

An estimation of the concentration effect based upon the measured amount of solvent removed from the solution reveals that significantly increased concentrations up to 5 to 6 times the initial protein concentration can be achieved, even with moderate initial protein and salt concentration, but dependent upon the temperature profile employed (see (Ryu 2010a)). As a consequence, varying degrees of supersaturation can be defined simply by selecting appropriate process parameters.

Unfortunately no measured solubility data at temperatures below 2 °C exist to date, and all solubility data used in (Ryu 2010a) are either estimated or extrapolated from higher temperature data by fitting a polynomial and extending the polynomial to the low temperature required. All supersaturation data reported are therefore approximate.

Qualitatively, however, the size and size distribution of product crystals is as expected, with larger supersaturation leading to smaller crystals and narrower size distributions, as determined through optical micrographs.

Activity measurements were carried out for the protein in all phases generated during the process, that is, for the ice layer, the mother liquor as well as for the protein crystals. Lysozyme catalyses the lysis of bacterial membranes and the method for activity determination used was that first reported by Shugar (Shugar 1952), where bacterial cell walls of *Micrococcus luteus* are suspended in a aqueous solvent under defined conditions (*Micrococcus lysodeikticus* and *M. luteus* are the same microorganism, *M. lysodeikticus* is an older name commonly found in the literature prior to the 1990s, current taxonomy uses the name *M. luteus*.). The transmittance of monochromatic light through this cell wall slurry is measured as a function of time. The turbidity of the solution decreases as the bacterial cell walls disintegrate under the action of the enzyme and the rate of (turbidity) decay is a measure of the activity of the enzyme. The specific activity can be determined with the aid of a separate protein assay and, in the experience of this author, the most reliable method of measuring lysozyme concentration is by UV-absorption at a wavelength of 280 nm.
Unfortunately the activity measurements presented by Ryu (Ryu 2010a) were inconclusive and no obvious effect of process conditions upon protein activity was observed.
In principle, the experimental efficiency of exploring a complex problem depending upon a large number of variables can be reduced significantly by means of statistical design of experiments (DOE). This is the approach adopted in a subsequent study by Diaz Borbon (Diaz Borbon 2013a), which takes a more systematic approach to investigate combined solvent solid layer melt crystallization and protein solution crystallization. Here, DOE is employed to identify the critical process variables that have the strongest influence upon the outcome of the combined process in terms of pre-defined responses of the system. The process variables investigated in the initial fractional factorial design are the initial protein concentration in the solution and the salt concentration, the temperature of the reactor jacket and the final temperature of as well as the cooling rate applied to the cold finger and its length, the intensity of mixing expressed as the rotational frequency of the impeller as well as the length of time the process spends at the final, constant temperature of the cold finger. The system responses used to quantify the influence of the process parameters are the mean particle size of the protein crystals generated, their yield, the volume of the ice layer generated as well as the fraction of protein lost to the ice layer through inclusion.
The fractional factorial design results in a set of 18 experiments, of which 16 represent the possible combinations of two selected limiting values (high and low) for each of the process variables and the two additional experiments represent centre-points where the process variables each take the average of the limiting values. The range of values chosen for the process variables is narrow, with the exception of the mixing intensity, and the selection of the limiting values is guided by an empirically determined ‘ideal pathway for crystal growth’, which is a qualitative estimation of those values, which result in well-formed, tetragonal lysozyme chloride crystals. The values for the length of the cold finger are limited by the equipment available and not subject to the initial parameter screen.
This first set of experiments shows, perhaps not quite unexpectedly, that the variables with the strongest influence upon the measured process responses are the final temperature of the cold

finger, the time the process spends at the final cold-finger temperature and the salt and initial protein concentrations. These variables define the final supersaturation of the solution as well as the rate of change of supersaturation and should be expected to have a significant effect upon the product. However, the results of the DOE clearly demonstrate that the process variables that have an influence upon the responses measured are not necessarily the same for all four criteria. The size of the particles obtained is effectively governed by the variables mentioned above, whereas the yield of protein crystals is significantly influenced only by the salt concentration, the final cold-finger temperature and the mixing intensity. Since the solubility of lysozyme decreases with decreasing temperature and increasing salt concentration, there is nothing unusual here. Mixing facilitates convective mass transport in the solution and providing that crystal growth is comparatively slow and process durations short, the observed effect can be rationalised.

The remaining two responses relate to the by-product of the process, the ice layer. The volume of ice obtained during the process is, again, a measure of the rate of change of supersaturation of the lysozyme-salt solution, while the amount of protein lost to the ice layer will reflect the growth mechanism of the ice layer growth (smooth *vs.* unstable growth), which ultimately has an impact upon the yield of the actual product. Mixing of the solution/slurry was observed to have a significant negative effect upon the amount of protein lost to the ice layer, *i.e.*, good mixing results in less protein inclusions in the solid layer and therefore less loss of product and is beneficial to the process. At the same time, increased mixing intensity reduces the ice volume formed. Again this can be rationalised by considering the consequence of good agitation upon the solid-liquid interface, the temperature gradient and mass transfer across this boundary and ultimately upon the concentration profile in the solution at the interface and local growth rate of the ice layer.

As a result of these initial findings, a further set of experiments was conducted using a central composite experimental design focussing upon these three parameters. In contrast to factorial design, composite design requires the experimental variables to take additional values both higher and lower than the limiting values mentioned previously, in addition to using the latter. The resulting set of experiments consists of all experiments representing the combination of the possible limiting values of the variables, a central point using the average value of the limiting values as well as two experiments for each variable exploring their extreme values while keeping the remaining variables at their average values (Brereton 2003). In the central composite design, Diaz Borbon (Diaz Borbon 2013b) considers only the final cold-finger temperature, the time spent at the final temperature and the mixing intensity. Although the salt concentration and initial protein concentration were shown to have a strong impact upon the responses, they were not considered, presumably as their role in the crystallization process is obvious and to reduce the experimental effort.

Considering the responses reported, the greatest variation is seen for the ice volume, while only small variations are observed for the protein yield and the loss of product to ice. The response diagrams (either as a function of a single variable or surfaces for pairs of variables) generated from these experiments (Diaz Borbon 2013b) map the ‘desirability’ of the values

for the process variables explored to the respective responses and provide a visual representation best value or combination of values for the process variables. As shown in (Diaz Borbon 2013b), the outcome of the statistical analysis for process yield shows that, when mapped to either the variable pair final temperature and process duration or process duration and mixing intensity, a low final temperature, long process duration and high mixing intensity are beneficial. However, when mapping the yield to the process duration and the mixing intensity, the mean stirring rate appears to be more desirable than either higher or lower rates, whereas the process duration seems to have little impact at constant mixing intensity.

In addition to the experiments discussed above, Diaz Borbon (Diaz Borbon 2013a) also investigated the change in enzymatic activity as a function of process conditions and observed a marginal decrease in activity for the product crystals when compared to the starting material.

The mean particle size used in the evaluation of the experimental variables was measured by laser light scattering and while not explicitly considered in the data analysis, the size distribution shows some variation with process conditions (Diaz Borbon 2013a) and consistent with expectations. For the majority of experiments the size distribution (represented as a volume fraction as a function of size in the work cited) of the tetragonal lysozyme chloride is fairly uniform and centred around a size of 10 μm to 20 μm, consistent with the optical microscopy images shown. The size distributions deviate from this general behaviour only when relatively high supersaturation is achieved in the process, where either a shift of the mean size to lower values or a significant tail towards small particles are observed, the latter occasionally accompanied by the emergence of a secondary maximum at small sizes. This is consistent with an increased nucleation rate at higher supersaturation, which leads to a greater surface area available for subsequent growth and smaller crystals.

Overall the DOE experiments carried out by Diaz Borbon essentially reveal that the crystallization of lysozyme by solvent withdrawal depends upon the usual variables supersaturation and rate of change of supersaturation, when quantified using the measures above. However, the value of the DOE approach applied here, lies in its ability to quantify the effect of all process variables examined and provide a clear insight into how these interact. For a complex process such as the crystallization of a protein, this is invaluable.

In addition to the DOE experiments already discussed, Diaz Borbon also investigated the effect of a protein impurity upon the crystallization of lysozyme chloride. For this purpose, ovalbumin was used as contaminant (Diaz Borbon 2012, Diaz Borbon 2013a), a protein that naturally occurs in the most abundant source for lysozyme, the hen egg white. Effective separation of the protein components in the solution was demonstrated.

5. Outlook

Large scale crystallization of proteins for the purpose of purification is clearly a promising and viable technology, as has been demonstrated here. Although crystallization of proteins has its own challenges and may differ from small molecule crystallization in the finer details, the fundamental principles governing the technology are the same as for small molecule crystallization. The level of difficulty in designing a suitable crystallization process is determined essentially by the following, intimately linked issues. First and foremost, rational process design requires knowledge of the physical properties of the protein for which a process is developed, in particular its solubility and both the nucleation and the growth kinetics. While most process development, from the point of view of the industrial process development scientist, can be carried out with only minimal knowledge of the kinetics of crystallization, a good understanding of the solubility and its change as a function of the relevant thermodynamic variables is essential. In contrast, the academic protein crystallization community has placed greater emphasis on understanding the kinetics of nucleation and crystal growth in the recent past, which in part explains the continuing paucity of solubility data available in the public domain. The difficulty in measuring solubility data with a limited amount of protein, for a wide range of solution compositions and temperatures as well as in a short period of time is a severe limitation, which has been addressed successfully by the development of a method for rapid solubility measurements described and discussed herein. One aspect of this technique that clearly requires further development is the amount of protein required in the measurements. More often than not the availability of material is the primary factor preventing systematic studies and miniaturisation of this dynamic equilibration method is highly desirable to address this issue. In principle there is little standing in the way of further miniaturisation and it is conceivable that the application of microfluidic technology with modern analytical equipment, together with parallelisation of measurements, can lead to significant efficiency gains in determining protein solubility.

The second challenging area is that related to the complexity of the source materials from which protein products are obtained. While the study of the thermodynamic properties of a pure, isolated protein in solution provides invaluable information for process design and knowledge of nucleation and growth kinetics is essential for process and product control, the fact that proteins stem from complex sources must not be neglected when transitioning to real systems. A few examples investigating the crystallization of proteins from solutions containing other proteins than just the target protein exist in the literature (Bhamidi 1999, Diaz Borbon 2012), both use artificial mixtures of proteins. A recent publication (Yu 2014) takes a slightly different approach, crystallizing lysozyme from a fermentation liquor. While still an artificial mixture, the complexity of the starting material is a more realistic representation of that encountered in a typical isolation and purification task.

Of course, other promising methods for the determination of solid-liquid equilibria in protein solutions exist, foremost turbidimetric solubility measurements. While here, too, the amount of solid required for a measurement is comparatively large, it is difficult to conceive how the

technique could be miniaturised much further in order to achieve a significant gain in efficiency. The measurement of second osmotic virial coefficients, much hailed as a substitute for solubility measurements, has been shown to be of limited use in process development, where real solubility data rather than solution compositions likely to yield crystals are required.

The flow-through method of equilibration for solubility measurements has, of course, other potential applications. Since concentration changes are monitored in real-time, the technique should prove useful in the study of crystal growth kinetics and the kinetics of phase transitions between different crystal modifications at a larger scale than merely the individual crystals.

The case studies presented herein demonstrate the power of a rigorous engineering approach to process development for protein crystallization, but also the significantly greater amount of effort required to fully characterise such a process. Combining existing technologies, as in the case of the combination of melt crystallization for solvent removal with simultaneous solution crystallization of the product is a promising strategy for further research. Indeed, the publication by Yu *et al.* (Yu 2014) mentioned above is a further development from the studies discussed in detail here. The potential for further academic research into these areas is great, and the amount of work required in order to establish large scale protein crystallization as a standard technology cannot be underestimated.

There are, of course, other, academically interesting approaches to manipulating protein solutions in order to crystallize and purify the constituent protein, most notably membrane based technologies (Curcio 2003, Di Profio 2003, Curcio 2005, Di Profio 2005a, Di Profio 2005b, Curcio 2006, Gugliuzza 2009, Weckesser 2009, Di Profio 2010). For the membrane-based technologies the same conclusion holds as for those discussed in detail here, in that they represent an interesting strategy that require a significant amount of further research, in particular with regard to how to remove the product form the membrane, to which it inadvertently adheres, in order to become mature and established technologies for the industrial crystallization of protein products.

6. Summary

Protein crystallization is promising technology for the industrial purification of these biological macromolecules. The work discussed herein represents the current state of the art in large scale protein crystallization. An overview of pertinent literature on the topics of protein solubility, nucleation and crystal growth, which form the physical basis for process development and underpin the research presented, is provided.

Based upon the need for a more efficient strategy for protein solubility measurement, a novel method has been developed which utilizes a static bed of protein crystals in contact with a flowing solution and allows continuous measurement of the solution concentration by means of UV photometry. This flow-through cell allows solubility data to be collected in a significantly shorter time when compared to methods relying on solution equilibration via a vapour phase such as the hanging drop/sitting drop methods or other batch equilibration methods and is also superior to these methodologies in that no sampling of the solutions is required since the solution concentration is monitored in situ and continuously. Application of this methodology has allowed the available solubility data to be expanded to modifications of lysozyme other than tetragonal lysozyme chloride and has also proven capable of delivering solubility data for regions of phase space, where a given modification is metastable. This provides direct access to transition points between different crystal modifications. The transition between tetragonal and the high temperature orthorhombic modification of lysozyme chloride has been characterised together with the transition between the low temperature and the high temperature orthorhombic modifications.

Two case studies applying crystallization technology to proteins have been presented. In the first, the extraction of urease from jack bean meal and its subsequent crystallization were thoroughly investigated with the aim of understanding the influence of the individual process steps and the relevant process parameters upon the quality of the product, which was defined in terms of purity, yield and enzymatic activity. It was shown, that modification of process parameters may have a conflicting impact upon yield and purity, necessitating optimisation of the process with respect to both these quality criteria.

A novel technology was developed and investigated, which employs a combination of melt crystallization for the removal of solvent from a protein solution and concurrent solution crystallization of the product. The melt crystallization serves to concentrate the mother liquor, increasing both the protein concentration as well as that of the precipitant. As a consequence the amount of precipitant required in the process can be reduced significantly, simultaneously reducing the environmental impact of the process. This approach was shown to deliver high quality crystals, retaining the enzymatic activity of lysozyme, which was used as the model substance for the investigations.

The work has also highlighted the need for further developments, both with regard to the determination of the physical properties of proteins relevant for process development, and also with regard to suitable technologies for large scale crystallization of this important class of crystalline product.

7. List of Symbols and Abbreviations

7.1 Symbols

a	Activity
A	Pre-exponential or variable parameter
B_2	Second osmotic virial coefficient
B_3	Third osmotic virial coefficient
c	concentration
c^*	equilibrium concentration (solubility)
c_A	Solute molal concentration
$c^{\ominus}$	Concentration of a reference state
Δc	Supersaturation (absolute)
g	Gravitational acceleration at the earth's surface
g'	Growth exponent (face growth rate)
g''	Growth exponent (mass deposition rate)
G	Overall linear growth rate
ΔG	Gibbs free energy
ΔG^{mix}	Gibbs free energy of mixing
ΔG_c^0	Gibbs free energy of a solute molecule in a cluster
ΔH	Enthalpy
J	Nucleation rate
k_2	Scale factor
k_B	Boltzmann's constant
K	Rate or equilibrium constant
m	Mass
M	Molar mass/molecular mass
M	Molarity

n	Number density
N	Number
N_A	Avogadro number
p	Pressure
r	radius
r_{crit}	Critical nucleus size
R	Ideal gas constant
R_G	Mass deposition rate
S	Supersaturation (relative)
ΔS	Entropy
t	Time
T	Temperature
T_c	Upper consolute temperature
U_0	Rate of cluster formation
U_1	Rate of cluster decay
$U(r)$	Potential of mean force
v	Volume of a 'building block' in a solid
$v_{(hkl)}$	Face growth rate for the crystal face (hkl)
V	Volume
x	Mol fraction
z	Number of nearest neighbours
Z	Zeldovich factor
α	Shape factor
γ	Activity coefficient
γ	Surface tension
ε	Extinction coefficient
η	Viscosity

λ	Wavelength
μ	Chemical potential
ρ	Density
σ	Interfacial tension
υ	Linear growth rate
υ^*	Frequency of attachment
Π	Osmotic pressure

7.2 Abbreviations

CNT	Classical nucleation theory
DCM	Discrete charge model
DLS	Dynamic light scattering
DLVO	Derjaguin-Landau-Verwey-Overbeek theory
DOE	Design of experiments
EDTA	Ethylenediamine tetraacetate
HTO	High temperature orthorhombic modification of lysozyme chloride
LCSP	Liquid-crystal spinodal
LLC	Liquid-liquid coexistence curve
LLSP	Liquid-liquid spinodal
LTO	Low temperature orthorhombic modification of lysozyme chloride
PEG	Poly(ethylene glycol)
SCM	Smeared charge model
SLE	Solid-liquid equilibrium
SLS	Static light scattering

8. References

Abel, J.J., Geiling, E.M.K., Roullier, C.A., Bell, F.K. and Wintersteiner, O., 1927, *Crystalline Insulin*. Journal of Pharmacology and Experimental Therapeutics, 31, 65-85.

Abraham, E.P., 1939, *Some properties of egg-white lysozyme.* Biochemical Journal, 33, 622-30.

Alagna, L., Hasnain, S.S., Piggott, B. and Williams, D.J., 1984, *The Nickel Ion Environment in Jack Bean Urease*. Biochemical Journal, 220, 591-595.

Alber, T., Hartman, F.C., Johnson, R.M., Petsko, G.A. and Tsernoglou, D., 1981, *Crystallization of Yeast Triose Phosphate Isomerase from Polyethylene Glycol - Protein Crystal Formation Following Phase Separation*. Journal of Biological Chemistry, 256, 1356-1361.

Aldabaibeh, N., Jones, M.J., Myerson, A.S. and Ulrich, J., 2009, *The Solubility of Orthorhombic Lysozyme Crystals Obtained at High pH*. Crystal Growth & Design, 9, 3313-3317.

Aldabaibeh, N., 2010, *Towards an Improved Understanding of the Variables Controlling Crystal Modifications and Phase Transitions in Lysozyme Crystals.* PhD Thesis, Illinois Institute of Technology, Chicago, USA.

Alderton, G., Ward, W.H. and Fevold, H.L., 1945, *Isolation of Lysozyme from Egg White*. Journal of Biological Chemistry, 157, 43-58.

Alford, J.R., Kendrick, B.S., Carpenter, J.F. and Randolph, T.W., 2008a, *Measurement of the second osmotic virial coefficient for protein solutions exhibiting monomer-dimer equilibrium*. Analytical Biochemistry, 377, 128-133.

Alford, J.R., Kwok, S.C., Roberts, J.N., Wuttke, D.S., Kendrick, B.S., Carpenter, J.F. and Randolph, T.W., 2008b, *High concentration formulations of recombinant human interleukin-1 receptor antagonist: I. Physical characterization*. Journal of Pharmaceutical Sciences, 97, 3035-3050.

Allahyarov, E., Lowen, H., Hansen, J.P. and Louis, A.A., 2003, *Nonmonotonic variation with salt concentration of the second virial coefficient in protein solutions*. Physical Review E: Statistical, Nonlinear, and Soft Matter Physics, 67, 051404/1-051404/13.

Annunziata, O., Payne, A. and Wang, Y., 2008, *Solubility of Lysozyme in the Presence of Aqueous Chloride Salts: Common-Ion Effect and Its Role on Solubility and Crystal Thermodynamics.* Journal of the American Chemical Society, 130, 13347-13352.

Artymiuk, P.J., Blake, C.C.F., Rice, D.W. and Wilson, K.S., 1982, *The Structures of the Monoclinic and Orthorhombic Forms of Hen Egg-White Lysozyme at 6 Å Resolution*. Acta Crystallographica Section B - Structural Science, 38, 778-783.

Asanov, A.N., DeLucas, L.J., Oldham, P.B. and Wilson, W.W., 1997, *Interfacial aggregation of bovine serum albumin related to crystallization conditions studied by total internal reflection fluorescence*. Journal of Colloid and Interface Science, 196, 62-73.

Astier, J.P., Bokern, D., Lapena, L. and Veesler, S., 2001, *α-amylase crystal growth investigated by in situ atomic force microscopy*. Journal of Crystal Growth, 226, 294-302.

Ataka, M. and Tanaka, S., 1986, *The Growth of Large Single-Crystals of Lysozyme*. Biopolymers, 25, 337-350.

Ataka, M. and Asai, M., 1988, *Systematic Studies on the Crystallization of Lysozyme - Determination and Use of Phase-Diagrams*. Journal of Crystal Growth, 90, 86-93.

Aymard, P., Durand, D. and Nicolai, T., 1996, *The effect of temperature and ionic strength on the dimerisation of β-lactoglobulin*. International Journal of Biological Macromolecules, 19, 213-221.

Balasubramanian, A. and Ponnuraj, K., 2010, *Crystal Structure of the First Plant Urease from Jack Bean: 83 Years of Journey from Its First Crystal to Molecular Structure*. Journal of Molecular Biology, 400, 274-283.

Barfoed, H.C., 1987, *Insulin Production Technology*. Chemical Engineering Progress, 83, 49-54.

Beckmann, W., 2013, *Crystallization*. Wiley-VCH, Weinheim, Germany.

Benas, P., Legrand, L. and Ries-Kautt, M., 2002, *Strong and specific effects of cations on lysozyme chloride solubility*. Acta Crystallographica Section D - Biological Crystallography, 58, 1582-1587.

Berger, B.W., Blamey, C.J., Naik, U.P., Bahnson, B.J. and Lenhoff, A.M., 2005a, *Roles of additives and precipitants in crystallization of calcium- and integrin-binding protein*. Crystal Growth & Design, 5, 1499-1507.

Berger, B.W., Gendron, C.M., Rlobinson, C.R., Kaler, E.W. and Lenhoff, A.M., 2005b, *The role of protein and surfactant interactions in membrane-protein crystallization*. Acta Crystallographica Section D - Biological Crystallography, 61, 724-730.

Berger, B.W., Gendron, C.M., Lenhoff, A.M. and Kaler, E.W., 2006, *Effects of additives on surfactant phase behavior relevant to bacteriorhodopsin crystallization*. Protein Science, 15, 2682-2696.

Bergeron, L., Filobelo, L.F., Galkin, O. and Vekilov, P.G., 2003, *Thermodynamics of the hydrophobicity in crystallization of insulin*. Biophysical Journal, 85, 3935-3942.

Berman, H.M., Westbrook, J., Feng, Z., Gilliland, G., Bhat, T.N., Weissig, H., Shindyalov, I.N. and Bourne, P.E., 2000, *The Protein Data Bank*. Nucleic Acids Research, 28, 235-242.

Berthou, J. and Jolles, P., 1974, *Phase-Transition in a Protein Crystal - Example of Hen Lysozyme*. Biochimica et Biophysica Acta, 336, 222-227.

Berthou, J. and Jolles, P., 1978, *Extension of Transition Phenomenon in Hen Egg-White Lysozyme Crystals - Case of Monoclinic Crystals*. Biochimie, 60, 209-210.

Bhamidi, V., Hanson, B.L., Edmundson, A., Skrzypczak-Jankun, E. and Schall, C., 1999, *The influence of a homologous protein impurity on lysozyme crystal growth*. Journal of Crystal Growth, 204, 542-552.

BIPM, 2006, *The International System of Units*. Bureau International des Poids et Mesures, Paris, France.

Biswal, B.K., Sukumar, N. and Vijayan, M., 2000, *Hydration, mobility and accessibility of lysozyme: structures of a pH 6.5 orthorhombic form and its low-humidity variant and a comparative study involving 20 crystallographically independent molecules*. Acta Crystallographica Section D - Biological Crystallography, 56, 1110-1119.

Boistelle, R., Astier, J.P., Marchismouren, G., Desseaux, V. and Haser, R., 1992, *Solubility, Phase-Transition, Kinetic Ripening and Growth-Rates of Porcine Pancreatic Alpha-Amylase Isoenzymes*. Journal of Crystal Growth, 123, 109-120.

Bolanos-Garcia, V.M., Mas-Oliva, J., Soriano-Garcia, M. and Moreno, A., 1998, *Precrystallization of human apoprotein A-I based on its aggregation behavior in solution studied by dynamic light scattering*. Journal of Molecular Structure, 440, 1-8.

Brader, M.L., Hughes, B.L., Li, S., Ng, K., Sukumar, M. and Wolff, R.K., 2000, *Insulin crystals for pulmonary administration.* PCT Int. Appl. WO 2000US08723 20000413.

Braun, M., Teichert, O. and Zweck, A., 2006, *Biokatalyse in der industriellen Produktion*. Zukünftige Technologien Consulting der VDI Technologiezentrum GmbH, Düsseldorf, Germany.

Brereton, R.G., 2003, *Chemometrics*. John Wiley & Sons, Chichester, UK.

Brinkmann, C., Weiss, M.S. and Weckert, E., 2006, *The structure of the hexagonal crystal form of hen egg-white lysozyme*. Acta Crystallographica Section D-Biological Crystallography, 62, 349-355.

Broutin, I., Rieskautt, M. and Ducruix, A., 1995, *Lysozyme Solubility in H_2O and D_2O Solutions as a Function of Sodium-Chloride Concentration*. Journal of Applied Crystallography, 28, 614-617.

Bruns, W., 1996, *The Second Osmotic Virial Coefficient of Polymer Solutions.* Macromolecules, 29, 2641-3.

Budayova, M., Astier, J.P., Veesler, S., Czjzek, M., Belaich, A. and Boistelle, R., 1999, *Characterization and crystallization of the Endoglucanase A from Clostridium Cellulolyticum in solution*. Journal of Crystal Growth, 196, 297-304.

Budayova-Spano, M., Lafont, S., Astier, J.P., Ebel, C. and Veesler, S., 2000, *Comparison of solubility and interactions of aprotinin (BPTI) solutions in H_2O and D_2O*. Journal of Crystal Growth, 217, 311-319.

Burton, J.A., Kolb, E.D., Slichter, W.P. and Struthers, J.D., 1953, *Distribution of Solute in Crystals Grown from the Melt .2. Experimental*. Journal of Chemical Physics, 21, 1991-1996.

Cacioppo, E., Munson, S. and Pusey, M.L., 1991a, *Protein Solubilities Determined by a Rapid Technique and Modification of That Technique to a Micromethod*. Journal of Crystal Growth, 110, 66-71.

Cacioppo, E. and Pusey, M.L., 1991b, *The Solubility of the Tetragonal Form of Hen Egg-White Lysozyme from pH 4.0 to 5.4*. Journal of Crystal Growth, 114, 286-292.

Cacioppo, E. and Pusey, M.L., 1992, *The Effects of Acid Treatment and Calcium-Ions on the Solubility of Concanavalin-A*. Journal of Crystal Growth, 122, 208-212.

Carbonnaux, C., Rieskautt, M. and Ducruix, A., 1995, *Relative Effectiveness of Various Anions on the Solubility of Acidic Hypoderma-Lineatum Collagenase at Ph 7.2*. Protein Science, 4, 2123-2128.

Chayen, N., Akins, J., Campbellsmith, S. and Blow, D.M., 1988, *Solubility of Glucose Isomerase in Ammonium Sulfate Solutions*. Journal of Crystal Growth, 90, 112-116.

Chen, D.L., Gerdts, C.J. and Ismagilov, R.F., 2005, *Using microfluidics to observe the effect of mixing on nucleation of protein crystals*. Journal of the American Chemical Society, 127, 9672-9673.

Chin, J.T., Wheeler, S.L. and Klibanov, A.M., 1994, *On protein solubility in organic solvents.* Biotechnology and Bioengineering, 44, 140-145.

Coen, C.J., Blanch, H.W. and Prausnitz, J.M., 1995, *Salting-out of Aqueous Proteins - Phase-Equilibria and Intermolecular Potentials*. AIChE Journal, 41, 996-1004.

Coen, C.J., Prausnitz, J.M. and Blanch, H.W., 1997, *Protein salting-out: Phase equilibria in two-protein systems*. Biotechnology and Bioengineering, 53, 567-574.

Cohn, E.J., 1922, *Studies in the Physical Chemistry of the Proteins : I. The Solubility of Certain Proteins at Their Isoelectric Points*. The Journal of General Physiology, 4, 697-722.

Cohn, E.J. and Hendry, J.L., 1923, *Studies in the Physical Chemistry of the Proteins : II. The Relation between the Solubility of Casein and Its Capacity to Combine with Base. The Solubility of Casein in Systems Containing the Protein and Sodium Hydroxide*. The Journal of General Physiology, 5, 521-54.

Cohn, E.J., Berggren, R.E. and Hendry, J.L., 1924, *Studies in the Physical Chemistry of the Proteins : IV. The Relation between the Composition of Zein and Its Acid and Basic Properties*. The Journal of General Physiology, 7, 81-98.

Cole, J.B., Bryan, M.L. and Bryan, W.P., 1969, *Thermodynamics of solution of lysozyme crystals.* Archives of Biochemistry and Biophysics, 130, 86-91.

Conway, E.J., FitzGerald, O. and McGeeney, K.F., 1966, *Urease. Studies in its isolation*. Irish Journal of Medical Science, No. 491, 502-6.

Curcio, E., Di Profio, G. and Drioli, E., 2003, *A new membrane-based crystallization technique: tests on lysozyme*. Journal of Crystal Growth, 247, 166-176.

Curcio, E., Simone, S., Di Profio, G., Drioli, E., Cassetta, A. and Lamba, D., 2005, *Membrane crystallization of lysozyme under forced solution flow*. Journal of Membrane Science, 257, 134-143.

Curcio, E., Fontananova, E., Di Profio, G. and Drioli, E., 2006, *Influence of the structural properties of poly(vinylidene fluoride) membranes on the heterogeneous nucleation rate of protein crystals*. Journal of Physical Chemistry B, 110, 12438-12445.

Curtis, R.A., Montaser, A., Prausnitz, J.M. and Blanch, H.W., 1998, *Protein-protein and protein-salt interactions in aqueous protein solutions containing concentrated electrolytes*. Biotechnology and Bioengineering, 57, 11-21.

DeMattei, R.C. and Feigelson, R.S., 1991, *The Solubility Dependence of Canavalin on pH and Temperature*. Journal of Crystal Growth, 110, 34-40.

Demoruelle, K., Guo, B., Kao, S.M., McDonald, H.M., Nikic, D.B., Holman, S.C. and Wilson, W.W., 2002, *Correlation between the osmotic second virial coefficient and solubility for equine serum albumin and ovalbumin*. Acta Crystallographica Section D - Biological Crystallography, 58, 1544-1548.

Deshpande, S.S. and Damodaran, S., 1989, *Effect of Phytate on Solubility, Activity and Conformation of Trypsin and Chymotrypsin*. Journal of Food Science, 54, 695-699.

Deszczynski, M., Harding, S.E. and Winzor, D.J., 2006, *Negative second virial coefficients as predictors of protein crystal growth: Evidence from sedimentation equilibrium studies that refutes the designation of those light scattering parameters as osmotic virial coefficients*. Biophysical Chemistry, 120, 106-113.

Di Profio, G., Curcio, E., Cassetta, A., Lamba, D. and Drioli, E., 2003, *Membrane crystallization of lysozyme: kinetic aspects*. Journal of Crystal Growth, 257, 359-369.

Di Profio, G., Curcio, E. and Drioli, E., 2005a, *Trypsin crystallization by membrane-based techniques*. Journal of Structural Biology, 150, 41-49.

Di Profio, G., Perrone, G., Curcio, E., Cassetta, A., Lamba, D. and Drioli, E., 2005b, *Preparation of enzyme crystals with tunable morphology in membrane crystallizers*. Industrial & Engineering Chemistry Research, 44, 10005-10012.

Di Profio, G., Curcio, E. and Drioli, E., 2010, *Supersaturation Control and Heterogeneous Nucleation in Membrane Crystallizers: Facts and Perspectives*. Industrial & Engineering Chemistry Research, 49, 11878-11889.

Diaz Borbon, V. and Ulrich, J., 2012, *Solvent freeze out crystallization of lysozyme from a lysozyme-ovalbumin mixture*. Crystal Research and Technology, 47, 541-547.

Diaz Borbon, V.P., 2013a, *Solvent Freeze Out (SFO) Technology for Protein Crystallization.* PhD Thesis, Martin-Luther-Universität Halle-Wittenberg, Halle (Saale), Germany.

Diaz Borbon, V.P. and Ulrich, J., 2013b, *SFO-solvent freeze out-technology for industrial proteins*. Journal of Crystal Growth, 373, 38-44.

Dounce, A.L., 1941, *An Improved Method for Recrystallizing Urease*. Journal of Biological Chemistry, 140, 307-308.

Dumetz, A.C., Snellinger-O'Brien, A.M., Kaler, E.W. and Lenhoff, A.M., 2007, *Patterns of protein - protein interactions in salt solutions and implications for protein crystallization*. Protein Science, 16, 1867-1877.

Dumetz, A.C., Chockla, A.M., Kaler, E.W. and Lenhoff, A.M., 2008, *Effects of pH on protein-protein interactions and implications for protein phase behavior*. Biochimica et Biophysica Acta - Proteins and Proteomics, 1784, 600-610.

Dumetz, A.C., Chockla, A.M., Kaler, E.W. and Lenhoff, A.M., 2009, *Comparative Effects of Salt, Organic, and Polymer Precipitants on Protein Phase Behavior and Implications for Vapor Diffusion*. Crystal Growth & Design, 9, 682-691.

Durbin, S.D., Carlson, W.E. and Saros, M.T., 1993, *In-Situ Studies of Protein Crystal Growth by Atomic Force Microscopy*. Journal of Physics D - Applied Physics, 26, B128-B132.

Edelhoch, H., 1967, *Spectroscopic Determination of Tryptophan and Tyrosine in Proteins*. Biochemistry, 6, 1948-&.

Espitalier, F., Cheng, Y.C. and Lenhoff, A.M., 2009, *Mechanism of formation of lysozyme crystals in concentrated ammonium sulfate solution from concentration profiles and equilibria: Influence of the 2nd osmotic virial coefficient*. Powder Technology, 190, 112-117.

Ewing, F., Forsythe, E. and Pusey, M., 1994, *Orthorhombic Lysozyme Solubility*. Acta Crystallographica Section D - Biological Crystallography, 50, 424-428.

Feeling-Taylor, A.R., Banish, R.M., Hirsch, R.E. and Vekilov, P.G., 1999, *Miniaturized scintillation technique for protein solubility determinations*. Review of Scientific Instruments, 70, 2845-2849.

Fleming, A., 1922, *Remarkable bacteriolytic element found in tissues and secretions.* Proceedings of the Royal Society of London, Series B: Biological Sciences, 93, 306-317.

Follmer, C., Pereira, F.V., da Silveira, N.P. and Carlini, C.R., 2004, *Jack bean urease (EC 3.5.1.5) aggregation monitored by dynamic and static light scattering*. Biophysical Chemistry, 111, 79-87.

Forsythe, E. and Pusey, M.L., 1994, *The Effects of Temperature and NaCl Concentration on Tetragonal Lysozyme Face Growth Rates*. Journal of Crystal Growth, 139, 89-94.

Forsythe, E.L. and Pusey, M.L., 1996, *The effects of acetate buffer concentration on lysozyme solubility*. Journal of Crystal Growth, 168, 112-117.

Forsythe, E.L., Judge, R.A. and Pusey, M.L., 1999a, *Tetragonal chicken egg white lysozyme solubility in sodium chloride solutions*. Journal of Chemical and Engineering Data, 44, 637-640.

Forsythe, E.L., Snell, E.H., Malone, C.C. and Pusey, M.L., 1999b, *Crystallization of chicken egg white lysozyme from assorted sulfate salts*. Journal of Crystal Growth, 196, 332-343.

Forsythe, R.H. and Foster, J.F., 1950, *Egg White Proteins .1. Electrophoretic Studies on Whole White*. Journal of Biological Chemistry, 184, 377-383.

Franco, L.F.M. and Pessoa Filho, P.d.A., 2013, *On the Relationship between the Solubility of Proteins and the Osmotic Second Virial Coefficient*. Brazilian Journal of Chemical Engineering, 30, 95-104.

Galeotti, G., 1906, *Equilibrium between proteids and electrolytes. III. Solubility of globulin in magnesium sulphate: influence of temperature.* Zeitschrift für Physiologische Chemie, 48, 473-80.

Galkin, O. and Vekilov, P.G., 1999, *Direct determination of the nucleation rates of protein crystals*. Journal of Physical Chemistry B, 103, 10965-10971.

Galkin, O. and Vekilov, P.G., 2000a, *Control of protein crystal nucleation around the metastable liquid-liquid phase boundary*. Proceedings of the National Academy of Sciences of the United States of America, 97, 6277-6281.

Galkin, O. and Vekilov, P.G., 2000b, *Are nucleation kinetics of protein crystals similar to those of liquid droplets?* Journal of the American Chemical Society, 122, 156-163.

Galkin, O. and Vekilov, P.G., 2001, *Nucleation of protein crystals: critical nuclei, phase behavior, and control pathways*. Journal of Crystal Growth, 232, 63-76.

Galkin, O., Pan, W., Filobelo, L., Hirsch, R.E., Nagel, R.L. and Vekilov, P.G., 2007, *Two-step mechanism of homogeneous nucleation of sickle cell hemoglobin polymers*. Biophysical Journal, 93, 902-913.

Garside, J. and Davey, R.J., 1980, *Secondary Contact Nucleation - Kinetics, Growth and Scale-Up*. Chemical Engineering Communications, 4, 393-424.

Georgalis, Y. and Saenger, W., 1993, *Time-Resolved Light Scattering Studies on Protein Precrystallization Fractal Clusters*. Advances in Colloid and Interface Science, 46, 165-183.

Georgalis, Y., Umbach, P., Raptis, J. and Saenger, W., 1997a, *Lysozyme aggregation studied by light scattering .1. Influence of concentration and nature of electrolytes*. Acta Crystallographica Section D - Biological Crystallography, 53, 691-702.

Georgalis, Y., Umbach, P., Zielenkiewicz, A., Utzig, E., Zielenkiewicz, W., Zielenkiewicz, P. and Saenger, W., 1997b, *Microcalorimetric and small-angle light scattering studies on nucleating lysozyme solutions*. Journal of the American Chemical Society, 119, 11959-11965.

Georgalis, Y., Umbach, P., Soumpasis, D.M. and Saenger, W., 1998, *Dynamics and microstructure formation during nucleation of lysozyme solutions*. Journal of the American Chemical Society, 120, 5539-5548.

George, A. and Wilson, W.W., 1994, *Predicting Protein Crystallization from a Dilute-Solution Property*. Acta Crystallographica Section D - Biological Crystallography, 50, 361-365.

Gibbs, J.W., 1928, *The Collected Works of J. Willard Gibbs*. C. Longmans, Green and Co., New York, USA.

Gill, S.C. and Vonhippel, P.H., 1989, *Calculation of Protein Extinction Coefficients from Amino-Acid Sequence Data*. Analytical Biochemistry, 182, 319-326.

Gillespie, C.M., Asthagiri, D. and Lenhoff, A.M., 2014, *Polymorphic Protein Crystal Growth: Influence of Hydration and Ions in Glucose Isomerase*. Crystal Growth & Design, 14, 46-57.

Gliko, O., Reviakine, I. and Vekilov, P.G., 2003, *Stable equidistant step trains during crystallization of insulin*. Physical Review Letters, 90, 225503-1 - 225503-4.

Gliko, O., Neumaier, N., Pan, W., Haase, I., Fischer, M., Bacher, A., Weinkauf, S. and Vekilov, P.G., 2005, *A metastable prerequisite for the growth of lumazine synthase crystals*. Journal of the American Chemical Society, 127, 3433-3438.

Gliko, O., Pan, W., Katsonis, P., Neumaier, N., Galkin, O., Weinkauf, S. and Vekilov, P.G., 2007, *Metastable liquid clusters in super- and undersaturated protein solutions*. Journal of Physical Chemistry B, 111, 3106-3114.

Gorin, G., Butler, M.F., Katyal, J.M. and Buckley, J.E., 1960, *Isolation of crystalline urease*. Proceedings of the Oklahoma Academy of Science, 40, 62-70.

Gorti, S., Forsythe, E.L. and Pusey, M.L., 2005, *Growth modes and energetics of (101) face lysozyme crystal growth*. Crystal Growth & Design, 5, 473-482.

Gray, R.J., Hou, W.B., Kudryavtsev, A.B. and DeLucas, L.J., 2001, *A new approach to the measurement of protein solubility by Michaelson interferometry*. Journal of Crystal Growth, 232, 10-16.

Green, A.A., 1931a, *Studies on the physical chemistry of proteins. VIII. The solubility of hemoglobin in concentrated salt solutions. A study of the salting out of proteins*. Journal of Biological Chemistry, 93, 495-516.

Green, A.A., 1931b, *Studies in the physical chemistry of the proteins. IX. The effect of electrolytes on the solubility of hemoglobin in solutions of varying hydrogen ion activity with a note on the comparable behavior of casein*. Journal of Biological Chemistry, 93, 517-542.

Green, A.A., 1932, *Studies in the physical chemistry of the proteins. X. The solubility of hemoglobin in solutions of chlorides and sulfates of varying concentrations*. Journal of Biological Chemistry, 95, 47-66.

Green, A.A., Cohn, E.J. and Blanchard, M.H., 1935, *Studies in the physical chemistry of the proteins. XII. The solubility of human hemoglobin in concentrated salt solutions*. Journal of Biological Chemistry, 109, 631-634.

Grimsley, G.R. and Pace, C.N., 2003, *Spectrophotometric determination of protein concentration*. Current Protocols in Protein Science, Supplement 33, 3.1.1 - 3.1.9.

Gripon, C., Legrand, L., Rosenman, I., Vidal, O., Robert, M.C. and Boue, F., 1997, *Lysozyme solubility in H_2O and D_2O solutions: A simple relationship*. Journal of Crystal Growth, 177, 238-247.

Gugliuzza, A., Aceto, M.C. and Drioli, E., 2009, *Interactive functional poly(vinylidene fluoride) membranes with modulated lysozyme affinity: a promising class of new interfaces for contactor crystallizers*. Polymer International, 58, 1452-1464.

Guilloteau, J.P., Riès-Kautt, M.M. and Ducruix, A.F., 1992, *Variation of Lysozyme Solubility as a Function of Temperature in the Presence of Organic and Inorganic Salts*. Journal of Crystal Growth, 122, 223-230.

Haas, C. and Drenth, J., 1998, *The protein-water phase diagram and the growth of protein crystals from aqueous solution*. Journal of Physical Chemistry B, 102, 4226-4232.

Haas, C., Drenth, J. and Wilson, W.W., 1999, *Relation between the solubility of proteins in aqueous solutions and the second virial coefficient of the solution*. Journal of Physical Chemistry B, 103, 2808-2811.

Haire, L.F. and Blow, D.M., 2001, *A novel spin filter method for the measurement of solubility*. Journal of Crystal Growth, 232, 17-20.

Hanabusa, K., 1961, *High-Yield Crystallization of Urease from Jack Bean*. Nature, 189, 551-553.

Harata, K., 1994, *X-Ray Structure of a Monoclinic Form of Hen Egg-White Lysozyme Crystallized at 313 K - Comparison of 2 Independent Molecules*. Acta Crystallographica Section D - Biological Crystallography, 50, 250-257.

Harata, K. and Akiba, T., 2004, *Phase transition of triclinic hen egg-white lysozyme crystal associated with sodium binding*. Acta Crystallographica Section D - Biological Crystallography, 60, 630-637.

Harata, K. and Akiba, T., 2006, *Structural phase transition of monoclinic crystals of hen egg-white lysozyme*. Acta Crystallographica Section D - Biological Crystallography, 62, 375-382.

Hazra, P., Adhikary, L., Dave, N., Khedkar, A., Manjunath, H.S., Anantharaman, R. and Iyer, H., 2010, *Development of a Process to Manufacture PEGylated Orally Bioavailable Insulin*. Biotechnology Progress, 26, 1695-1704.

Heijna, M.C.R., Van Enckevort, W.J.P. and Vlieg, E., 2007, *Crystal growth in a three-phase system: diffusion and liquid-liquid phase separation in lysozyme crystal growth*. Physical Review E, 76, 011604.

Henning, S. and Ulrich, J., 1997, *Description of the migration of liquid inclusions in growing crystalline layers*. Chemical Engineering Research & Design, 75, 233-236.

Hofmeister, F., 1890, *Ueber die Darstellung von krystallisirtem Eieralbumin und die Krystallisirbarkeit colloider Stoffe*. Zeitschrift für Physiologische Chemie, 14, 165-172.

Howard, S.B., Twigg, P.J., Baird, J.K. and Meehan, E.J., 1988, *The Solubility of Hen Egg-White Lysozyme*. Journal of Crystal Growth, 90, 94-104.

Hünefeld, F.L., 1840, *Der Chemismus in der thierischen Organisation*. F.A. Brockhaus, Leipzig, Germany.

Ildefonso, M., Candoni, N. and Veesler, S., 2011, *Using Microfluidics for Fast, Accurate Measurement of Lysozyme Nucleation Kinetics*. Crystal Growth & Design, 11, 1527-1530.

Ildefonso, M., Candoni, N. and Veesler, S., 2013, *Heterogeneous Nucleation in Droplet-Based Nucleation Measurements*. Crystal Growth & Design, 13, 2107-2110.

Ison, A., Odeh, I.N. and Margerum, D.W., 2006, *Kinetics and mechanisms of chlorine dioxide and chlorite oxidations of cysteine and glutathione*. Inorganic Chemistry, 45, 8768-8775.

Israelachvili, J.N., 2011, *Intermolecular and Surface Forces*. Academic Press, Waltham, Massachussetts, USA.

Jolles, P. and Berthou, J., 1972, *High-Temperature Crystallization of Lysozyme - Example of Phase-Transition*. FEBS Letters, 23, 21-23.

Jones, M.J. and Ulrich, J., 2005, *Industrial crystallisation of proteins - A question of activity*. Chemie Ingenieur Technik, 77, 1527-1534.

Jones, M.J. and Ulrich, J., 2010, *Are Different Protein Crystal Modifications Polymorphs? A Discussion*. Chemical Engineering & Technology, 33, 1571-1576.

Juarez-Martinez, G., Garza, C., Castillo, R. and Moreno, A., 2001, *A dynamic light scattering investigation of the nucleation and growth of thaumatin crystals*. Journal of Crystal Growth, 232, 119-131.

Judge, R.A., Johns, M.R. and White, E.T., 1995, *Protein Purification by Bulk Crystallization - the Recovery of Ovalbumin*. Biotechnology and Bioengineering, 48, 316-323.

Judge, R.A., Johns, M.R. and White, E.T., 1996, *Solubility of ovalbumin in ammonium sulfate solutions*. Journal of Chemical and Engineering Data, 41, 422-424.

Judge, R.A., Forsythe, E.L. and Pusey, M.L., 2010, *Growth Rate Dispersion in Protein Crystal Growth.* Crystal Growth & Design, 10, 3164-3168.

Kadima, W., McPherson, A., Dunn, M.F. and Jurnak, F.A., 1990, *Characterization of Precrystallization Aggregation of Canavalin by Dynamic Light-Scattering*. Biophysical Journal, 57, 125-132.

Kadima, W., McPherson, A., Dunn, M.F. and Jurnak, F., 1991, *Precrystallization Aggregation of Insulin by Dynamic Light-Scattering and Comparison with Canavalin*. Journal of Crystal Growth, 110, 188-194.

Kam, Z., Shore, H.B. and Feher, G., 1978, *On the Crystallization of Proteins*. Journal of Molecular Biology, 123, 539-555.

Kashchiev, D., Vekilov, P.G. and Kolomeisky, A.B., 2005, *Kinetics of two-step nucleation of crystals*. Journal of Chemical Physics, 122, 244706-1 - 244706-6.

Kashimoto, E., Sazaki, G., Hasegawa, K., Nakada, T., Miyashita, S., Komatsu, H., Sato, K., Matsuura, Y. and Tanaka, H., 1998, *Crystallization studies on a concanavalin A crystal with high-index faces*. Journal of Crystal Growth, 186, 461-470.

Katsonis, P., Brandon, S. and Vekilov, P.G., 2006, *Corresponding-states laws for protein solutions*. Journal of Physical Chemistry B, 110, 17638-17644.

Kodama, K., 1922, *The solubility of globulin in neutral salt solution.* Journal of Biochemistry, 1, 419-432.

Korolev, V.F., 1939, *The properties and conditions for the formation of sodium chloride dihydrate.* Byull. Tsentral. Nauch.-Issledovatel. Solyanoi Lab., 56-78.

Kroeff, E.P., Owens, R.A., Campbell, E.L., Johnson, R.D. and Marks, H.I., 1989, *Production Scale Purification of Biosynthetic Human Insulin by Reversed-Phase High-Performance Liquid-Chromatography*. Journal of Chromatography, 461, 45-61.

Kubacki, V., Brown, K.D. and Laskowski, M., 1949, *Electrophoresis and Solubility of Chymotrypsinogen-B and Chymotrypsin-B*. Journal of Biological Chemistry, 180, 73-78.

Kunitz, M. and Northrop, J.H., 1938, *Solubility of proteins as a test of purity. The solubility of chymotrypsin and chymotrypsinogen.* Comptes Rendus des Travaux du Laboratoire Carlsberg, Serie Chimique, 22, 288-94.

Laemmli, U.K., 1970, *Cleavage of Structural Proteins During Assembly of Head of Bacteriophage-T4*. Nature, 227, 680-685.

Lafont, S., Veesler, S., Astier, J.P. and Boistelle, R., 1994, *Solubility and Prenucleation of Aprotinin (BPTI) Molecules in Sodium-Chloride Solutions*. Journal of Crystal Growth, 143, 249-255.

Lafont, S., Veesler, S., Astier, J.P. and Boistelle, R., 1997, *Comparison of solubilities and molecular interactions of BPTI molecules giving different polymorphs*. Journal of Crystal Growth, 173, 132-140.

Landau, L.D. and Lifshitz, E.M., 1996, *Statistical Physics, Part 1*. Elsevier Butterworth-Heineman, Oxford, UK.

Landsteiner, K. and Heidelberger, M., 1923, *Differentiation of oxyhemoglobins by means of mutual solubility tests.* Journal of General Physiology, 6, 131-135.

Legrand, L., Ries-Kautt, M. and Robert, M.C., 2002, *Two polymorphs of lysozyme nitrate: temperature dependence of their solubility*. Acta Crystallographica Section D - Biological Crystallography, 58, 1564-1567.

Lens, J., 1946, *The Solubility Curve and the Purity of Insulin*. Journal of Biological Chemistry, 164, 223-231.

Li, Y., Lubchenko, V. and Vekilov, P.G., 2011, *The use of dynamic light scattering and Brownian microscopy to characterize protein aggregation*. Review of Scientific Instruments, 82, 053106-1 - 053106-8.

Lim, K., Nadarajah, A., Forsythe, E.L. and Pusey, M.L., 1998, *Locations of bromide ions in tetragonal lysozyme crystals*. Acta Crystallographica Section D - Biological Crystallography, 54, 899-904.

Lipinski, C.A., Lombardo, F., Dominy, B.W. and Feeney, P.J., 2001, *Experimental and computational approaches to estimate solubility and permeability in drug discovery and development settings*. Advanced Drug Delivery Reviews, 46, 3-26.

Lipinski, C.A., Lombardo, F., Dominy, B.W. and Feeney, P.J., 2012, *Experimental and computational approaches to estimate solubility and permeability in drug discovery and development settings*. Advanced Drug Delivery Reviews, 64, 4-17.

Liu, J., Yin, D.-C., Guo, Y.-Z., Wang, X.-K., Xie, S.-X., Lu, Q.-Q. and Liu, Y.-M., 2011, *Selecting Temperature for Protein Crystallization Screens Using the Temperature Dependence of the Second Virial Coefficient*. Plos One, 6, e17950.

Liu, Y., Pietzsch, M. and Ulrich, J., 2014, *Determination of the phase diagram for the crystallization of L-asparaginase II by a turbidity technique.* Crystal Research and Technology, 49, 262-268.

Longsworth, L.G., Cannan, R.K. and MacInnes, D.A., 1940, *An electrophoretic study of the proteins of egg white.* Journal of the American Chemical Society, 62, 2580-2590.

Lowry, O.H., Rosebrough, N.J., Farr, A.L. and Randall, R.J., 1951, *Protein Measurement with the Folin Phenol Reagent*. Journal of Biological Chemistry, 193, 265-275.

Lu, J., Wang, X.J. and Ching, C.B., 2003, *Effect of additives on the crystallization of lysozyme and chymotrypsinogen A*. Crystal Growth & Design, 3, 83-87.

Lu, J., Jiang, X.-L., Li, Z., Rohani, S. and Ching, C.-B., 2011, *Solubility of a Lysozyme in Polyelectrolyte Aqueous Solutions.* Journal of Chemical & Engineering Data, 56, 4808-4812.

Lynn, K.R., 1967, *Some Properties and Purification of Urease*. Biochimica et Biophysica Acta, 146, 205-218.

Madhusudan, Kodandapani, R. and Vijayan, M., 1993, *Protein Hydration and Water Structure - X-Ray-Analysis of a Closely Packed Protein Crystal with Very Low Solvent Content*. Acta Crystallographica Section D-Biological Crystallography, 49, 234-245.

Majeed, S., Ofek, G., Belachew, A., Huang, C.C., Zhou, T.Q. and Kwong, P.D., 2003, *Enhancing protein crystallization through precipitant synergy*. Structure, 11, 1061-1070.

Malkin, A.J., Kuznetsov, Y.G., Glantz, W. and McPherson, A., 1996, *Atomic force microscopy studies of surface morphology and growth kinetics in thaumatin crystallization*. Journal of Physical Chemistry, 100, 11736-11743.

Maosoongnern, S., Borbon, V.D., Flood, A.E. and Ulrich, J., 2012, *Introducing a Fast Method to Determine the Solubility and Metastable Zone Width for Proteins: Case Study Lysozyme*. Industrial & Engineering Chemistry Research, 51, 15251-15257.

McPherson, A., 1999, *Crystallization of Biological Macromolecules*. Cold Spring Harbor Laboratory Press, Cold Spring Harbour, NY, USA.

Meyer, K., Thompson, R., Palmer, J.W. and Khorazo, D., 1936, *The purification and properties of lysozyme.* Journal of Biological Chemistry, 113, 303-309.

Mihalyi, E., 1968, *Numerical values of the absorbances of the aromatic amino acids in acid, neutral, and alkaline solutions.* Journal of Chemical and Engineering Data, 13, 179-182.

Mikol, V. and Giege, R., 1989a, *Phase-Diagram of a Crystalline Protein - Determination of the Solubility of Concanavalin a by a Microquantitation Assay*. Journal of Crystal Growth, 97, 324-332.

Mikol, V., Hirsch, E. and Giege, R., 1989b, *Monitoring Protein Crystallization by Dynamic Light-Scattering*. FEBS Letters, 258, 63-66.

Moré, S. and Saenger, W., 1995, *Growth Mechanism of Concanavalin A Crystals*. Journal of Crystal Growth, 153, 35-41.

Moreno, A., Mas-Oliva, J., Soriano-Garcia, M., Salvador, C.O. and Bolanos-Garcia, V.M., 2000, *Turbidity as a useful optical parameter to predict protein crystallization by dynamic light scattering*. Journal of Molecular Structure, 519, 243-256.

Moretti, J.J., Sandler, S.I. and Lenhoff, A.M., 2000, *Phase equilibria in the lysozyme-ammonium sulfate-water system*. Biotechnology and Bioengineering, 70, 498-506.

Müller, C., 2012, *How to describe protein crystals correctly? - case study of lysozyme crystals.* PhD Thesis, Martin-Luther-Universität Halle-Wittenberg, Halle (Saale), Germany.

Mullin, J.W., 2001, *Crystallization*. Butterworth-Heineman, Oxford, UK.

Mutaftschiev, B., 2001, *The Atomistic Nature of Crystal Growth*. Springer Verlag, Berlin, Germany.

Myerson, A.S., 1993, *Handbook of Industrial Crystallization*. Butterworth-Heinemann, Stoneham, MA, USA.

Nadarajah, A., Forsythe, E.L. and Pusey, M.L., 1995, *The Averaged Face Growth-Rates of Lysozyme Crystals - the Effect of Temperature*. Journal of Crystal Growth, 151, 163-172.

Nagendra, H.G., Sudarsanakumar, C. and Vijayan, M., 1995, *Characterization of Lysozyme Crystals with Unusually Low Solvent Content*. Acta Crystallographica Section D - Biological Crystallography, 51, 390-392.

Nagendra, H.G., Sudarsanakumar, C. and Vijayan, M., 1996, *An X-ray analysis of native monoclinic lysozyme. A case study on the reliability of refined protein structures and a comparison with the low-humidity form in relation to mobility and enzyme action*. Acta Crystallographica Section D-Biological Crystallography, 52, 1067-1074.

Nakazato, K., Homma, T. and Tomo, T., 2004, *Rapid solubility measurement of protein crystals as a function of precipitant concentration with micro-dialysis cell and two-beam interferometer*. Journal of Synchrotron Radiation, 11, 34-37.

Neal, B.L., Asthagiri, D., Velev, O.D., Lenhoff, A.M. and Kaler, E.W., 1999, *Why is the osmotic second virial coefficient related to protein crystallization?* Journal of Crystal Growth, 196, 377-387.

Ninomiya, K., Yamamoto, T., Oheda, T., Sato, K., Sazaki, G. and Matsuura, Y., 2001, *Morphology and solubility of multiple crystal forms of Taka-amylase A*. Journal of Crystal Growth, 222, 311-316.

Noble, J.E. and Bailey, M.J.A., 2009, *Quantitation of Protein*. In: Guide to Protein Purification, Second Edition, Methods in Enzymology, 463, 73-95.

Noskov, B.A., 2014, *Protein conformational transitions at the liquid-gas interface as studied by dilational surface rheology.* Advances in Colloid and Interface Science, 206, 222-238.

Ohara, M. and Reid, R.C., 1973, *Modelling Crystal Growth Rates from Solution*. Prentice-Hall Inc., Englewood, N.J., USA.

Oki, H., Matsuura, Y., Komatsu, H. and Chernov, A.A., 1999, *Refined structure of orthorhombic lysozyme crystallized at high temperature: correlation between morphology and intermolecular contacts*. Acta Crystallographica Section D - Biological Crystallography, 55, 114-121.

Onuma, K. and Kanzaki, N., 2007, *Multi-angle static and dynamic light scattering investigation of lysozyme association: From crystallization to liquid-liquid phase separation*. Journal of Crystal Growth, 304, 452-459.

Osborne, T.B. and Campbell, G.F., 1900, *Protein constituents of egg white.* Journal of the American Chemical Society, 22, 422-450.

Osborne, T.B. and Harris, I.F., 1905, *Solubility of globulin (edestin) in salt solutions.* American Journal of Physiology, 14, 151-171.

Pace, C.N., Vajdos, F., Fee, L., Grimsley, G. and Gray, T., 1995, *How to Measure and Predict the Molar Absorption-Coefficient of a Protein*. Protein Science, 4, 2411-2423.

Pan, W., Galkin, O., Filobelo, L., Nagel, R.L. and Vekilov, P.G., 2007, *Metastable mesoscopic clusters in solutions of sickle-cell hemoglobin*. Biophysical Journal, 92, 267-277.

Pan, X. and Glatz, C.E., 2003, *Solvent effects on the second virial coefficient of subtilisin and solubility*. Crystal Growth & Design, 3, 203-207.

Pan, X.J. and Glatz, C.E., 2002, *Solvent effects on the growth kinetics of subtilisin crystals*. Journal of Crystal Growth, 240, 549-559.

Payne, R.W., Nayar, R., Tarantino, R., Del Terzo, S., Moschera, J., Di, J., Heilman, D., Bray, B., Manning, M.C. and Henry, C.S., 2006, *Second virial coefficient determination of a therapeutic peptide by self-interaction chromatography*. Biopolymers, 84, 527-533.

Petsev, D.N., Thomas, B.R., Yau, S.T. and Vekilov, P.G., 2000, *Interactions and aggregation of apoferritin molecules in solution: Effects of added electrolytes*. Biophysical Journal, 78, 2060-2069.

Petsev, D.N., Thomas, B.R., Yau, S.T., Tsekova, D., Nanev, C., Wilson, W.W. and Vekilov, P.G., 2001, *Temperature-independent solubility and interactions between apoferritin monomers and dimers in solution*. Journal of Crystal Growth, 232, 21-29.

Pjura, P.E., Lenhoff, A.M., Leonard, S.A. and Gittis, A.G., 2000, *Protein crystallization by design: Chymotrypsinogen without precipitants*. Journal of Molecular Biology, 300, 235-239.

Plomp, M., McPherson, A., Larson, S.B. and Malkin, A.J., 2001, *Growth mechanisms and kinetics of trypsin crystallization*. Journal of Physical Chemistry B, 105, 542-551.

Poznanski, J., Szymanski, J., Basinska, T., Slomkowski, S. and Zielenkiewicz, W., 2005, *Aggregation of aqueous lysozyme solutions followed by dynamic light scattering and ^{1}H NMR spectroscopy*. Journal of Molecular Liquids, 121, 21-26.

Przybycien, T.M. and Bailey, J.E., 1989, *Solubility-Activity Relationships in the Inorganic Salt-Induced Precipitation of α-Chymotrypsin*. Enzyme and Microbial Technology, 11, 264-276.

Pusey, M.L., 1986, *An Apparatus for Protein Crystal Growth Studies*. Analytical Biochemistry, 158, 50-54.

Pusey, M.L. and Gernert, K., 1988, *A Method for Rapid Liquid-Solid Phase Solubility Measurements Using the Protein Lysozyme*. Journal of Crystal Growth, 88, 419-424.

Pusey, M.L., 1991, *Estimation of the Initial Equilibrium Constants in the Formation of Tetragonal Lysozyme Nuclei*. Journal of Crystal Growth, 110, 60-65.

Retailleau, P., RiesKautt, M. and Ducruix, A., 1997, *No salting-in of lysozyme chloride observed at how ionic strength over a large range of pH*. Biophysical Journal, 73, 2156-2163.

Retailleau, P., Ducruix, A. and Ries-Kautt, M., 2002, *Importance of the nature of anions in lysozyme crystallisation correlated with protein net charge variation*. Acta Crystallographica Section D - Biological Crystallography, 58, 1576-1581.

Riès-Kautt, M.M. and Ducruix, A.F., 1989, *Relative Effectiveness of Various Ions on the Solubility and Crystal-Growth of Lysozyme*. Journal of Biological Chemistry, 264, 745-748.

Riès-Kautt, M.M. and Ducruix, A.F., 1991, *Crystallization of Basic Proteins by Ion-Pairing*. Journal of Crystal Growth, 110, 20-25.

Roberts, E.A.H. and Wells, A.Q., 1937, *The preparation and properties of purified egg-white lysozyme.* Quarterly Journal of Experimental Physiology, 27, 89-98.

Rosenbaum, D., Zamora, P.C. and Zukoski, C.F., 1996a, *Phase behavior of small attractive colloidal particles*. Physical Review Letters, 76, 150-153.

Rosenbaum, D.F. and Zukoski, C.F., 1996b, *Protein interactions and crystallization*. Journal of Crystal Growth, 169, 752-758.

Rosenberger, F., Howard, S.B., Sowers, J.W. and Nyce, T.A., 1993, *Temperature-Dependence of Protein Solubility - Determination and Application to Crystallization in X-Ray Capillaries*. Journal of Crystal Growth, 129, 1-12.

Ruppert, S., Sandler, S.I. and Lenhoff, A.M., 2001, *Correlation between the osmotic second virial coefficient and the solubility of proteins*. Biotechnology Progress, 17, 182-187.

Ryu, B.H., 2010a, *Protein Crystallization by Solvent Freeze-Out Technology.* PhD Thesis, Martin-Luther-Universität Halle-Wittenberg, Halle (Saale), Germany.

Ryu, B.H., Jones, M.J. and Ulrich, J., 2010b, *Crystallization of Hen Egg White Lysozyme by Solvent Freeze-Out: Effect of Cooling Rate on Protein Inclusion in the Ice Layer*. Chemical Engineering & Technology, 33, 1695-1698.

Saito, Y., 1996, *Statistical Physics of Crystal Growth*. World Scientific Publishing Co. Pte. Ltd., Singapore.

Sapan, C.V., Lundblad, R.L. and Price, N.C., 1999, *Colorimetric protein assay techniques*. Biotechnology and Applied Biochemistry, 29, 99-108.

Schlichtkrull, J., 1956, *Insulin Crystals .2. Shape of Rhombohedral Zinc-Insulin Crystals in Relation to Species and Crystallization Media*. Acta Chemica Scandinavica, 10, 1459-1464.

Schlichtkrull, J., 1957a, *Insulin Crystals .5. The Nucleation and Growth of Insulin Crystals*. Acta Chemica Scandinavica, 11, 439-460.

Schlichtkrull, J., 1957b, *Insulin Crystals .6. The Anisotropic Growth of Insulin Crystals*. Acta Chemica Scandinavica, 11, 484-486.

Schlichtkrull, J., 1957c, *Insulin Crystals .7. The Growth of Insulin Crystals*. Acta Chemica Scandinavica, 11, 1248-1256.

Scholz, R., Wangnick, K. and Ulrich, J., 1993, *On the Distribution and Movement of Impurities in Crystalline Layers in Melt Crystallization Processes*. Journal of Physics D - Applied Physics, 26, B156-B161.

Schwert, M.H. and Neurath, H., 1950, *The Precipitation of Insulin by Thiocyanate*. Journal of the American Chemical Society, 72, 2784-2786.

Selimovic, S., Jia, Y. and Fraden, S., 2009, *Measuring the Nucleation Rate of Lysozyme using Microfluidics*. Crystal Growth & Design, 9, 1806-1810.

Shih, Y.C., Prausnitz, J.M. and Blanch, H.W., 1992, *Some Characteristics of Protein Precipitation by Salts*. Biotechnology and Bioengineering, 40, 1155-1164.

Shim, J.-U., Cristobal, G., Link, D.R., Thorsen, T. and Fraden, S., 2007, *Using microfluidics to decouple nucleation and growth of protein crystals*. Crystal Growth & Design, 7, 2192-2194.

Shugar, D., 1952, *The Measurement of Lysozyme Activity and the Ultra-Violet Inactivation of Lysozyme*. Biochimica et Biophysica Acta, 8, 302-309.

Sibille, L. and Pusey, M.L., 1994, *Investigation of Nucleating Lysozyme Solutions*. Acta Crystallographica Section D - Biological Crystallography, 50, 396-397.

Skouri, M., Lorber, B., Giege, R., Munch, J.P. and Candau, J.S., 1995, *Effect of Macromolecular Impurities on Lysozyme Solubility and Crystallizability - Dynamic Light Scattering, Phase Diagram, and Crystal Growth Studies*. Journal of Crystal Growth, 152, 209-220.

Sleutel, M., Willaert, R., Gillespie, C., Evrard, C., Wyns, L. and Maes, D., 2009, *Kinetics and Thermodynamics of Glucose Isomerase Crystallization*. Crystal Growth & Design, 9, 497-504.

Smith, S.C., Johnson, S., Andrews, J. and McPherson, A., 1982, *Biochemical Characterization of Canavalin, the Major Storage Protein of Jack Bean*. Plant Physiology, 70, 1199-1209.

Soral-Smietana, M., Swigon, A., Amarowicz, R. and Sijtsma, L., 1998, *The solubility of trypsin pea protein hydrolysates*. Nahrung-Food, 42, 217-218.

Sörensen, M., 1934, *Carbohydrate content of the proteins from egg white.* Biochemische Zeitschrift, 269, 271-284.

Steinrauf, L.K., 1959, *Preliminary X-Ray Data for Some New Crystalline Forms of β-Lactoglobulin and Hen Egg-White Lysozyme*. Acta Crystallographica, 12, 77-79.

Steinrauf, L.K., 1998, *Structures of monoclinic lysozyme iodide at 1.6 Å and of triclinic lysozyme nitrate at 1.1 Å*. Acta Crystallographica Section D - Biological Crystallography, 54, 767-779.

Strube, J., Grote, F., Josch, J.P. and Ditz, R., 2011, *Process Development and Design of Downstream Processes*. Chemie Ingenieur Technik, 83, 1044-1065.

Sukumar, N., Biswal, B.K. and Vijayan, M., 1999, *Structures of orthorhombic lysozyme grown at basic pH and its low-humidity variant*. Acta Crystallographica Section D - Biological Crystallography, 55, 934-937.

Sumner, J.B., 1919, *The Globulins of the Jack Bean, Canavalia Ensiformis. Preliminary Paper*. Journal of Biological Chemistry, 37, 137-142.

Sumner, J.B., 1926a, *Note. The Recrystallization of Urease*. Journal of Biological Chemistry, 70, 97-98.

Sumner, J.B., 1926b, *The Isolation and Crystallization of the Enzyme Urease. Preliminary Paper*. Journal of Biological Chemistry, 69, 435-441.

Sumner, J.B. and Hand, D.B., 1928a, *Crystalline Urease. II*. Journal of Biological Chemistry, 76, 149-162.

Sumner, J.B. and Holloway, R.G., 1928b, *Crystalline Urease. III. Variations in Jack Bean Meal as Affecting the Yield of Crystals*. Journal of Biological Chemistry, 79, 489-492.

Suzuki, Y., Sawada, T., Miyashita, S., Komatsu, H., Sazaki, G. and Nakada, T., 2000, *An interferometric study of the solubility of lysozyme crystals under high pressure*. Journal of Crystal Growth, 209, 1018-1022.

Suzuki, Y., Konda, E., Hondoh, H. and Tamura, K., 2011, *Effects of temperature, pressure, and pH on the solubility of triclinic lysozyme crystals*. Journal of Crystal Growth, 318, 1085-1088.

Tamagawa, R.E., Miranda, E.A. and Berglund, K.A., 2002, *Raman spectroscopic monitoring and control of aprotinin supersaturation in hanging-drop crystallization*. Crystal Growth & Design, 2, 263-267.

Tanford, C. and Wagner, M.L., 1954, *Hydrogen Ion Equilibria of Lysozyme*. Journal of the American Chemical Society, 76, 3331-3336.

Tavare, N.S., 1985, *Crystal growth rate dispersion.* Canadian Journal of Chemical Engineering, 63, 436-442.

Tessier, P.M., Lenhoff, A.M. and Sandler, S.I., 2002a, *Rapid measurement of protein osmotic second virial coefficients by self-interaction chromatography*. Biophysical Journal, 82, 1620-1631.

Tessier, P.M., Vandrey, S.D., Berger, B.W., Pazhianur, R., Sandler, S.I. and Lenhoff, A.M., 2002b, *Self-interaction chromatography: a novel screening method for rational protein crystallization*. Acta Crystallographica Section D - Biological Crystallography, 58, 1531-1535.

Tessier, P.M., Johnson, H.R., Pazhianur, R., Berger, B.W., Prentice, J.L., Bahnson, B.J., Sandler, S.I. and Lenhoff, A.M., 2003a, *Predictive crystallization of ribonuclease A via rapid screening of osmotic second virial coefficients*. Proteins - Structure Function and Genetics, 50, 303-311.

Tessier, P.M. and Lenhoff, A.M., 2003b, *Measurements of protein self-association as a guide to crystallization*. Current Opinion in Biotechnology, 14, 512-516.

Thomson, J.A., Schurtenberger, P., Thurston, G.M. and Benedek, G.B., 1987, *Binary-Liquid Phase-Separation and Critical Phenomena in a Protein Water Solution*. Proceedings of the National Academy of Sciences of the United States of America, 84, 7079-7083.

Tiller, W.A., Jackson, K.A., Rutter, J.W. and Chalmers, B., 1953, *The redistribution of solute atoms during the solidification of metals.* Acta Metallurgica, 1, 428-437.

Ulrich, J., 1989, *Growth rate dispersion - a review.* Crystal Research and Technology, 24, 249-257.

Ulrich, J. and Glade, H., 2003, *Melt Crystallization - Fundamentals Equipment and Applications*. Shaker Verlag, Aachen, Germany.

Ulrich, J., 2004, *Verfahren und Apparate zur Kristallisation aus Schmelzen*. In: Kristallisation in der industriellen Praxis, Wiley-VCH Verlag, Weinheim, Germany, 248 - 262.

Umbach, P., Georgalis, Y. and Saenger, W., 1998, *Time-resolved small-angle static light scattering on lysozyme during nucleation and growth*. Journal of the American Chemical Society, 120, 2382-2390.

Valente, J.J., Verma, K.S., Manning, M.C., Wilson, W.W. and Henry, C.S., 2005, *Second virial coeffcient studies of cosolvent-induced protein self-interaction*. Biophysical Journal, 89, 4211-4218.

Van Driessche, A.E.S., Gavira, J.A., Patino Lopez, L.D. and Otalora, F., 2009, *Precise protein solubility determination by Laser confocal differential interference contrast microscopy*. Journal of Crystal Growth, 311, 3479-3484.

Vaney, M.C., Maignan, S., RiesKautt, M. and Ducruix, A., 1996, *High-resolution structure (1.33 Å) of a HEW lysozyme tetragonal crystal grown in the APCF apparatus. Data and structural comparison with a crystal grown under microgravity from SpaceHab-01 mission*. Acta Crystallographica Section D - Biological Crystallography, 52, 505-517.

Vaney, M.C., Broutin, I., Retailleau, P., Douangamath, A., Lafont, S., Hamiaux, C., Prange, T., Ducruix, A. and Ries-Kautt, M., 2001, *Structural effects of monovalent anions on polymorphic lysozyme crystals*. Acta Crystallographica Section D - Biological Crystallography, 57, 929-940.

van't Hoff, J.H., 1898, *Vorlesungen über theoretische und physikalische Chemie*. Friedrich Viehweg und Sohn, Braunschweig, Germany.

Veesler, S., Ferte, N., Costes, M.S., Czjzek, M. and Astier, J.P., 2004, *Temperature and pH effect on the polymorphism of aprotinin (BPTI) in sodium bromide solutions*. Crystal Growth & Design, 4, 1137-1141.

Vekilov, P.G., Monaco, L.A., Thomas, B.R., Stojanoff, V. and Rosenberger, F., 1996, *Repartitioning of NaCl and protein impurities in lysozyme crystallization*. Acta Crystallographica Section D - Biological Crystallography, 52, 785-798.

Vekilov, P.G., Feeling-Taylor, A.R., Yau, S.T. and Petsev, D., 2002, *Solvent entropy contribution to the free energy of protein crystallization*. Acta Crystallographica Section D - Biological Crystallography, 58, 1611-1616.

Vekilov, P.G., 2003, *Solvent entropy effects in the formation of protein solid phases*. In: Macromolecular Crystallography, Part C, Methods in Enzymology, ACADEMIC PRESS INC, San Diego, 368, 84-105.

Vekilov, P.G., 2004, *Dense liquid precursor for the nucleation of ordered solid phases from solution*. Crystal Growth & Design, 4, 671-685.

Vekilov, P.G., 2005, *Two-step mechanism for the nucleation of crystals from solution*. Journal of Crystal Growth, 275, 65-76.

Vekilov, P.G., 2010, *Nucleation*. Crystal Growth & Design, 10, 5007-5019.

Vekilov, P.G., 2011, *Nucleation of protein condensed phases*. Reviews in Chemical Engineering, 27, 1-13.

Vekilov, P.G., 2012a, *A two-step mechanism for crystal nucleation without supersaturation - general discussion*. Faraday Discussions, 159, 139-180.

Vekilov, P.G., 2012b, *The Two-Step Mechanism and the Solution-Crystal Spinodal for Nucleation of Crystals in Solution*. In: Kinetics and Thermodynamics of Multistep Nucleation and Self-Assembly in Nanoscale Materials, Advances in Chemical Physics, 151, 79-109.

Velev, O.D., Kaler, E.W. and Lenhoff, A.M., 1998, *Protein interactions in solution characterized by light and neutron scattering: Comparison of lysozyme and chymotrypsinogen*. Biophysical Journal, 75, 2682-2697.

Velev, O.D., Pan, Y.H., Kaler, E.W. and Lenhoff, A.M., 2005, *Molecular effects of anionic surfactants on lysozyme precipitation and crystallization*. Crystal Growth & Design, 5, 351-359.

Visuri, K. and Nummi, M., 1972, *Purification and Characterization of Crystalline β-Amylase from Barley*. European Journal of Biochemistry, 28, 555-565.

Visuri, K.J., 1987, *Stable Glucose Isomerase Concentrate and a Process for the Preparation Thereof.* PCT Int. Appl. WO1986000336 A1.

Visuri, T.K., 2000, *Protein crystallization is an exacting task but can be successfully applied in industry*. Kemia - Kemi, 27, 180-183.

Vivares, D. and Bonnete, F., 2002, *X-ray scattering studies of Aspergillus flavus urate oxidase: towards a better understanding of PEG effects on the crystallization of large proteins*. Acta Crystallographica Section D - Biological Crystallography, 58, 472-479.

Vollmer, M., 1939, *Kinetik der Phasenbildung*. Verlag von Thoeodor Steinkopf, Dresden und Leipzig.

Vuolanto, A., Uotila, S., Leisola, M. and Visuri, K., 2003, *Solubility and crystallization of xylose isomerase from Streptomyces rubiginosus*. Journal of Crystal Growth, 257, 403-411.

Walsh, G., 2002, *Proteins Biochemistry and Biotechnology*. John Wiley & Sons Ltd, Chichester, United Kingdom.

Walsh, M.A., Schneider, T.R., Sieker, L.C., Dauter, Z., Lamzin, V.S. and Wilson, K.S., 1998, *Refinement of triclinic hen egg-white lysozyme at atomic resolution*. Acta Crystallographica Section D - Biological Crystallography, 54, 522-546.

Wang, Z.-Z., Xiao, H.-Z., Han, Y., Jiang, P.-P. and Zhou, Z.-J., 2011, *The Effect of Four Imidazolium Ionic Liquids on Hen Egg White Lysozyme Solubility.* Journal of Chemical & Engineering Data, 56, 1700-1703.

Wanka, J. and Peukert, W., 2011, *Optimized Production of Protein Crystals: From 1D Crystallization Slot towards 2D Supersaturation B_{22} Diagram*. Chemical Engineering & Technology, 34, 510-516.

Warner, R.C., 1954, *Egg proteins.* In: The Proteins, Academic Press Inc., New York, Volume 2, Part A, 435 - 485.

Weatherburn, M.W., 1967, *Phenol-Hypochlorite Reaction for Determination of Ammonia*. Analytical Chemistry, 39, 971-974.

Weber, M., Jones, M.J., Hertel, T., Pietzsch, M. and Ulrich, J., 2005, *An Improved Protein Solubility Measurement Method: Solubility of Hen Egg White Lysozyme*. In: 12th International Workshop on Industrial Crystallization (BIWIC 2005), Halle (Saale), Germany, 232 - 239.

Weber, M., 2008a, *Industrial Purification of the Enzyme Urease from Jack Beans Using Crystallization.* PhD Thesis, Martin-Luther-Universität Halle-Wittenberg, Halle (Saale), Germany.

Weber, M., Jones, M.J. and Ulrich, J., 2008b, *Optimisation of isolation, and purification of the jack bean enzyme urease by extraction and subsequent crystallization*. Food and Bioproducts Processing, 86, 43-52.

Weber, M., Jones, M.J. and Ulrich, J., 2008c, *Crystallization as a Purification Method for Jack Bean Urease: On the Suitability of Poly(Ethylene Glycol), Li_2SO_4, and NaCl as Precipitants*. Crystal Growth & Design, 8, 711-716.

Weckesser, D., 2009, *Membrangestützte Kristallisation.* PhD Thesis, Friedrich-Alexander-Universität Erlangen-Nürnberg, Erlangen, Germany.

Widmark, E.M., 1923, *Observations on the Solubility of Insulin*. The Biochemical journal, 17, 668-70.

Wilcox, W.R., 1968, *Removal of inclusions from crystals by gradient techniques.* Industrial and Engineering Chemistry, 60, 12-23.

Wills, P.R., Nichol, L.W. and Siezen, R.J., 1980, *Indefinite Self-Association of Lysozyme - Consideration of Composite-Dependent Activity-Coefficients*. Biophysical Chemistry, 11, 71-82.

Wilson, W.W., 1990, *Monitoring crystallization experiments using dynamic light scattering: assaying and monitoring protein crystallization in solution*. Methods, 1, 110-17.

Winterbourne, D.J., 1986, *Cell-Growth Determined by a Dye-Binding Protein Assay*. Biochemical Society Transactions, 14, 1179-1179.

Winzor, D.J., Deszczynski, M., Harding, S.E. and Wills, P.R., 2007, *Nonequivalence of second virial coefficients from sedimentation equilibrium and static light scattering studies of protein solutions*. Biophysical Chemistry, 128, 46-55.

Young, E.G., 1937, *The separation and characterization of the proteins of egg white.* Journal of Biological Chemistry, 120, 1-9.

Yu, X., Wang, J. and Ulrich, J., 2014, *Purification of Lysozyme from Protein Mixtures by Solvent-Freeze-Out Technology*. Chemical Engineering & Technology, In the press,

Zhang, Y. and Cremer, P.S., 2009, *The inverse and direct Hofmeister series for lysozyme*. Proceedings of the National Academy of Sciences of the United States of America, 106, 15249-15253.

Zogg, M., 1993, *Einführung in die Mechanische Verfahrenstechnik*. B.G. Teubner Verlag, Stuttgart, Germany.

Erklärung

Hiermit erkläre ich gemäß der Habilitationsordnung des Zentrums für Ingenieurwissenschaften der Martin-Luther-Universität Halle-Wittenberg vom 21.01.2008, dass ich die vorliegende Arbeit mit dem Titel „On the Industrial Crystallization of Proteins“ selbständig und ohne fremde Hilfe verfasst, andere als die von mir angegebenen Quellen und Hilfsmittel nicht verwendet habe und die den verwendeten Werken wörtlich oder inhaltlich entnommenen Stellen als solche kenntlich gemacht habe.

Apolda, den 11. Juli 2014 Matthew J. Jones

Lebenslauf

Persönliche Daten

Name:	Matthew Jonathan Jones
Geburtsdatum und Ort:	06. August 1967, Rinteln, Deutschland
Familienstand:	Ledig

Schulbildung

1973 – 1974	Ralston Village School, Ralston, Canada.
1974 – 1975	Clive School, Belm, Deutschland.
1975 – 1977	St. Bernhardschule, Rulle, Deutschland.
1977 – 1979	Thomas-Morus-Schule, Osnabrück, Deutschland.
1979 – 1986	Ernst-Moritz-Arndt-Gymnasium, Osnabrück, Deutschland.
1986	Erlangung der Allgemeinen Hochschulreife.

Studium

1986 – 1992	Studium der Chemie an der Westfälischen-Wilhelms-Universität, Münster, Deutschland.
1991 – 1992	Anfertigung der Diplomarbeit am Institut für Festkörperforschung, Forschungszentrum Jülich, Deutschland.
1992	Erlangung des akademischen Grades Diplom-Chemiker.
1992 – 1997	Promotionsstudium in physikalischer Chemie, zunächst an der University of St. Andrews, ab 1993 an der University College London, Großbritannien.
1997	Erlangung des akademischen Grades Doctor of Philosophy (PhD).

Wissenschaftliche Tätigkeit und Berufsleben

1996 – 1998	Post Doctoral Research Assistant, School of Chemistry, University of St. Andrews, St. Andrews, Großbritannien.
1998 – 2000	Post Doctoral Research Associate, Department of Mechanical and Chemical Engineering, Heriot-Watt University, Edinburgh, Großbritannien.
2000 – 2003	Teaching Fellow (ab dem 01.08.03 Senior Teaching Fellow), School of Process, Environmental and Materials Engineering, University of Leeds, Großbritannien.
2003 – 2008	Wissenschaftlicher Assistant, Verfahrenstechnik/TVT, Martin-Luther-Universität Halle-Wittenberg, Halle (Saale), Deutschland.
2008 – 2010	Associate Principal Scientist, Process Engineering, AstraZeneca R&D, Södertälje, Schweden.
2010 – 2012	Senior Scientist, Physical Science, AstraZeneca R&D, Södertälje, Schweden.
Seit 2013	Senior Scientist, Jesalis Pharma GmbH, Jena, Deutschland.